IDŐJÁRÁS

QUARTERLY JOURNAL
OF THE HUNGARIAN METEOROLOGICAL SERVICE

CONTENTS

****

http://www.met.hu/Journal-Idojaras.php

VOL. 115 * NO. 3 * JULY – SEPTEMBER 2011

IDŐJÁRÁS

Quarterly Journal of the Hungarian Meteorological Service

Editorial Office: Kitaibel P.u. 1, H-1024 Budapest, Hungary
P.O. Box 38, H-1525 Budapest, Hungary
E-mail: journal.idojaras@met.hu
Fax: (36-1) 346-4669

Indexed and abstracted in Science Citation Index Expanded™ and Journal Citation Reports/Science Edition
Covered in the abstract and citation database SCOPUS®

Subscription by

mail: IDŐJÁRÁS, P.O. Box 38, H-1525 Budapest, Hungary
E-mail: journal.idojaras@met.hu

IDŐJÁRÁS

Quarterly Journal of the Hungarian Meteorological Service
Vol. 115, No. 3, July–September 2011, pp. 123–145

Atmospheric chemistry – Bridging the chemical air composition with the climate

Detlev Möller

Chair for Atmospheric Chemistry and Air Pollution Control,
Brandenburg Technical University, P.O. Box 10 13 44, D-03013 Cottbus, Germany
Volmerstr. 13, D-12489 Berlin, Germany
E-mail: moe@btu-lc.fta-berlin.de

(Manuscript received in final form June 14, 2011)

Abstract—Studying the environment is an extremely complex issue, comprising all natural sciences and regarding the "key" compartments water, air, and soil, often defined as the climate system. Without any doubt, the atmosphere is the most important one, it is highly dynamic and globally interlinking the biosphere. Nowadays, the humans are shortly before reaching the "tipping point" between moving into the (climate) catastrophe or the sustainable development. This paper introduces a new discipline, the "chemistry of the climate system". Atmospheric chemistry, without using this term before the 1950s, was a fundamental approach in the beginning of modern chemistry (air analysis and understanding combustion) some 200 years ago, and it is now enlarging to the interfaces ("interfacial chemistry") with the biosphere and hence our climate system. Humans created a new dimension (the "anthroposphere") by globally modified biogeochemical cycles. Climate control means learning from nature and creating closed man-made material cycles, first of all that of carbon. Our environmental problem is not the limited energy but creating unbalanced reservoir distributions of substances with different characteristic timescales out of steady-state conditions.

Key words: atmospheric chemistry, air pollution, climate, climate change, chemical climate, sustainable chemistry, human evolution, anthroposphere, biogeochemistry

1. Introduction

Out of the recognized complexity of nature, the three basic sciences arose: physics, chemistry, and biology. Further progress in the understanding of natural processes created numerous sub-disciplines and cross-disciplines, termed with a variety of prefixes and combinations, often creating misunderstandings unless careful definitions are used. In order to overcome disciplinary borders, a new

super-science was established,the earth system science, to study the earth as a system, with an emphasis on observing, understanding, and predicting global environmental changes involving interactions between land, atmosphere, water, ice, biosphere, societies, technologies, and economies. Humans – by decoupling their life cycle from natural conditions – have altered "natural" biogeochemical cycles. The Russian geochemist, *Vladimir Ivanovich Vernadsky*, understood a new dimension of the biosphere called noosphere (or anthroposphere by *Paul Crutzen*) a new dimension of the biosphere, developing under the evolutionary influence of humans on natural processes (*Vernadsky*, 1926).

We will define air (or atmospheric) chemistry as the discipline dealing with the origin, distribution, transformation, and deposition of gaseous, dissolved, and solid substances in air. This chain of matter provides the atmospheric part of the biogeochemical cycles. A more general definition, but one that is appealing as a wonderful phrase, was given by the German air chemist, *Christian Junge* "Air chemistry is defined ... as the branch of atmospheric science concerned with the constituents and chemical processes of the atmosphere ..." (*Junge*, 1963). In other words, air chemistry is the science concerned with the origin and fate of the components in air. The origin of air constituents concerns all source and formation processes, the chemicals of air itself, but also emissions by natural and man-made processes into the atmosphere. The fate of air constituents includes distribution (which is the main task of meteorology), chemical conversion, phase transfers and partitioning (reservoir distribution), and deposition of species. Deposition is going on via different mechanisms from gas, particulate, and droplet phases to the earth's ground surface, including uptake by plants, animals, and humans. Removal from the atmosphere is the input of matter to another sphere (see *Fig. 1*).

The term "atmospheric chemistry" appears to have been used for the first time in German by *Hans Cauer* in 1949 (*Cauer*, 1949). It was soon used as the label for a new discipline. The first monograph in the field of this new discipline was written by *Junge*, entitled "Air Chemistry and Radioactivity" (New York and London, 1963), soon after he had published a first long chapter entitled "Atmospheric Chemistry" in a book in 1958 (*Junge*, 1958). This clear term identifies a sub-discipline of chemistry and not meteorology or physics. The "discipline" was called "chemical meteorology" before that time. However, before the 1950s, chemical meteorology was mainly looking for the relationship between condensation nuclei, its chemical composition, and the formation of clouds and rain.

Basically, there is no need to prefix the sciences (environmental, ecological, geo-, air, hydro-, etc.). Other sciences such as geology and meteorology, for example, can be reduced to the natural sciences. It is worth noting the language roots of "geo" and "meteor". In Greek, γή (ge) means earth, land, and ground (poetically γαία (gaia))[1]. In the composition of words, Greek γέα (gea), γης

[1] In Latin, the word for earth, land, and ground is "tellūs" (in sense of the celestial body) and "terra" (in sense of matter).

(ges), γην (gen), and γεω (geo) occur. Already before the year 600 B.C., the Greek word μετέωρος (metéoros) was in use, meaning "a thing in the air, altitude, or above ground"[2]. Until the end of the eighteenth century, μετέωρος denoted all celestial phenomena: aqueous, vaporous, solid, and light. *Aristotle*'s "Meteorologia" is a book on natural philosophy (in modern terms: earth science). Hence, in a more narrow (historical) sense, geosciences (geology, geography, geochemistry, geophysics, etc.) deal with the subject of the solid earth (the geosphere). Geochemistry studies the composition and alterations of the solid matter of the earth; geology is the scientific study of the origin, history, and structure of the earth; geography studies the earth and its features and the distribution of life on the earth, including human life and the effects of human activity. Geography (which is an old discipline, founded as a modern science by Humboldt) is thus the science of the earth's surface – the physical and human landscapes, the processes that affect them, how and why they change over time, and how and why they vary spatially. In other words, geography is an interfacial science between the solid and the gaseous earth (the atmosphere); indeed some geographers consider climatology to be a sub-discipline of geography (and vice versa, some meteorologists do not include climatology in meteorology). Finally, the liquid earth (the hydrosphere) is the subject of hydrology[3]. It is important to note that gaseous water (vapor) in the atmosphere is not considered to be an object in hydrology, but liquid water in the atmosphere is. Logically we now can state that the science of studying the "gaseous earth" (atmosphere) is meteorology. Older (synonymous) terms for the science of the study of earth's atmosphere are aerology and atmospherology. For example, meteorology has been defined as the physics and chemistry of the atmosphere (*Scharnow et al.*, 1965) but also reduced to just the physics of the atmosphere (*Liljequist* and *Cehak*, 1984). Some definitions focus meteorology on weather processes and forecasting, which surely was the beginning of that science. A satisfactory definition is "the study dealing with the phenomena of the atmosphere, including physics, chemistry, and dynamics, extending to the effects of the atmosphere on the earth's surface and the oceans". Hence, meteorology is more than "only" the physics and chemistry of the atmosphere. Nowadays, the term "atmospheric sciences" is also used to summarize all the sub-disciplines needed to explain atmospheric phenomena and processes. To return to chemistry, (atmospheric)

[2] μετέωρολογια [metéorologia] means the "science of celestial, heavenly things" but also "vague talk" and "philosophical shenanigans" (*Benselers* Greek-German School Dictionary (*Griechisch-Deutsches Schulwörterbuch*, Leipzig and Berlin 1911).

[3] In Greek ὕδωρ (idor) means originally rain water and generally water; it appears in composite words as ύδρο (idro). This is the derivation of the prefix "hydro" (the pronunciation of Greek letter ὐ and ύ is like "hy"). In Latin, water as a substance is "aqua", but natural waters are referred to as "unda", derived from the Greek "hy-dor" (ὕδωρ); ὕδρα (Greek), and hydra (Latin) is the many-headed water snake in Greek mythology. From Gothic "vato" and Old High German "waz-ar", are clearly seen the roots of English "water" and German "Wasser".

chemistry is just one of the sciences to understand the (chemical) processes in the atmosphere (see above for definition of atmospheric chemistry).

Antoine Lavoisier, who revolutionized the science of chemistry in the eighteenth century and replaced the mythical "phlogiston" with the term and concept of oxygen, clearly understood the importance of accurate definitions. In his words: "We cannot improve the language of any science without at the same time improving the science itself; nor can we, on the other hand, improve a science without improving the language or nomenclature" (*Lavoisier*, 1789). *Imre Lakatos* (1981) wrote "Philosophy of science without history is empty; history of science without philosophy is blind".

2. Air and atmosphere – a multiphase and multi-component system

The typical dictionary definition of atmosphere is "the mixture of gases surrounding the earth and other planets" or "the whole mass of an aeriform fluid surrounding the earth". The terms air and atmosphere are widely used as synonyms. The word "air" derives from Greek άήρ and Latin aer or ær. The term "atmosphere", however, originated from the Greek ατμόσ (= vapor) and σφαιρα (= sphere), and was not regularly used before the beginning of the nineteenth century. The Dutch astronomer and mathematician *Willebrord van Roijen Snell* translated the term "damphooghde" into Latin "atmosphæra" in 1608. *Otto von Guericke*, who invented the air pump and worked on his famous experiments concerning the physics of the air in the 1650s, used the term "ærea sphæra" (*Guericke*, 1672). In addition, in the nineteenth century the term "Air Ocean" was also used, in analogy to the sea.

It makes even more sense to define the atmosphere as being the reservoir (space) surrounding our (and any) planet, and air to be the mixture of substances filling the atmospheric space. With this in mind, the term air chemistry is more adequate than atmospheric chemistry. From a chemical point of view, it is possible to say that air is the substrate with which the atmosphere is filled. This is in analogy to the hydrosphere where water is the substance. Furthermore, air is an atmospheric suspension containing different gaseous, liquid (water droplets), and solid (dust particles) substances, and therefore, it provides a multiphase and multi-component chemical system. Solar radiation is the sole primary driving force in creating gradients in pressure, temperature, and concentration which result in transport, phase transfer, and chemical processes (*Fig. 1*).

The physical and chemical status of the atmosphere is called climate (see Section 4 for details). Supposing that the incoming solar radiation shows no trend over several hundred years, and accepting that natural biogenic and geogenic processes vary but also do not show trends on these time scales, it is only mankind's influence on land use and emissions into the atmosphere that changes air chemical composition, and thus, the climate. Human activities have

an influence on natural processes (biological, such as plant growth and diversity, and physical, such as radiation budget), resulting in a cascade of consequent physical and chemical developments (feedback).

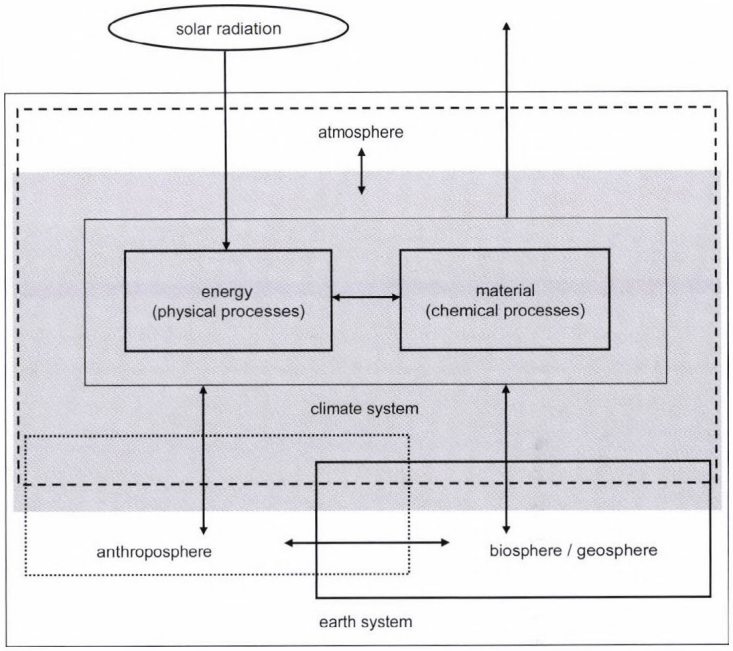

Fig. 1: Scheme of the physico-chemical interactions between the atmosphere, biosphere, and anthroposphere (the climate system).

We will initially set the climate system in a chain of subsystems:

Cosmic system → solar system → earth system → climate system →
→ sub-systems (e.g., atmosphere).

In other words, each system to be defined lies in another "mother" system, the surrounding or environment where an exchange of energy and material is realized via the interfaces. Consequently, there are no fully closed systems in our world.

The chemical composition of air depends on the natural and man-made sources of the constituents (their distribution and source strength in time and space) as well as on the physical (e.g., radiation, temperature, humidity, wind) and chemical conditions (other trace species), which determine transportation and transformation. Thus, atmospheric chemistry is not a pure chemistry but it also includes other disciplines which are important for describing the

interactions between atmosphere and other surrounding reservoirs (biosphere, hydrosphere, etc.). Measurements of chemical and physical parameters in air will always contain a "geographical" component, i.e., the particularities of the locality. That is why the terms "chemical weather" and "chemical climate" have been introduced. For example, diurnal variation of the concentration of a substance may occur for different reasons. Therefore, general conclusions or transfer of results to other sites should be done with care. On the other hand, the basic task in atmospheric chemistry is not only to present local results of chemical composition and its variation in time, but also to find general relationships between trace species and their behavior under different conditions.

Without discussing the biological and physical processes within the climate system in any details, the chemical composition of the atmosphere and its variation in time and space, as well as its trends, are essential for an understanding of climate change. Atmospheric substances with their physical and chemical properties will have many effects in the climate system; we list the most important ones together with their impacts (there are many more impacts, parallel and synergistic effects):

- formation of cloud condensation nuclei (CCN) and subsequent cloud droplets: hydrological cycle;
- greenhouse gases (GHG): radiative interaction (warming the atmosphere);
- ozone-depleting substances (ODS): radiative interaction (increasing UV radiation penetration into the lower troposphere);
- formation of atmospheric aerosol: radiative interaction (cooling the atmosphere);
- oxidation capacity: lifetime of pollutants;
- acidity: chemical weathering;
- toxicity: poisoning the environment (affecting life functions and biodiversity);
- nutrition: bioavailability of compounds essential for life but also eutrophication.

We see that the climate system has physical and chemical components, interacting and (at least partly) determining each other. Physical quantities in the climate system show strong influences on chemical processes:

- temperature and pressure: reactions, rates, and (chemical and phase) equilibria;
- radiation (wavelength and intensity): photochemistry,
- motion: fluxes of matter (bringing substance together for chemical reactions).

Let us now turn to the atmosphere as a multiphase system. While gases and particles (from molecules via molecular clusters to nano- and micro-particles) are always present in the air, although with changing concentrations, condensed water (hydrometeors) is occasionally present in air, depending on the presence of so-called cloud condensation nuclei (CCN) and water vapor supersaturation at the site of fog and cloud formation. With the formation, transportation, and evaporation of clouds, huge amounts of atmospheric energy are transferred. This results in changing radiation transfer and thus "makes" the weather, and, on a long-term scale, the climate. Furthermore, clouds provide an effective "chemical reactor" and transport medium and cause redistribution of trace species after evaporation. When precipitating, clouds remove trace substances from the air (we term it wet deposition) to the earth's surface. As a consequence, beside the continuous process of dry deposition, clouds may occasionally lead to large inputs of trace substances into ecosystems. The amount of condensed water in clouds and fog is very small, with around 1 g/m^3 air or, in the dimensionless term, liquid water content $1 \cdot 10^{-6}$ (identical with 1 ppb). Thus, 99.99% or more of total atmospheric water remains in the gaseous phase of an air parcel. Hydrometeors may be solid (ice crystals in different shapes and forms) or liquid (droplets ranging from a few μm up to some tens of μm). We distinguish the phenomenon of hydrometeors into clouds, fog, and precipitation (rain, drizzle, snow, hail, etc.). This atmospheric water is always a chemical aqueous solution where the concentration of dissolved trace matter (related to the bulk quantity of water) is up to several orders of magnitude higher than in the gaseous state of air. This analytical fact is the simple explanation why collection and chemical analysis of hydrometeors began much earlier than gas-phase measurements.

Due to permanent motion, namely advection and turbulent diffusion, having stochastic characteristics on different time and spatial scales, it is extremely complicated to model chemistry and transport (so-called chemistry-transport models, CTM, which are also a basis for climate modeling) in space and time. At the earth-air interface, exchange of matter occurs, emission as well as deposition.

3. Changes in air chemical composition: air pollution

Changes in the chemical composition of air caused by humans are termed air pollution. The terms air pollution and pollutant need some comments. To start with, the term pollutant should be used only for man-made (anthropogenic) emitted substances, despite the fact that most of them are also of natural origin. Air pollution represents a deviation from a natural chemical composition of air (providing a reference level) at a given site. Depending on the residence time of the pollutant, we can characterize the scale of pollution from local via regional to global. Air pollution nowadays is a global phenomenon because long-lived pollutants can be found to be increasing at any sites of the globe. Remote air just

means that the site is located far away from the sources of emissions and, consequently, this air has lower concentrations of short-lived (reactive) substances compared with sites close to sources of pollutants. Although polluted air is human-influenced air, clean air is not synonymous with natural air. The natural atmosphere no longer exists; it was the chemical composition of air without man-made influences. However, this definition is also not exact, because humans are part of nature. In nature situations may occur, such as volcanic eruptions, sand storms and biomass burning, where the air is being "polluted" (rendered unwholesome by contaminants) or in other words, concentrations of substances of natural origin are increased. Therefore, the reference state of natural air is a climatological figure where a mean value with its variation must be considered. The term clean air is also used politically in air pollution control as a target, i.e., to make our air cleaner (or less polluted) in the sense of pollutant abatement. A clean atmosphere is a political target, it represents an air chemical composition (defined in time and scale) which should permit sustainable development. The largest difficulty, however, lies in the definition of what sustainable means. This term comprises the whole range of categories from simple scientific questions (for example, impact threshold) to political decisions (global ecomanagement) and also to philosophical questions (for example, what human life needs).

Therefore, air pollution in terms of the changing chemical composition of the atmosphere must be identified through a problem, not simply by measured concentrations. The problem lies between "dangerous" and "acceptable" climate impact, a definition that is beyond the direct role of the scientific community despite the fact that scientists have many ideas about it (*Schneider*, 2006).

Doubtless, the air of settlements and towns was extremely polluted in the past. Heavy metals have been found in Greenland ice cores dating back to the Roman Empire; thus demonstrating that metallurgical operations of immense volume took place in that era. The modern quality of air pollution, since the industrial revolution of the nineteenth century, is best characterized by a continuous worldwide increase in emissions as the era of fossil fuel combustion began. In the last 150 years, serious air pollution problems have been described, analyzed, and solved (to an extent, by end-of-pipe technologies), such as soot, dust and smoke plagues, winter and summer smog, and acid rain. The chemicals (or emitted compounds) behind these phenomena are soot, sulfur dioxide (SO_2), nitrogen oxides (NO_x), and volatile organic compounds (VOC) – all of them short-lived species, but because of global use of fossil fuels, the pollution problem is distributed globally. Some air pollution problems connected with long-lived compounds – now in terms of persistent compounds, such as agricultural chemicals (food chain accumulation) and halogenated organic compounds (ozone layer destruction) – have been solved by legislation banning their use. Unfortunately, some long-lived emitted compounds, the so-called greenhouse gases, have increased significantly in global mean concentration (*Table 1*).

Table 1. Increase of some climate relevant gases in air (in ppb)

Substance	1850	2008	Increase (in ppb)	Increase (in %)
Carbon dioxide CO_2	285,000	383,000	98,000	34
Methane CH_4	700	1700	1000	143
Nitrous oxide N_2O	300	320	20	7
Ozone O_3	10	20	10	100

Ozone is not among long-lived species but globally it is a secondary product from methane oxidation. CH_4 and N_2O (mainly byproducts of agriculture) as well as CO_2 (a byproduct of fossil fuel combustion) are coupled with the two columns of human existence; food and energy. There is no doubt that the CO_2 problem can be solved only through sustainable technology change. It should be noted that these three pollutants (CO_2, CH_4, and N_2O), even with much higher atmospheric concentrations, are harmless for life. They are in fact key substances in biogeochemical cycles, but there is also no doubt that these three substances contribute to about 90% of global warming. Besides, N_2O acts as an ozone-depleting substance in the stratosphere, while CH_4 contributes to O_3 formation in the troposphere and is probably responsible for up to 80% of the global O_3 increase. Future air pollution control is synonymous with climate control and must be focused on CO_2, CH_4, and N_2O.

4. Climate and the climate system

The physical and chemical status of the atmosphere on a medium-range timescale (by definition 30 years) is called climate. The expression climate is currently often used in connection with climate change (a term widely popularized in recent years). Synonymously, the expression climate alteration (a more scientific term) is used. In the United Nations Framework Agreement on Climate Change, which was signed by 34 countries and was approved in New York on May 9, 1992, climate change is defined as "changes in climate, that are directly or indirectly attributable to anthropogenic activities, which change the composition of the atmosphere and which add up to the natural climatic changes observed over comparable periods of time". This definition is circumscribed, as natural processes are included in the sense of climate change but not in the sense of climate alteration. However, it can only be observed that climate change is due to all factors. Possible anthropogenic factors having an effect on climate (and, therefore, on its alteration) are manifold and stretch from an alteration in the use of land (altered surface properties) to emissions, whereas direct energetic influences (e.g., warmth islands) are at most (first) of local importance. Thus, a climatic change is the difference between two states of climate. A state of climate is described through the static condition of the climatic system. A

climatic fluctuation can therefore be described as a periodic climatic change, independent of the respective scale of time. Climate is a function of space and time – and is continuously changing (*Schneider-Carius*, 1961).

The climate system is too complex to be clearly mathematically described. In all likelihood, this will be valid in the future as well. Our knowledge about many single processes in this system is still imperfect. Nevertheless, immense progress has been made in the past twenty years and the description of the principal processes is considered as assured (*Hansen et al.*, 2007). It is all the more surprising, that a (quasi)-linear relationship between the GMT (global mean temperature) and the cumulative CO_2 emission was found; on the other hand, the atmospheric CO_2 concentration also shows a strong linear relation with the cumulative CO_2 emission since about 1910 (*Möller*, 2010).

Both climate researchers and historians of climate science have conceived of climate as a stable and well defined category, but such a conception is flawed. Of particular interest becomes the impact of climate on human beings and the environment. In modern climate research, at the close of the twentieth century, the concept of climate lost its temporal stability. Instead, climate change has become a core feature of the understanding of climate and a focus of research interest. Climate has also lost its immediate association with specific geographical places and become global. Interest is now focused on the impact of human beings on climate (*Heymann*, 2009).

Alexander von Humboldt's often cited definition of climate shows three remarkable particularities: the relation of changes instead of a mean status (as defined later in the nineteenth century), the inclusion of the chemical status of the atmosphere (by using the terms cleanness and pollution), and the restriction on parameters affecting human organisms but also the whole biosphere:

> "The term climate, taken in its most general sense, indicates all the changes in the atmosphere which sensibly affect our organs, as temperature, humidity, variations in the barometric pressure, the calm state of the air or the action of opposite winds, the amount of electric tension, the purity of the atmosphere or its admixture with more or less noxious gaseous exhalations, and, finally the degree of ordinary transparency and clearness of the sky, which is not only important with respect to the increased radiation from the earth, the organic development of plants, and the ripening of fruits, but also with reference to its influence on the feeling and mental condition of men." (*Humboldt*, 1850–1852)

The father of the physical definition of climate is *Julius Hann* who defined the climate as "the entirety of meteorological phenomena which describe the mean status of the atmosphere at any given point of the earth's surface"[4] (*Hann*,

[4] " ...Gesamtheit meteorologischer Erscheinungen, welche den mittleren Zustand der Atmosphäre an irgendeiner Stelle der Erdoberfläche charakterisieren."

1883). He further stated that "climate is the entirety of the weathers[5] of a longer or shorter period as occurring on average at a given time of the year". The aim of climatology is to establish the mean states of the atmosphere over different parts of the earth's surface, including describing its variations (anomalies) within longer periods for the same location (*Hann*, 1883). *Hann* also introduced the term climatic element emphasizing that measurements must characterize these through numerical values. He also freed the term "climate" from the close relation to humans and plants, and related it to the time before life appeared on the earth (without using the term palaeoclimate).

Köppen (1906) adopted *Hann*'s definition ("mean weather at a given location") but stated in contrast to *Hann* that it is meaningless to define a climate without focus on human beings; hence only factors (elements) influencing "organic life" should be considered. *Köppen* explicitly presents a "second definition" of climate "... as the entirety of atmospheric conditions, which make a location on earth more or less habitable for men, animals and plants" (*Köppen*, 1906). He wrote that "with the progress in knowledge new subjects will be included in the number of climatic elements when their geographical characteristics are unveiled" (*Köppen*, 1923). During the last 60 years the idea of climate has broadened in so far that, in the definition of climate, apart from the mean value, higher statistical moments are included. According to the new definition, climate describes the "statistical behavior of the atmosphere, which is characteristic for a relatively large temporal order of magnitude" (*Hantel et al.*, 1987).

For an understanding of the dynamics of climate, that is, the processes that determine the average state and variability of the atmosphere over longer periods, the meteorological definition is inadequate, as over longer periods, changes in the atmosphere are considerably affected by interdependencies of the atmosphere, the ocean, vegetation and ice masses (*Claußen*, 2006). For this reason, in climate dynamics, climate is defined by the state and the statistical behavior of the climatic system, as can be read in modern textbooks on meteorology and climate physics (e.g., *Peixoto* and *Oort*, 1992; *Kraus*, 2004; *Lutgens et al.*, 2009). *Claußen* (2006) distinguishes between a meteorological and a system-analytical definition. Note that it is essential to include the statistics into the idea of climate, i.e., climate means not simply the "mean weather". It follows that

- climate is a function of space and time;
- climate cannot be described as a single unit.

[5] There is no direct English translation of German Witterung. The translation as "weather" (German Wetter) is not fully correct because Witterung denotes short-term averaged weather (a weather period).

In the history of mankind and the exploration of air and atmosphere, the concept of climate has been subject to change, but also various descriptions have existed at the same time. It is beyond the scope of this paper to address them here. Here, one can conclude that different definitions of climate are also in use. A priori, this is a contradiction, as there is only one climate system on the Earth. Obviously, this results from a pragmatic approach to the cognition and description of the climatic system by

- diverse disciplinary points of view,
- different objectives (e.g., description of subsystems), and/or
- differentiated knowledge of the system relationships.

The climate system can be described (and widely quantified through measurements) by the

- natural energy system,
- hydrologic cycle,
- carbon cycle and
- other biogeochemical cycles.

The subsystems are linked to each other through flows of energy, impulse, and matter. To the flows of matter, the transport of chemical substances and the processes of their transformation need to be added, as far as these substances, e.g., greenhouse gases or nutrients of the biosphere are directly or indirectly related to the energy budget. The definition of the climate system is not derived from superior principles, but is a pragmatic restriction of the subject to be examined by classification in subsystems and interpretation of the respective system environment. The separation of the climate system from its environment is carried out in that way, as no significant flow of matter between the system and its environment occurs on timescales relevant for examination.

In a broader sense, the climate system can be seen as an interlayer within the earth system, buffering a habitable zone from uninhabitable physical and chemical conditions in altitude (upper atmosphere) and depth (deep lithosphere); see *Fig. 2*. In a more narrow sense, the human-habitable zone is limited to the gas-solid interface (earth-surface/atmosphere) with a very small extension of a few tens of meters. The anthroposphere (or noosphere), however, is permanently expending in space – also out of the climate system – due to the fact that humans are creating inhabited and uninhabited closed habitable systems in an uninhabitable surrounding.

In the literature, the total of climate system and anthroposphere is defined as the earth system (*Schellnhuber* and *Wenzel*, 1998; *Schellnhuber*, 1999; *Claußen*, 1998, 2001). *Hantel* (2001) presents a very pregnant definition "The

climate is not a subject-matter but a property. Its carrier is the climate system. The climate is the entirety of the properties of the climate system."

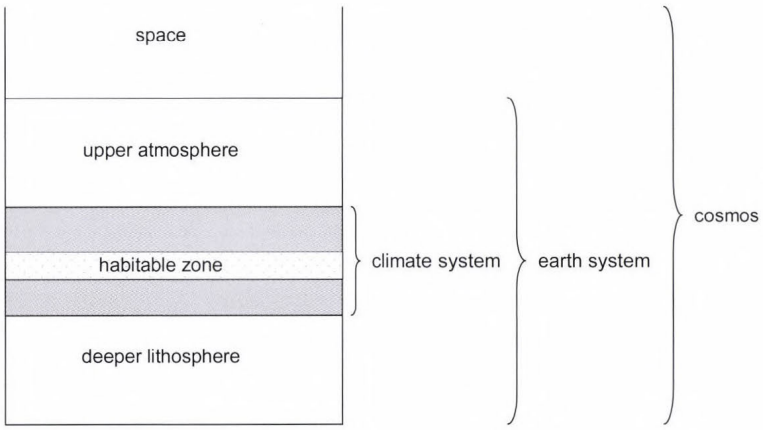

Fig. 2. Layer structure of the climate system.

According to the definition of "chemical weather" given by *Lawrence et al.* (2005), we arrive at a formal definition of chemical climate as: "The synthesis of chemical weather conditions in a given area, characterized by long-term statistics (mean values, variances, probabilities of extreme values, etc.) of the chemical substances in that area."

Instead of "meteorological elements", we have "chemical substances". When – as implicitly mentioned earlier – meteorology feels responsible as a discipline for the description of the chemical state of the atmosphere, the list of "meteorological elements" can simply be expanded to accommodate all relevant chemical variables as well. So as not to raise misunderstandings, "chemical aspects" and not "chemistry" are dealt with the extension of the term climate, since climatology is not a subdiscipline of physics.

I would like to define climate in a general sense as follows:

> Climate describes the mean status of the atmosphere at a given site of the earth's surface, represented by the statistical total properties (mean values, frequencies, durations etc.) of a long enough time period.

It is understood, and, therefore, no differentiation between a meteorological and a system-related definition of climate according to *Claußen* shall be undertaken, that the atmosphere is only one part of the climatic system, and therefore, climate can only correctly be described in a physical-chemical manner taking into consideration material and energetic interdependencies with the other subsystems. Advantageously, a climatic state (i.e., the scientific, broadly mathematical description of the climate) can be defined:

A climate state is given by the whole description of the statistical status of the internal climate system.

The conclusion that the climate is permanently but slowly changing is true. Now, however, we have the likely situation of man-made abrupt climate change. An abrupt climate change occurs when the climate system is forced into transition to a new state at a rate that is determined by the climate system itself, and which is more rapid than the rate of change of the external forcing. Moreover, with this background we understand climate change better, because it means that one or more of the earth-system determining climate elements is changing by a qualitative jump. In nature there is no jump, as nature itself composes of jumps. The idea of interactive changes from quality to quantity and vice versa is a main principle of dialectics. The fact, that our subjective thinking and the objective world underlies the same laws, and therefore, cannot be contradictory in their results, but correspond, rules our complete theoretical thinking. It is an unconscious and unconditional premise. The materialism of the eighteenth century studied this premise according to its vitally metaphysical character on its content only. It limited itself to the proof that the content of all thinking and knowledge descends from sensual experience, and reconstructed the sentence: *Nihil est in intellectu, quod non fuerit in sensu.* (Nothing is in the mind, which has not been in the senses before). Dialectics as the science of the common laws of all movement was first scientifically postulated by *Friedrich Engels*. Despite the linguistic simplification, we should not forget the complexity of the system: even the most advanced mathematical models running on the biggest (and networked) computers are still unable to produce a true picture of the climate system sufficient to draw reliable conclusions. Experimental validation of the model outputs, however, is only possible after climate change – that is the dilemma! Parts of the model (or the system) can be validated with relevant experimental approaches, for example, cooling of the atmosphere by particulate matter after large volcanic eruptions.

5. Chemical evolution and the role of humans

The term evolution was used first in the field of biology at the end of the nineteenth century. In the context of biology, evolution is simply the genetic change in populations of organisms over successive generations. Evolution is widely understood as a process that results in greater quality or complexity (a process in which something passes by degrees to a different stage, especially a more advanced or mature stage). However, depending on the situation, the complexity of organisms can increase, decrease, or stay the same, and all three of these trends have been observed in biological evolution. Nowadays, the word has a number of different meanings in different fields. The term chemical evolution is not well-defined and used in different senses.

Chemical evolution is not simply the change and transformation of chemical elements, molecules, and compounds as it is often asserted – that is the nature of chemistry itself. It is essentially the process by which increasingly complex elements, molecules, and compounds develop from the simpler chemical elements that were created in the Big Bang. The chemical history of the universe began with the generation of simple chemicals in the Big Bang. Depending on the size and density of the star, the fusion reactions can end with the formation of carbon or they can continue to form all the elements up to iron.

The origin of life is a necessary precursor for biological evolution, but understanding that evolution occurred once organisms appeared and investigating how this happens do not depend on understanding exactly how life began. The current scientific consensus is that the complex biochemistry that makes up life came from simpler chemical reactions, but it is unclear how this occurred. Not much is certain about the earliest developments in life, the structure of the first living things, or the identity and nature of any last universal common ancestor or ancestral gene pool. Consequently, there is no scientific consensus on how life began, but proposals include self-replicating molecules such as RNA, and the assembly of simple cells. Astronomers have recently discovered the existence of complex organic molecules in space. Small organic molecules were found to have evolved into complex aromatic molecules over a period of several thousand years. Chemical evolution is an exciting topic of study, because it yields insight into the processes which lead to the generation of the chemical materials essential for the development of life. If the chemical evolution of organic molecules is a universal process, life is unlikely a uniquely terrestrial phenomenon, instead, it is likely to be found wherever the essential chemical ingredients occur.

In colloquial contexts, evolution usually refers to development over a long time scale, and the question is not important whether evolution tends toward more complexity. Many definitions tend to postulate or assume that complexity expresses a condition of numerous elements in a system and numerous forms of relationships among the elements. At the same time, deciding on what is complex and what is simple is relative and changes with time.

A modern understanding of evolution includes continuous development, but also leaps (catastrophes). This is referred to as "transformation of quantity into quality" (dialectic leap) and may characterize the current discussion on the impacts of climate change. However, it is hard to envisage a physical situation in which a quantifiable parameter can increase indefinitely without a critical condition occurring. Physical processes – starting with the Big Bang – created the first atoms (which form chemical elements) and physical conditions, permanently affecting the subsequent chemical and biological evolution. Compared with the Big Bang as the beginning of physical evolution, the creation of molecules and life can be referred to as the starting point of a chemical and biological evolution, respectively. Life became a geological force

with oxygenic photosynthesis and created an interactive feedback with chemical and physical evolution. After forming the geosphere and the first atmosphere in the sense of a potentially habitable system, and later the biosphere with the modern atmosphere, a habitable climate system evolved.

If water was as common in the solar system as it is implied by the facts, that would suggest that there were many environments in the solar system where the conditions were right for the development of life. What is life? For instance, *Lynn Margulis* (quoted by *Horgan*, 1997) has stated that to proceed "...from a bacterium to people is less of a step than to go from a mixture of amino acids to that bacterium". At the beginning of the seventeenth century, the ultimate origin of life was considered to be primarily a theological issue. However, it was thought possible that small creatures, such as maggots and even mice, could arise from non-living material by spontaneous generation, a theory first propounded by Aristotle. Today, there is no doubt that bacterial life is created, exists, and survives in space (*Maurette*, 2006). But, what is life? Where did we come from? These two fundamental questions remain (still) unanswered in science. The existence of humans (and all animals) depends on free oxygen in the atmosphere, and this compound is almost completely produced from oceanic cyanobacteria. Hence, the origin of life lies in the darkness of the evolution of molecules in structured systems (a chemical plant that we call a cell) to provide work-sharing synthesis via non-equilibrium electron transfer processes (in other terms, redox processes). Cells represent a dissipative structure, whose organization and stability is provided by irreversible processes running far from equilibrium. *Falkowski* and *Godfrey* (2008) state that the question posed above reflects our ignorance of basic chemistry of the electron transfers, that bring the ensemble of molecules in cells to "life".

But life created a further dimension, human intelligence, which becomes another geological force (human evolution – today approaching a critical condition which we call crisis). Human intelligence disengaged humankind from the rigorous necessities of nature and provided unlimited scope for reproduction (at least in the past). Man, in all his activities and social organizations is part of, and cannot stand in opposition to or be a detached or external observer of, the nature. However, the new dimension (or quality) of human intelligence as a result of biological evolution – without some global ecomanagement – could change the climate system in a direction not providing the internal principle of self-preservation. Mankind converts the biosphere into a noosphere. Chemical evolution is now interloped with human evolution. Changing fluxes and concentrations of chemicals in bio- (or rather noo-) geochemical cycles with a subsequent changing climate system seems to be the creation of a human-chemical evolution.

Vernadsky was the first to propose the idea of biogeochemical cycling (having asked: What is the impact of life on geology and chemistry of the earth?). *Vernadsky*, who had met *Suess* in 1911, popularized the term biosphere in his book The Biosphere (first published in Russian in 1926, not translated into

a full English version until more than 60 years later), hypothesizing that life is the geological force that shapes the earth (*Vernadsky*, 1926; 1944; 1945). *Vernadsky* first took the term "noosphere" in 1931, as a new dimension of the biosphere under the evolutionary influence of humankind (*Vernadsky*, 1944). He wrote: "The Noosphere is the last of many stages in the evolution of the biosphere in geological history" (*Vernadsky*, 1945). The biosphere became a real geological force that is changing the face of the earth, and the biosphere is changing into the noosphere. In Vernadsky's interpretation, the noosphere is a new evolutionary stage of the biosphere, when human reason will provide further sustainable development both of humanity and the global environment

> "In our century the biosphere has acquired an entirely new meaning; it is being revealed as a planetary phenomenon of cosmic character... In the twentieth century, man, for the first time in the history of earth, knew and embraced the whole biosphere, completed the geographic map of the planet earth, and colonized its whole surface. Mankind became a single totality in the life on earth... The noosphere is the last of many stages in the evolution of the biosphere in geological history." (*Vernadsky*, 1945).

Today the term "anthroposphere" is also used. The idea of a close interrelation between the humans and the biosphere is topical in understanding the "earth system", i.e., the climate change, and is used by *Schellnhuber* (1999) with the terminology "global mind" and by *Crutzen* and *Stoermer* (2000) with "anthropocene" to characterize the present epoch[6].

We also may state that the climate is first a result of geophysical and chemical processes, and that evolving life adapts to these conditions. We know that oxygen is definitively a result of the photosynthesis of plants, hence it is of biological origin. Without any doubt we can state that life did change the climate – with "sense" or without –, and that feedback did influence the evolution of life. What is life or a living thing? Each living thing is composed of "lifeless" molecules, independently of its dimension and complexity, which are subject to the physical and chemical laws that are characteristic of inanimate bodies. A living thing (to avoid the definition of "life") has certain characteristics which are common to living matter but not found in nonliving objects, such as:

- the capacity for self-replication (they grow and reproduce in forms identical in mass, shape, and internal structure),
- the ability to extract, transform, and use energy from their environment (in the form of nutrients and sunlight), and
- an organized structure, where each component unit has a specific purpose or function.

[6] *Zalasiewicz et al.* (2008) published the first proposal for the formal adoption of the Anthropocene epoch by geologists, and this adoption is now pending.

All these characteristics result in non-equilibrium with themselves and with their environment. Non-living things tend to exist in equilibrium with their surroundings. An earth-like planet, not developing life, would therefore be oxidized with aging. Only photolytic dissociation and thermal degradation would occur, depending on incoming radiation (distance from the Sun) and available thermal heat (planetary size). At a final stage, the atmosphere would be composed solely of oxides and acids. The large CO_2 content would increase the atmospheric temperature. Missing free oxygen (because it is fixed in oxides, volatile and non-volatile) in the atmosphere (and subsequent ozone) would prevent a UV-absorbing layer and, therefore, allow almost all photodissociations close to the planetary surface. With time, all water would disappear due to photolytic splitting into hydrogen, which escapes into space. The oxygen from water splitting cannot accumulate until all primordial reduced atoms are oxidized. Finally, free oxygen could be possible in the case of an excess over the equivalent of atoms in reduced state. Conversely, no free oxygen would occur when the reduction equivalent exceeds that of oxygen. The planet becomes irreversibly uninhabitable, especially because of absence of water. There is no doubt that this process would occur over a long time, potentially over the planetary lifetime.

The non-living world tends to dissipate structures and, therefore, to increase entropy. However, because of its huge energy pools, the earth's internal geothermal heat and the Sun's radiation, both are likely to remain over the entire expected lifetime of the earth, provide gradients to force geochemical cycling with the irreversible direction of oxidation and acidification (*Fig. 3*).

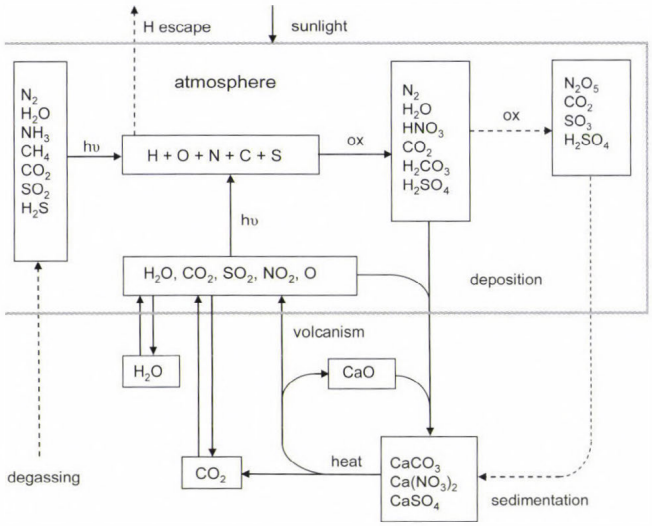

Fig. 3. Scheme of geochemical cycling over geological epochs.

Only the living world is able to reduce entropy by creating structures, or in other words, to move the system back from equilibrium. Indeed, the central role

of life (more exactly, autotrophic organisms) is to maintain the cycle shown in *Fig. 4*, starting with light-induced electrolytic water splitting, and subsequent parallel – but, important to note, in separated organs – reduction of CO_2 into hydrocarbons and the oxidation of them back to CO_2. Globally, this cycle represents a dynamic equilibrium. Consequently, there are established stationary concentrations in the climate system.

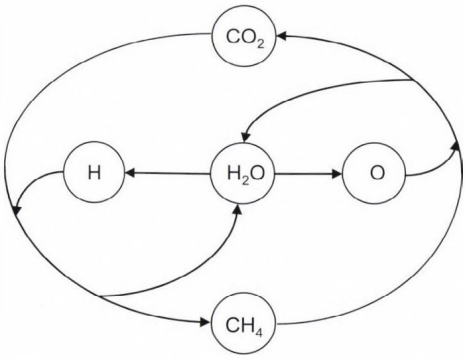

Fig. 4. Scheme of the water-carbon interlinked cycle.

Under the evolution of the earth and the climate system, we will simply understand the historical development from earliest times until the present. Theories for how the atmosphere and ocean formed must begin with an idea of how the Earth itself originated (*Kasting*, 1993). An understanding of our atmosphere and climate system is incomplete without going into the past. "The farther backward you can look the farther forward you can see." (*Winston Churchill*).

6. Conclusion: toward sustainability

In recent decades, humans have become a very important force in the earth system, demonstrating that emissions and land use changes are the cause of many of our environmental issues. These emissions are responsible for the major global reorganizations of biogeochemical cycles. With humans as part of nature and the evolution of a man-made changed earth's system, we also have to accept that we are unable to remove the present system into a preindustrial or even prehuman state, because this means disestablishing humans. The key question is which parameters of the climate system allow the existence of humans (and how many) under which specific conditions.

The chemical composition of air is now contributed by both natural and man-made sources. The chemical composition of air has been changing since the settlement of humans. In addition to the scale problem (from local to global), we

have to regard the time scale. Natural climate variations (e.g., due to ice ages) had a minimum time scale of 10.000 years. The man-made changes in our atmosphere over the last 2000 years were relatively small before the 1850s. In the past 150 years (but almost all after 1950), however, the chemical composition has changed drastically. For many atmospheric compounds anthropogenic emissions have grown to the same or even larger order of magnitude than natural ones. Because of the huge population density, the need (or consumption)[7] of materials and energy has drastically forced the earth's system. "The Great Acceleration is reaching criticality. Whatever unfolds, the next few decades will surely be a tipping point in the evolution of the Anthropocene" write *Steffen et al.* (2007).

The time scale of the adaptation and restoration of natural systems is much larger than the time scale of man-made stresses (or changes) to the climate system. We should not forget that "nature" cannot assess its own condition. In other words, the biosphere will accept all chemical and physical conditions, even worse (catastrophic) ones. Only humans possess the facility to evaluate the situation, accepting it or not, and coming to the conclusion of making it sustainable. But humans also do have all the facilities to turn the "chemical revolution" into a sustainable chemical evolution. That does not mean "back to nature".

Let us define a sustainable society as one that balances the environment, other life forms, and human interactions over an indefinite time period. A global sustainable chemistry first needs a paradigm change, namely the awareness that growth drives each system towards a catastrophe. The basic principle of global sustainable chemistry, however, is to transfer matter for energetic and material use only within global cycles without changing reservoir concentrations above a critical level, which is "a quantitative estimate of an exposure to one or more pollutants below which significant harmful effects on specified sensitive elements of the environment do not occur according to present knowledge" (*Nilsson* and *Grennfelt*, 1988).

The value in identifying current trends and viewing them in a historical light is that the results can be used to inform ongoing policy and investment decisions. The planet could not support the six to seven billion people that exist today without the commercialization of first coal, and then oil and gas. Whereas historical increases in energy consumption had been gradual, once indust–rialization occurred, the rate of consumption increased dramatically over a

[7] This is an interesting question: do we need all this consumption? What consumption do we need to realize a *cultural* life? Of course we move from natural (earth sciences) to a social and political dimension (life sciences) in answering these questions. But there is a huge potential to economize and save resources in answering these questions and implementing it. *Karl Marx* wrote "The philosophers have only managed to interpret the world in various ways. The point is to change it". (This is still fixed in the main hall of the central building of the Humboldt University in Berlin, Germany). However, the key point is how and in which direction we have to change the world to receive sustainability.

period of just a few generations. In fact, the rate of energy use from all sources has been growing even faster than, the world population growth. Thus, from 1970 to 1995, energy use increased at a rate of 2.5% per year (doubling in every 30 years) compared with a worldwide population growth of 1.7% per year (doubling in every 40 years). During the next 20 years, energy use is projected to increase at a rate of 4.5% per year (doubling in every 16 years) compared with a population growth rate of 1.3% per year (doubling in every 54 years). Although about 50% of all the solar energy captured by worldwide photosynthesis is used by humans, this amount is still inadequate to meet all human needs for food and other purposes (*Pimentel* and *Pimentel*, 2007). Hence, only the direct conversion of solar energy (heat and radiation) into electricity and chemically stored energy can overcome the future gap.

A global sustainable chemistry first needs a paradigm change, namely the awareness that growth drives each system towards a catastrophe. Sustainable chemistry, also known as green chemistry, is a chemical philosophy encouraging the design of products and processes that reduce or eliminate the use and generation of hazardous substances.

Permanent growth – as stated by politicians – will not solve life problems such as employment; this is a question of reorganizing society. In nature, many processes follow a simple law Eq. (1), which expresses that the change of a quantity N (for example population, mass, energy) is proportional to the quantity itself. In other words, exponential growth occurs when some quantity regularly increases by a fixed percentage. The proportionality coefficient λ characterizes the process (biology, chemistry, physics, economy, etc.) as follows:

$$\frac{dN}{dt} = \lambda N = F, \qquad N(t) = N_o \exp(\lambda t). \tag{1}$$

We see that dN/dt denotes a flux F; according to the sign, it could result in a growth (positive sign) or decline (negative sign). It is clearly seen that a negative flux will end with $N(t) = 0$ with $t \to \infty$ when there is no permanent source (positive flux) of N to maintain a pool of this quantity. After productivity (expressed as constant annual turnover) satisfies social consumption needs, stationary conditions are then achievable, i.e., λ becomes zero in Eq. (1). Naturally, the human population will (and must) tend to a constant number. This limitation process is likely to go on over the next 200 years. Another limitation must be set through per capita consumption to provide social and cultural standards. The growth, however, is going on this century. Without revolutionary technological changes, the climate becomes out of control. As stated above, the atmospheric CO_2 increase must be stopped within the next few decades. There are several ways, simultaneously linked with the solution of the energy problem:

- reducing fossil fuel combustion and (drastically) replaceing by solar energy (e.g., desertec conception),
- CO_2 capture from exhaust gases and storage (CCS technology) – likely for future reuse and cycling (CCC technology), and
- CO_2 capture from ambient air and recycling (or sequestration achieving a negative flux) to establish a global carbon/CO_2 man-made cycle.

References

Cauer, H., 1949: Aktuelle Probleme der atmosphärischen Chemie. In *Meteorologie und Physik der Atmosphäre* (ed.: *R. Mügge*). *19*: *Naturforschung und Medizin in Deutschland 1936-1946.* Dietrich'sche Verlagsbuchhandlung, Wiesbaden, 277-291.

Claußen, M., 1998: Von der Klimamodellierung zur Erdsystemmodellierung: Konzepte und erste Versuche. *Ann. der Meteorol. (Neue Folge) 36*, 119-130.

Claußen, M., 2001: Earth system models. In *Understanding the Earth System: Compartments, Processes and Interactions* (eds.: *E. Ehlers* and *T. Krafft*). Springer-Verlag, Berlin, 145-162.

Claußen, M., 2006: Klimaänderungen: Mögliche Ursachen in Vergangenheit und Zukunft. In: *Klimawandel - vom Menschen verursacht? 8. Symposium Mensch – Umwelt* (ed.: *D. Möller*). *Acta Acad. Scientiarum* (Academy of the Arts and Sciences Useful to the Public in Erfurt) *10*, 217.

Crutzen, P.J. and. *Stoermer, E.F.*, 2000: The "Anthropocene". *Glob. Change Newsletters 41*, 17-18.

Falkowski, P.G. and *Godfrey, L.V.*, 2008: Electrons, life and the evolution of Earth's oxygen cycle. *Philosop. Transact. Roy. Soc., Ser. B 363*, 2705-2716.

Guericke, O. von, 1672: Neue „Magdeburgische" Versuche über den leeren Raum. In: *Ostwald's Klassiker der exakten Naturwiss.. 59. Unveränderter Nachdruck (Drittes Buch).* Akademische Verlagsgesellschaft (*ca.* 1930), Leipzig, 116.

Hann, J. von, 1883: Handbuch der Klimatologie. In: *Bibliothek geographischer Handbücher* (ed. *F. Ratzel*), J. Engelhorn, Stuttgart, 764. (translated into English: *Handbook of Climatology: Part I. General Climatology*, Macmillan Company, 1903).

Hansen, J., Sato, M., Kharecha, P., Russel, G., Lea, D.W. and *Siddall, M.*, 2007: Climate change and trace gases. *Philos. Transact. of the Roy. Sciety A 365*, 1925-1954.

*Hantel, M., Kraus, H.*and. *Schönwiese, C.-D.,* 1987 :Climate definition. In: *Landolt-Börnstein - Group V Geophysics. Numerical Data and Functional Relationships in Science and Technology. Subvolume C1 'Climatology. Part 1' of Volume 4 'Meteorology'*. Springer-Verlag, Berlin, 5.

Hantel, M., 2001: Klimatologie. In: *Bergmann-Schaefer Lehrbuch der Experimentalphysik*, *7*: *Erde und Planeten* (ed. *W. Raith*), de Gruyter, Berlin and New York, 311-426.

Heymann, M., 2009: Klimakonstruktionen. Von der klassischen Klimatologie zur Klimaforschung. *NTM Zeitschrift für Geschichte der Wissenschaften, Technik und Medizin 17*, 171-197.

Horgan, J., 1997: The end of science: Facing the limits of knowledge in the twilight of the scientific age. Broadway Books, New York, 319.

*Humboldt, A.*V., 1850-1852: Cosmos: A sketch of a physical description of the universe. Translated from German by *E. C. Otté*. Harper & Brothers, New York, *1*. 1850: 275., *2*. 1850: 367., *3*. 1851: 219., *4*. 1852: 234.

Junge, C.E., 1958: Atmospheric chemistry. In: *Advances in geophysics. IV*, Acad. Press. New York, (separate volume), *108*.

Junge, C.E., 1963: Air chemistry and radioactivity. *Int. Geophys. Ser.* (ed. *J. van Mieghem*) 4, Academic Press, New York and London, 382.

Kasting J.F., 1993: Earth´s early atmosphere. *Science 259*, 920-926.

Köppen, W. 1906: Klimakunde I: Allgemeine Klimakunde. Göschen, Leipzig, *8*; 132.

Köppen, W., 1923: Die Klimate der Erde. Grundriß der Klimakunde. 1. Auflage. de Gruyter, Berlin, *3*; 369.

Kraus, H., 2004: Die Atmosphäre der Erde. Eine Einführung in die Meteorologie. Springer-Verlag, 422.

Lakatos, I., 1980: History of science and its rational reconstructions. In: *Scientific revolutions* (ed. *J. Hacking*), Oxford University Press, 107-127.

Lavoisier, A.-L., 1789: Elements of Chemistry in a new systematic order, containing all the modern discoveries. (Transl. by *R. Kerr*) reprint 1965, Dover Publ. New York, 511.

Lawrence, M.G., Hov, O., Bekmann, M., Brandt, J., Elbern, H., Eskes, H., Feichter H. and *Takigawa, M.*, 2005: The chemical weather. *Environ. Chemist. 2*, 6-8.

Liljequist, G.H. and *Cehak, K.*, 1984: Allgemeine Meteorologie. Fr. Vieweg und Sohn, Braunschweig, 368.

Lutgens, F.K., Tarbuck, E.J. and *Tasa, D.*, 2009: The atmosphere: An introduction to meteorology. (11th edition). Prentice Hall, Toronto, 544.

Maurette, M., 2006: Micrometeorites and the mysteries of our origins. Springer-Verlag, Berlin, 200.

Möller, D., 2010: Chemistry of the climate system. De Gruyter, Berlin 722.

Nilsson, J. and *Grennfelt, P., e*ds. 1988: Critical loads for sulphur and nitrogen. *UNECE/Nordic Council workshop report*, Skokloster, Sweden. March 1988. Nordic Council of Ministers: Copenhagen.

Peixoto, J.P. and *Oort, A.H.*, 1992: Physics of climate. Springer, New York, 520.

Pimentel, D. and *Pimentel, M.H.*, 2007: Food, energy, and society. (3rd edition), CRC Press, 380.

Scharnow, U., Berth, W. and *Keller, W.* 1965: Wetterkunde. VEB Verlag für Verkehrswesen, Berlin, 415.

Schellnhuber, H.-J. and *Wenzel, V.*, eds. 1998: Earth system analysis - integrating science for sustainability. Springer-Verlag, Berlin, 530.

Schellnhuber, H.-J., 1999: Earth system analysis and the second Copernican Revolution. *Nature, Suppl. 402*, C19-C23.

Schneider, St.H., 2006: Climate change: Do we know enough for policy action? *Sci. Engineer. Ethics 12*, 607-636.

Schneider-Carius, K., 1961: Das Klima, seine Definition und Darstellung. Zwei Grundsatzfragen der Klimatologie. In: *Veröffentlichungen der Geophysik*, Institut der Universität Leipzig, 2. Serie, Bd. *XVII*, Heft 2, Berlin.

Steffen, W., Crutzen, P.J. and *McNeill, J.R.*., 2007: The Anthropocene: Are humans now overwhelming the Great Forces of Nature? *Ambio 36*, 614-621.

Vernadski, V.I.. 1926: Biosphera (in Russian). *Nautschnyi-chim.-techn.* Izdateltsvo, Leningrad 48 pp. Translated into French (*La Biosphére*, 1929), German (*Biosphäre*, 1930), and English (*The Biosphere*, 1998; a reduced version in English appeared in 1986)

Vernadski, V.I., 1944: Some words on noosphere (in Russian). *Успехи соврем. биол. (uspechi sovrem. biol. 18*, 113-120.

Vernadsky, V.I., 1945: The biosphere and the noosphere. *Scient. Amer. 33*, 1-12.

Zalasiewicz, J., Williams,, M., Smith, A., Barry, T.L., Coe, A.L., Bown, P.R., Brenchley, P., Cantrill, D., Gale, A., Gibbard, P., Gregory, F.J., Hounslow, M.W., Kerr, A.C., Pearson, P., Knox, R., Powell, J., Waters, C., Marshall, J., Oates, M., Rawson P. and *Stone, P,*. 2008: Are we now living in the Anthropocene? *GSA Today 18*, 4-8.

IDŐJÁRÁS

Quarterly Journal of the Hungarian Meteorological Service
Vol. 115, No. 3, July–September 2011, pp. 147–165

Numerical simulation of the cycle of aerosol particles in stratocumulus clouds with a two-dimensional kinematic model

Beáta Szabó -Takács

University of Pécs, Institute of Environmental Sciences
Ifjúság u. 6, H-7624 Pécs, Hungary;
E-mail: takacs.beata@gamma.ttk.pte.hu

(Manuscript received in final form October 20, 2010)

Abstract—The purpose of the paper was to develop a numerical model to study the cycle of aerosol particles in stratocumulus clouds in different air mass types. A detailed microphysical scheme was incorporated into an idealized two-dimensional kinematic model to investigate the role of the aerosol particles in the formation of the water droplets, regeneration of the aerosol particles due to evaporation of the water drops, and the washout of the aerosol particles. The calculations were made with different cloud condensation nuclei (CCN) size distributions and concentrations typical for maritime, rural, and remote continental air mass types, furthermore, with two different updraft profiles. The water droplets were formed on soluble ammonium-sulfate aerosol particles. The ratio of the number concentration of the soluble and insoluble aerosol particles depended on their size. The drops grew by condensation and collision coalescence in the updraft core, but they evaporated due to the subsaturation in the downdraft region.

The model clearly simulated the regeneration of the aerosol particles. The majority of the water soluble particles were scavenged due to the water drop formation. The efficiency of the scavenging of the water insoluble particles depended on the concentration of the water soluble aerosol particles. While Brownian effect played an important role in capturing these particles, only few of them were washed out due to the phoretic- and gravitational forces. Results of the numerical simulation show that in the case of the stratocumulus clouds the number concentration of insoluble aerosol particles larger than 0.1 μm is hardly modified due to different scavenging mechanisms.

Key-words: aerosol particles, drop formation, condensational growth, collision coalescence, aerosol scavenging, aerosol regeneration

1. Introduction

In the 20th century the interest in the effect of the aerosol particles in the clouds has been increased. The aerosol particles play important role in the formation of the clouds. Their characteristics strongly affect both the optical properties of the clouds and precipitation formation. The impact of aerosol particles on the clouds is strongly affected by the physical and chemical attributes of the particles, which depend on the various air mass types (*Hoose et al.*, 2008; *Sassen et al.*, 1999). While the dynamical processes in general define where supersaturated environments occur in the atmosphere, the cloud attributes are determined by aerosol-cloud interaction (*Targino et al.*, 2007). This interaction includes variety of microphysical processes that affect the concentration, size distribution, and chemical composition of cloud droplets (*Gilliani et al.,* 1995). Clouds play an important role in the redistribution of aerosol particles in the atmosphere. The wet scavenging can be separated into two categories. The in-cloud scavenging refers to nucleation and interstitial scavenging. Another category is the below-cloud scavenging, when the aerosol particles are collected by hydrometeors that fall out from the cloud (*Feng*, 2007). The majority of the water-soluble particles are removed by nucleation scavenging (water drops form on the particle).

Results of numerical simulations about the effect of the size distribution and chemical composition on the albedo and the precipitation formation of the stratocumulus clouds have been published in numerous papers (*Geresdi et al.*, 2006; *Caro et al.*, 2004; *Geresdi* and *Rasmussen*, 2005; *Zhang et al.,* 2004; *Bott*, 2000; *Feingold et al.,* 1996; *Ackerman et al.,* 1995). In our research we have focused on the aerosol–cloud interactions that occur in stratocumulus clouds. Not only the role of the aerosol particles in the precipitation formation was investigated, but also how the water insoluble aerosol particles are washed out. We also studied the regeneration of the aerosol particles in the subsaturated regions.

These processes were investigated in stratocumulus clouds due to their relatively simple dynamics. The weak convective updrafts generate shallow, horizontally extensive cloud layers due to the overlaying drier and stable air that blocks the vertical development of the air mass. Stratocumulus clouds play an important role in climate change due to their high albedo, which causes a significant negative contribution to the overall radiative forcing.

In the present paper we discuss our results on the cycle of the aerosol particles in stratocumulus clouds under different dynamic and environmental conditions.

2. Model description

The microphysical processes that occur in a stratocumulus cloud were simulated in a dynamic framework of the idealized two-dimensional kinematic model developed by *Szumowski et al.* (1998) and *Morrison* and *Grabowski* (2007) with

2D MPDATA routine written by Smolarkiewicz (*Smolarkiewicz* and *Margolin*, 1998). The two-dimensional domain includes both updraft and downdraft regions. The updraft and downdraft regions were characterized with two different maximum velocities. The horizontal and vertical extensions of the domain were 2000 m and 750 m, respectively. The resolution was 20 m in horizontal direction and it was 15 m in vertical direction.

Detailed microphysical scheme was used in the research (see the details in *Geresdi*, 1998; *Geresdi* and *Rasmussen*, 2005). The size distribution of water drops and wet aerosol (haze) particles were divided into 55 bins. At the left side edge of the first bin, the particle mass was 3.048×10^{-20} kg with doubling the mass in the bin edges ($m_{k+1} = 2\ m_k$). The size distribution of the dry aerosol particles were divided into 36 bins. At the left side edge of the first bin, the particle mass was the same in the case of the dry aerosol particles and haze particles (wet aerosol particles). While the density of the aerosol particles was assumed to be size independent (1600 kg/m^3), the density of the haze particles depended on the molar concentration of the solution. The aerosol particles were divided into two categories: water soluble and water insoluble ones. The uncertainties about the size dependence of number concentration of water soluble ammonium-sulfate particles are large. The field observations show that number concentration of the soluble ammonium-sulfate particles comparing with the total aerosol concentration is relatively large in size range of 0.1 μm to 1 μm (*Masahiro et al.*, 2003; *Charlson et al.*, 1983; *Kulmala et al.*, 1997; *Mertes et al.*, 2005; *Svenningsson et al.*, 1997). On the base of these observations the ratio of the number concentration of soluble aerosol particles and the total aerosol particle concentration was chosen to be 0.5 when the radius of the aerosol particles was less than 0.012 μm (in the first 10 bins), and this ratio was 0.7 in case of the larger sizes. The purpose of using external mixture was to investigate the different scavenging mechanisms. The aerosol particles contained water soluble fraction can be washed out mostly by water drop formation (nucleation scavenging). The water insoluble aerosol particles can be collected by water drops through other different scavenging mechanisms (Brownian, phoretic, and gravitational collection).

In this study the following microphysical processes were taken into consideration: (i) drop formation on water soluble aerosol particles, (ii) condensational growth/evaporation of water drops, (iii) collision - coalescence of water drops, and (iv) aerosol particles collection by water drops due to Brownian, phoretics and gravitational motion. Some theoretical studies suggest that the turbulence enhances the water drops – aerosol particles collection efficiency. However, efficient turbulent collection was found for collector drops near 200 μm in combination with particles with diameter of 2–4 μm (*Zhang* and *Vet*, 2006). Because in the stratocumulus clouds the drops size generaly less than 200 μm, the effect of turbulent collision was not taken into account in this study.

The water soluble aerosol particles were transferred into the water drop category, if the relative humidity was larger then 90%. The transfer of dry aerosol particles to wet aerosol particles due to vapor diffusion starts at subsaturated condition. In the case of the small water soluble particles (< 0.1 μm), this process occurred at relative humidity larger than 95%, at larger particles size the transfer occurred at 90%. If the mass of the water in a wet aerosol particle decreased to be equal to the mass of the aerosol inside, the wet aerosol particles were transferred to the dry aerosol particle category. Thirty minutes of cloud life time was simulated using 1 s time step.

The diffusional growth of these particles were calculated by using hybrid bin method. More details about this method can be found in the papers published by *Chen* and *Lamb* (1994) and *Geresdi* and *Rasmussen* (2005). The collision–coalescence processes of water drops were calculated by using two-moments method. These moments – the concentration (N_k) and the mixing ratio (M_k) inside the kth bin – were approximated by the following linear equations:

$$N_k(m,t) = f_k \cdot \left(\frac{m_{k+1} - m}{m_{k+1} - m_k} \right) + \psi_k \cdot \left(\frac{m - m_k}{m_{k+1} - m_k} \right) = a_k + b_k \cdot m, \tag{1}$$

$$M_k(m,t) = m_k \cdot f_k \cdot \left(\frac{m_{k+1} - m}{m_{k+1} - m_k} \right) + m_{k+1} \cdot \psi_k \cdot \left(\frac{m - m_k}{m_{k+1} - m_k} \right) = c_k + d_k \cdot m, \tag{2}$$

where m_k and m_{k+1} are the particle mass at the bin boundaries, hereafter m is the mass of the particles. The f and ψ parameters were calculated by using the following equation:

$$M_k^j = \int_{x_k}^{x_{k+1}} m^j n_k(m,t) dx, \tag{3}$$

where M_k^0 and M_k^1 are the concentration (N_k) and mixing ratio (M_k) in the kth bin, respectively.

To calculate the kinetic collection equation of water drops, the Smoluchowski equation was used (*Tzivion et al.*, 1999). The water drop–water drop collision efficiencies used in the model are based on the data published by *Hall* (1980). The collision efficiencies for the given sizes of water drops were calculated by linear interpolation. The Brownian motion, the phoretic effect, and the gravitational collection were taken into consideration when the scavenging of the aerosol particles was simulated (*Ackerman et al.*, 1995; *Gwen et al.*, 2004; *Jian*, 2007; *Mircea et al.*, 2000).

The Brownian motion affects the collision between hydrometeors and very small aerosol particles ($r_p < 0.01$ μm). The following equation gives the number of collected aerosol particles in unit time due to Brownian motion:

$$\left.\frac{dN_p}{dt}\right|_B = 4\pi r_d D_p n_p f_p, \tag{4}$$

where r_d is the radius of the water drop, n_p is the number concentration of the aerosol particles, D_p is the diffusion coefficient for the aerosol particles, f_p is a correction factor which depends on the Reynolds and Schmidt numbers of the aerosol particles (*Pruppacher* and *Klett*, 1997). The motion of aerosol particles due to temperature gradients near to the drop surface is called thermophoresis. Particle motion due to the spatial vapor density gradient is called diffusiophoresis. The sum of the thermophoretic and diffusiophoretic forces is known as phoretic force. The following equation gives the number of collected aerosol particles in unit time due to phoretic forces:

$$\left.\frac{dN}{dt}\right|_{th+df} = \frac{4\pi r_d n_p s f_v}{\left[\frac{L_v}{k_a T_\infty}\left(\frac{L_v}{R_v T_\infty} - 1\right) + \frac{R_v T_\infty}{D_v e_s(T_\infty)}\right]}\left(\frac{C}{\rho_a} - \frac{L_v f_{th}}{p}\right), \tag{5}$$

where $s, T_\infty, k_a, p, \rho_a$, and D_v are the supersaturation, temperature, thermal conductivity, pressure, density of air, and diffusivity of vapor in the air, respectively; R_v is the gas constant for the water vapor, L_v is the evaporation heat, e_s is the saturation vapor pressure over flat water surface. f_v and f_{th} represent the ventilation coefficient and thermophoretic force, respectively (*Pruppacher* and *Klett*, 1997). C is the Cunningham-correction, which value depends on the Knudsen number. While in the case of evaporating drop the motion of the aerosol particles is directed toward the surface of the water drop (the right side term in Eq. (5) is larger than zero), in the case of diffusional growth the direction of the motion is opposite (the right side term in Eq. (5) is less than zero). The effect of the phoretic forces is dominant if the size of the aerosol particles is about 0.1 μm (*Wang*, 2002). The phoretic force results in collision between the submicron aerosol particles and the water drops in the subsaturated regions where the drops evaporate. This condition is realized in the precipitation zone and at the lateral edge of the cloud.

If the radius of the aerosol particles is larger than 1 μm, the phoretic forces hardly affect their motion. They are collected by the water drops due to the gravitational collection. The following equation gives the number of aerosol particles collected by a water drop in unit time due to gravitational force:

$$\left.\frac{dN_p}{dt}\right| = E(r_d + r_p)^2 \pi v_t(r_d) n_p, \tag{6}$$

where E is the collection efficiency, r_d and r_p are the radius of the water drop and the aerosol particles, respectively. v_t is the terminal velocity of the water drop.

3. Results

Formation of the water drops and washout of the aerosol particles were examined in the case of three different air mass types: maritime, rural, and remote continental. Initial size distributions of the aerosol particles (*Fig. 1*) were given by equations published by *Jaenicke* (1988). These equations are frequently used in numerical experiments (e.g., *Bott*, 2000; *Leroy et al.*, 2006; *Caro et al.*, 2004; *Mircea et al.*, 2000).

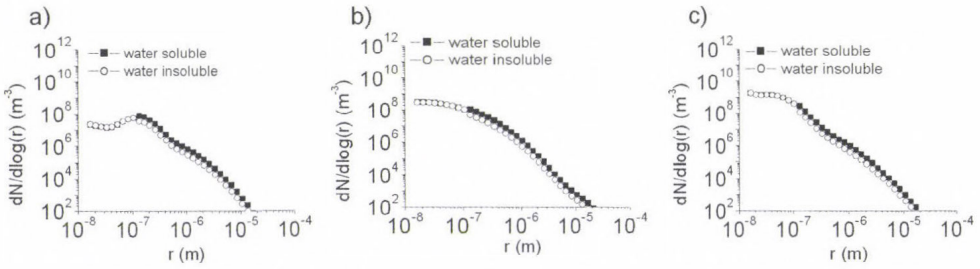

Fig. 1. Initial size distribution of the water soluble (square symbol) and water insoluble (circle symbol) aerosol particles in three different air mass types: (a) maritime, (b) rural, and (c) remote continental.

The spatial distribution of the supersaturation gives information about the development of the cloud. In addition, the phoretic force depends on the subsaturation (see Eq. (5)). The supersaturation is affected by the adiabatic rising of the moist air and by the formation and condensational growth of water drops (*Cohard et al.*, 1998). The supersaturation rapidly increases above the cloud base until it reaches its maximum value. Thereafter it decreases gradually, and at about 100 m above the cloud base it becomes near constant. Most of the haze particles reach their critical size in the updraft region, near to the cloud base where supersaturation is the largest. *Fig. 2* shows the simulated vertical profile of the supersaturation at 0.5 m/s and 1.2 m/s maximum updraft velocities at different aerosol concentrations.

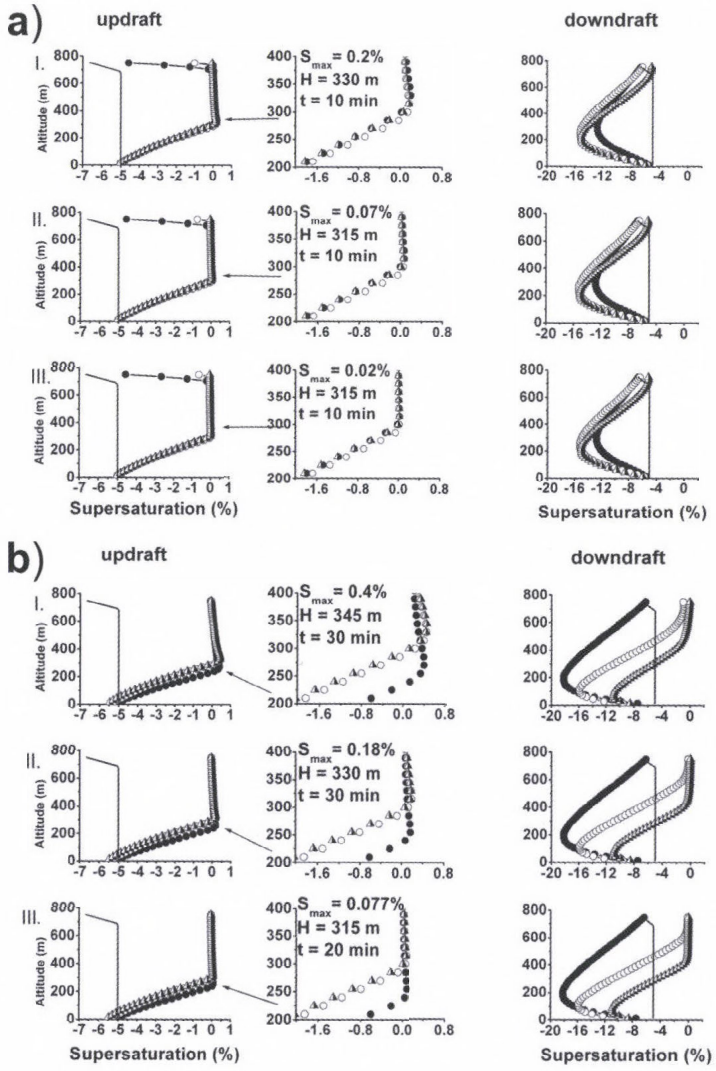

Fig. 2. Vertical profile of the supersaturation in case of maritime (I), rural (II), and remote continental (III) air masses at t = 10 min (black cycle), t = 20 min (white cycle) and t = 30 min (black and white triangle) according to initial supersaturation (solide line) at maximum updraft velocity of 0.5 m/s (a) and 1.2 m/s (b).

In case of weaker maximum updraft velocity (w_{max} = 0.5 m/s), the supersaturation reached its maximum value at about 300 m above the surface, and after a small diminution it became nearly constant with increasing altitude. The largest maximum supersaturation value occurred in the case of the maritime air mass, because the low CN concentration resulted in lower concentration of droplets. Above the cloud top, the saturation suddenly decreased in all

simulation times. With increasing time, reduction rate decreased. In the downdraft region, the relative humidity decreased at lower altitude. After 30 minute of simulation time, the rate of the depletion significantly decreased. Below the cloud base, the relative humidity slightly increased due to the evaporation of falling droplets.

When the maximum updraft velocity was stronger ($w_{max} = 1.2$ m/s) the maximum supersaturation occurred at lower altitude at the beginning (10th minute) than in the case of weaker maximum updraft. With increasing time, the position of the maximum of the supersaturation rose to higher altitude. In the downdraft core, the relative humidity depended on the adiabatic descend of the air and the evaporation of the water drops. While the warming due to adiabatic descend reduces the relative humidity, the evaporation of the water drops increases it. The decrease of the relative humidity until about the 10th minute of the simulation was the consequence of the dry adiabatic descend of the air. The appearance of water drops after the 10th minute resulted in increase of the relative humidity everywhere in the downdraft. This explains that the relative humidity was lower in the case of stronger updraft until the 10th minute of the simulation than in the case of weaker updraft. The increase of the relative humidity was the consequence of the evaporation of the water drops in the down draft core. While this process confined to near to the top of the domain in the case of weaker updraft, evaporation of the water drops occurred in an about 400 m deep layer in the case of the stronger updraft. (See the layer where the supersaturation is eaqual to zero in the right coloumn in *Fig. 2b.*) The effect of evaporation was the largest in the case of remote continental air mass type (IIIrd row in *Fig. 2b.*). This can be explained by the fact, that the total surface area of the water drops was the largest in this case.

Some features of simulation are summarized in *Tables 1* and *2*. The domain integrated number concentration or mixing ratios (M), furthermore, the domain and time integrated production terms (P) were calculated by the following equation:

$$M = \sum_{i,j} M_{i,j} \rho_a \Delta x \Delta y, \qquad P = \sum_{n=1}^{n_{\max}} \Delta t \sum_{i,j} p_{i,j} \rho_a \Delta x \Delta y, \tag{7}$$

where Δx and Δy are the horizontal and vertical distances between the grid points, respectively, ρ_a is the density of air, Δt is the time step, $n_{\max}$ is the number of time steps used during the simulation; $p_{i,j}$ is the production term calculated at the grid point i, j and $M_{i,j}$ is the number concentration or the mixing ratio of the aerosol particles.

Table 1 shows the time and domain integrated production term for the condensation of vapor, change of the number concentration, mixing ratio and

aerosol mass of the wet aerosol particles due to condensation, and the change of the concentration of the water drops due to the collision-coalescence.

Table 1. The following domain integrated production term: change of the mass of wet aerosol particles-water drops due to condensation (ΔM_c); transfer of the dry aerosol particles to wet aerosol particles due to the increase of the relative humidity. Number (column a), mass of water plus aerosol (column b), only aerosol mass (column c); decrease of the number of the water drops due to drop-drop collision

	ΔM_c	N (a)	M_w (b)	M_a (c)	N_w	Updraft
	(kg m^{-1})	(m^{-1})	(kg m^{-1})	(kg m^{-1})	(m^{-1})	m/s
Maritime	1.31×10^{2}	9.54×10^{13}	4.80×10^{-2}	2.40×10^{-2}	-4.50×10^{11}	
Rural	1.31×10^{2}	4.43×10^{14}	5.37×10^{-2}	2.68×10^{-2}	-4.45×10^{11}	0.5
Remote continental	1.31×10^{2}	2.02×10^{15}	6.19×10^{-2}	3.09×10^{-2}	-3.81×10^{11}	
Maritime	2.07×10^{2}	9.72×10^{13}	4.80×10^{-2}	2.40×10^{-2}	-1.84×10^{12}	
Rural	2.09×10^{2}	4.62×10^{14}	5.37×10^{-2}	2.68×10^{-2}	-1.42×10^{12}	1.2
Remote continental	2.11×10^{2}	2.12×10^{15}	6.21×10^{-2}	3.10×10^{-2}	-1.08×10^{12}	

The increase of the total water content was caused by the condensational growth of the wet aerosol particles and water drops. Both the wet aerosol particles and water drops evaporated in the subsaturated region. Similarly to the results published by *Szumowski* et al. (1998), our results show that the water drops, that remained in the updraft core, permanently grow, and the water drops that fall out from the updraft into the outflow, remain small, or completely evaporate. This is demonstrated by the joint size distributions of the water drops and of wet aerosol particles in *Figs. 3* and *4*. The mean size of the water drops increases in the updraft core and decreases in the downdraft regions. Another important feature of the size distributions is that while they were getting narrower in the ascending air due to the condensational growth of the water drops and due to the evaporation of the wet aerosol particles which did not reach the critical size, they got wider due to the evaporation of the water drops in the downdraft. Near to the surface in the downdraft region, the size distribution should be similar to that of the initial size distribution of the aerosol particles due to the complete evaporation of the water drops. The differences can be the consequence of the following reasons: (i) some of the water soluble aerosol particles can be captured by the water drops due to different scavenging mechanisms; (ii) numerical deficiency. During the calculation, the discrete bin width limits the information about the mass of the aerosol particle inside of the drops. This uncertainty of the mass of aerosol particles inside the water drops caused fluctuations in the number concentration of the regenerated aerosol particles at the submicron size in the downdraft core. To avoid this effect, the size distribution can be smoothed by calculation of the mean value of the concentration in three neighboring bins (n_{k-1}, n_k, n_{k+1}) (*Geresdi* and *Rasmussen*, 2005).

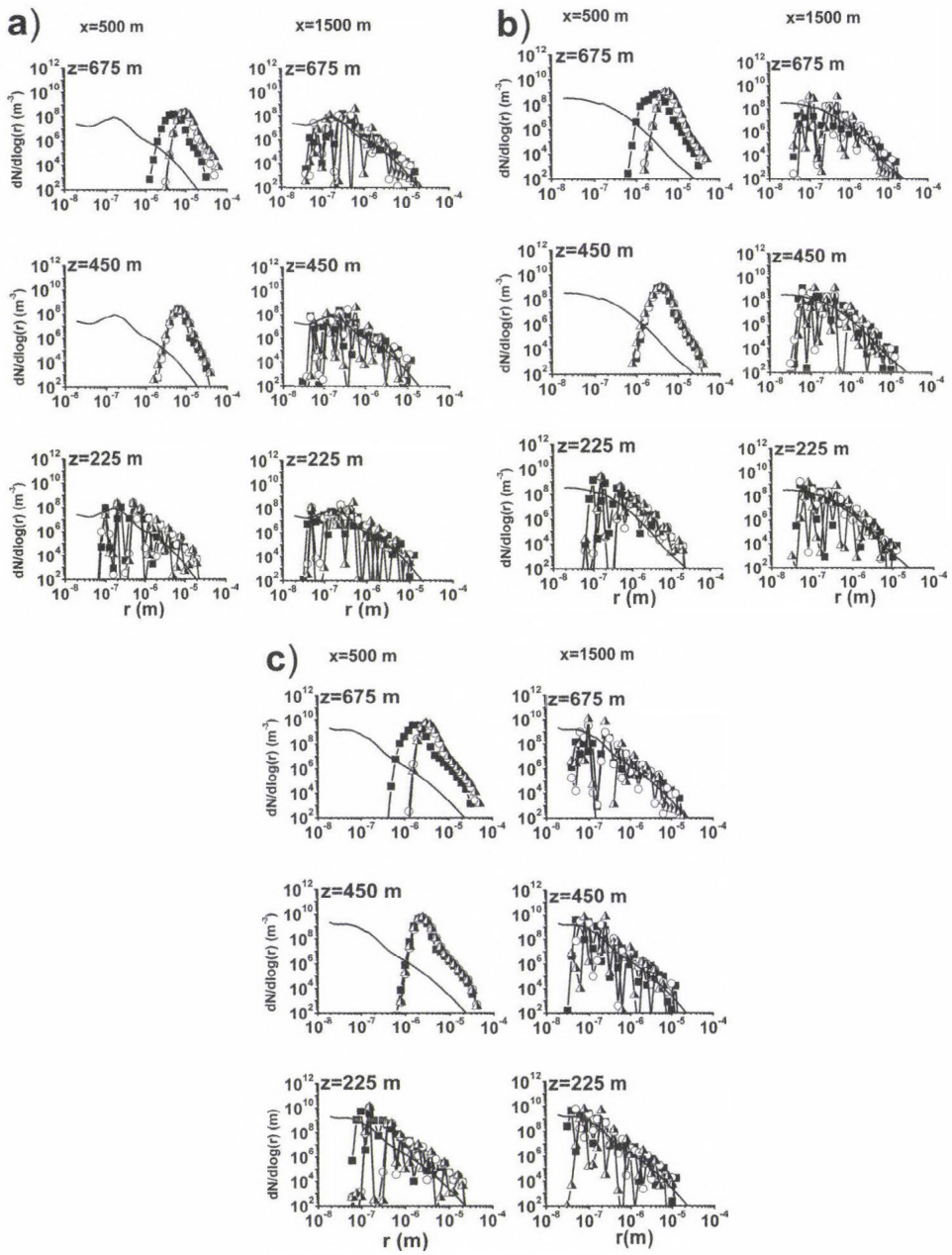

Fig. 3. The evolution of size distribution of the water drops in maritime (a), rural (b) and remote continental (c) air masses at t = 10 min (black square), at t = 20 min (white cycle) and at t = 30 min (black and white triangle) according to initial size distribution of water soluble aerosol particles at 0.5 m/s maximum updraft velocity in the updraft core (x = 500 m) and in the downdraft core (x = 1500 m).

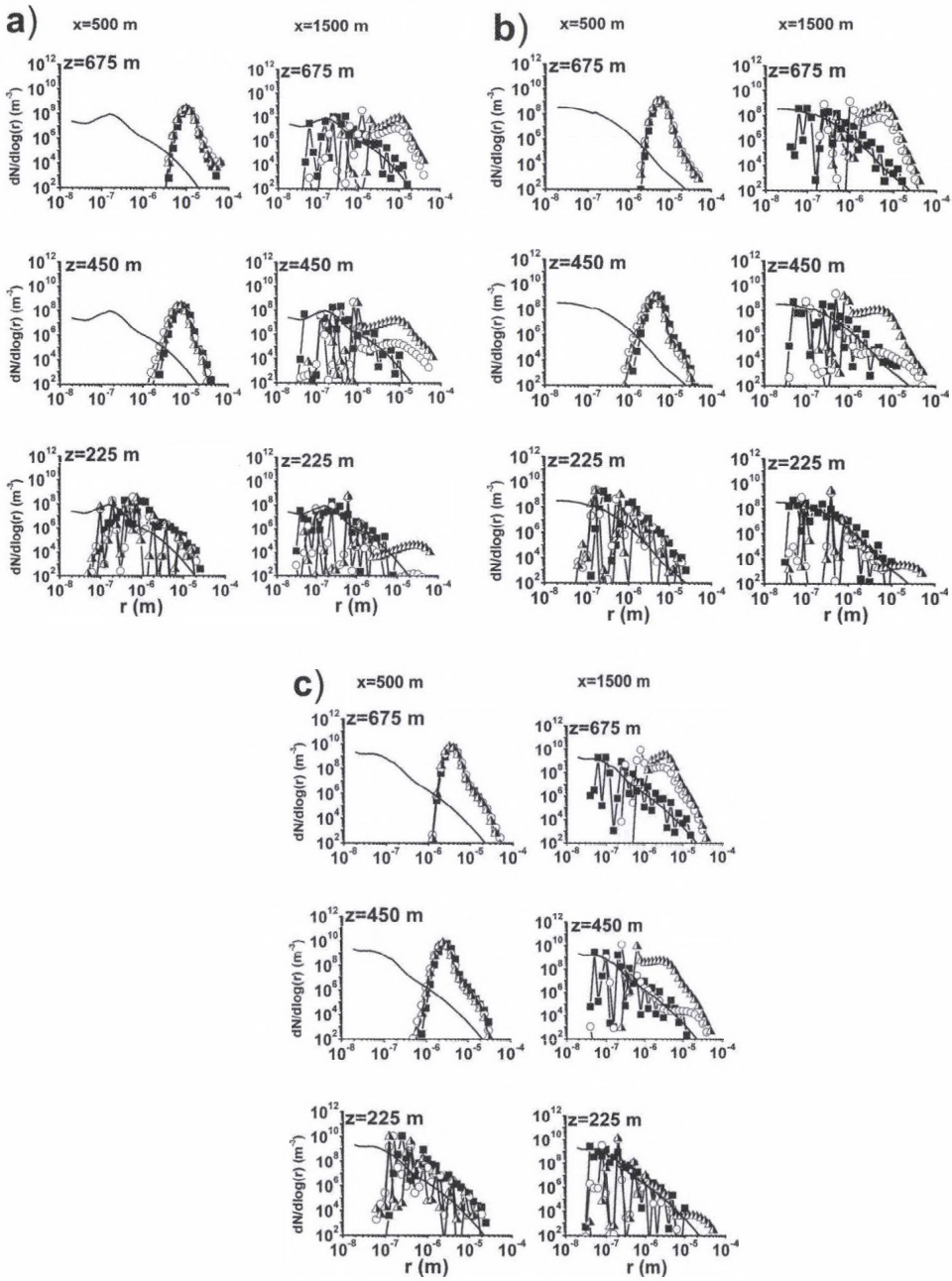

Fig. 4. The evolution of size distribution of the water drops in maritime (a), rural (b) and remote continental (c) air masses at t = 10 min (black square), t = 20 min (white cycle) and t = 30 min (black and white triangle) according to initial size distribution of water soluble aerosol particle at maximum updraft velocity of 1.2 m/s in the updraft core (x = 500 m) and in the downdraft core (x = 1500 m).

The initial size distribution of the water soluble aerosol particles significantly affects the size distribution of the water drops form on them. The concentration of the water drops less than 25 μm was the smallest in the case of maritime air mass and it was the largest in the case of remote continental one (*Fig. 5*).

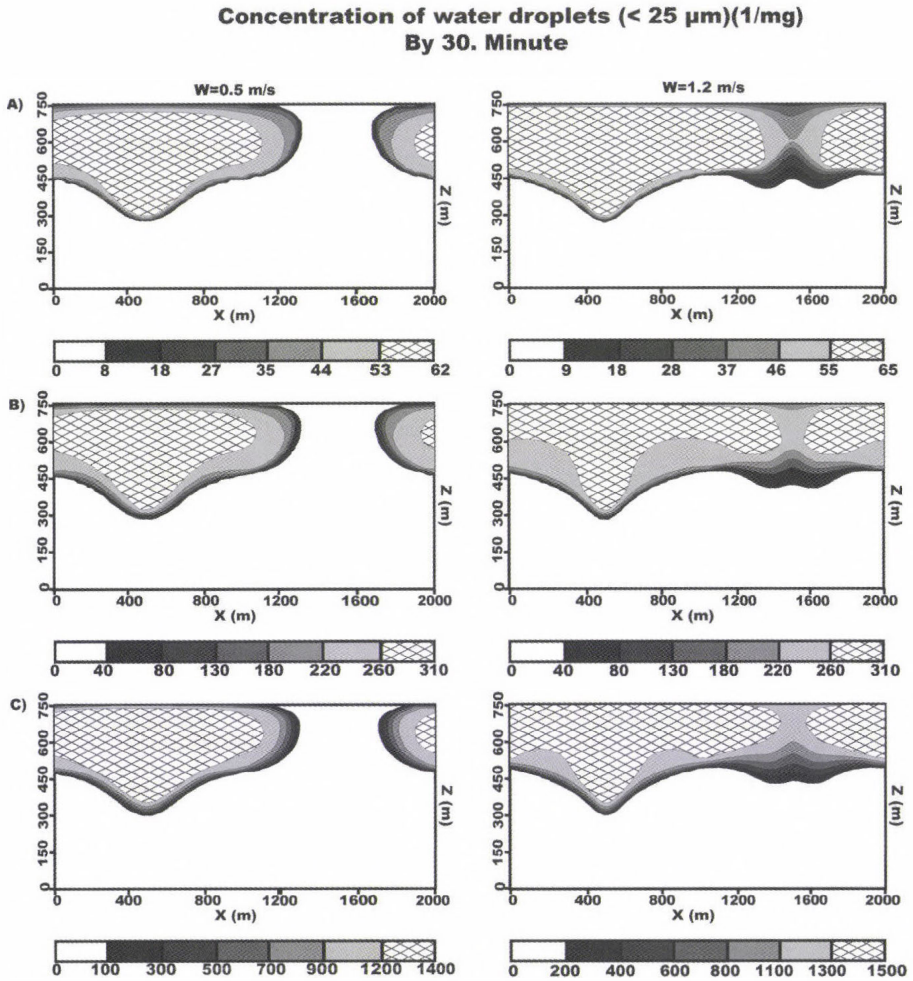

Fig. 5. The evolution of size distribution of the water drops in maritime (a), rural (b), and remote continental (c) air masses at maximum updraft velocity of 0.5 and 1.2 m/s.

Due to the small concentration of water soluble aerosol particles less water drops formed in the maritime airmass. Hence, more water vapor condensed on each of these drops. As a result, the mean mass of drops was larger in the maritime airmass than in the rural and remote continental airmasses. This result was reported also by *Leroy et al.* (2006), *Reisin et al.* (1996), and *Rasmussen et*

al. (2002). As the efficiency of the collision-coalescence of the water drops strongly depends on the mean size of the drops, the concentration of the drizzle size water drops ($r > 25$ μm) was the highest in the maritime case. The mixing ratio of these drops was ten times larger in the maritime case than in the rural air mass case (*Fig. 6*). The water drops were rising until their terminal velocity was equal to the vertical velocity of air and, thereafter, they began to fall down. The fall-out of the rain drops began earlier in the maritime air mass due to the larger terminal velocity of the rain drops.

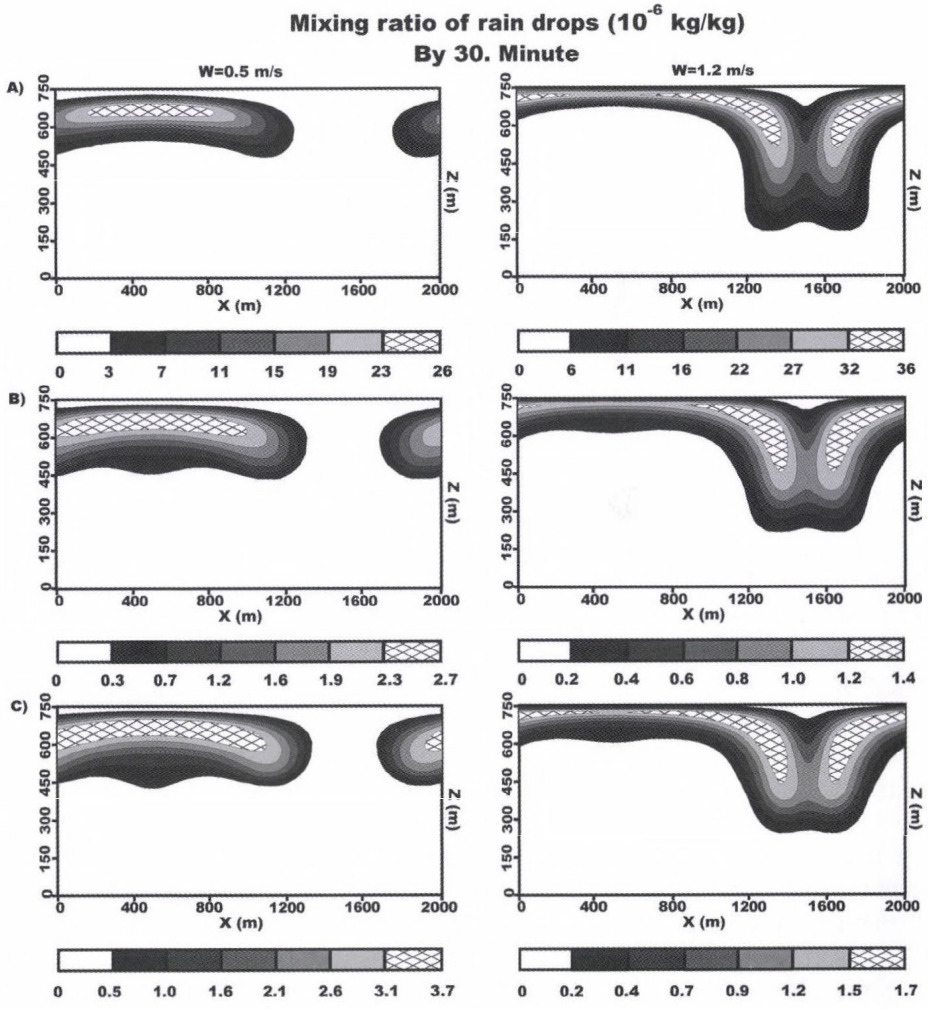

Fig. 6. Mixing ratio of the rain drops in maritime (a), rural (b), and remote continental (c) air mass types at two different maximum updraft velocities by the end of simulation. Scale is given in kg/kg.

Table 2 shows the domain and time integrated values of the production terms, that give the change of number and mass of the water soluble and water insoluble aerosol particles due to Brownian and phoretics effects.

Table 2. Domain and time integrated value of the change of concentration (ΔN_s) and mixing ratio (ΔM_s) of water soluble and insoluble (ΔN_{is}, ΔM_{is}) aerosol particles due to Brownian and phoretic collision with water drops, initial domain integrated concentration and mixing ratio of the water soluble and insoluble aerosol particles

	ΔN_s (m^{-1})	ΔM_s (kg m^{-1})	ΔN_{is} (m^{-1})	ΔM_{is} (kg m^{-1})	**Updraft** m/s
Maritime	-6.09×10^{8}	-3.65×10^{-10}	-6.33×10^{11}	-5.55×10^{-6}	
Rural	-1.22×10^{10}	-3.26×10^{-9}	-1.36×10^{13}	-1.40×10^{-5}	0.5
Remote continental	-5.59×10^{10}	-1.45×10^{-8}	-1.45×10^{14}	-6.69×10^{-5}	
Maritime	-4.98×10^{8}	-2.97×10^{-10}	-1.35×10^{12}	-7.87×10^{-6}	
Rural	-9.69×10^{9}	-2.56×10^{-9}	-3.03×10^{13}	-3.27×10^{-5}	1.2
Remote continental	-4.48×10^{10}	-1.16×10^{-8}	-3.03×10^{14}	-1.43×10^{-4}	
	N_{s0} (m^{-1})	M_{s0} (kg m^{-1})	N_{is0} (m^{-1})	M_{is0} (kg m^{-1})	
Maritime	9.86×10^{13}	2.40×10^{-2}	6.60×10^{13}	8.34×10^{-3}	
Rural	4.75×10^{14}	2.69×10^{-2}	4.28×10^{14}	9.52×10^{-3}	0.5
Remote continental	2.19×10^{15}	3.11×10^{-2}	2.11×10^{15}	1.19×10^{-2}	
Maritime	9.86×10^{13}	2.40×10^{-2}	6.60×10^{13}	8.34×10^{-3}	
Rural	4.75×10^{14}	2.69×10^{-2}	4.28×10^{14}	9.52×10^{-3}	1.2
Remote continental	2.19×10^{15}	3.11×10^{-2}	2.11×10^{15}	1.19×10^{-2}	

For the depletion rate of aerosol particle due to nucleation scavenging we got similar result to that of published by *Zhang et al.* (2004). They investigated aerosol scavenging by low-level, warm stratiform clouds and precipitation using a one-dimensional model with detailed cloud microphysics and size resolved aerosol particles and hydrometeors. By the end of the simulation, more than 90% of the water soluble aerosol particles and more than 99% of the mass of the water soluble aerosol particles were depleted due to the formation of water drops in each case. The rate of condensation increased with the strength of the updraft. Negligible fraction of water soluble particles was scavenged due to the Brownian and phoretics effects. These results also agree with that of published by *Zhang et al.* (2004). *Fig. 7* shows the time integrated change of the concentration of the water insoluble aerosol particles in the case of 0.5 m/s and 1.2 m/s maximum updraft velocities by the 30th minute of the simulation. In case of smaller clouds (weaker updraft) the aerosol particles were scavenged just inside the clouds. While in case of larger clouds (stronger updraft) the drops collected the particles at the edge of clouds and in the downdraft core too. Collection was most significant in the upper divergence region. The high collection rate in the remote continental and rural airmass was the consequence of the larger total surface area of the droplets in a unit volume of the air.

Comparing the initial and final size distributions of the aerosol particles, the total number of water insoluble aerosol particles decreased by 1% and 2% in the case of maritime airmass, 3% and 7% in the case of rural airmass, and 7% and 14% in the case of remote continental airmass at maximum vertical velocities of 0.5 m/s and 1.2 m/s, respectively.

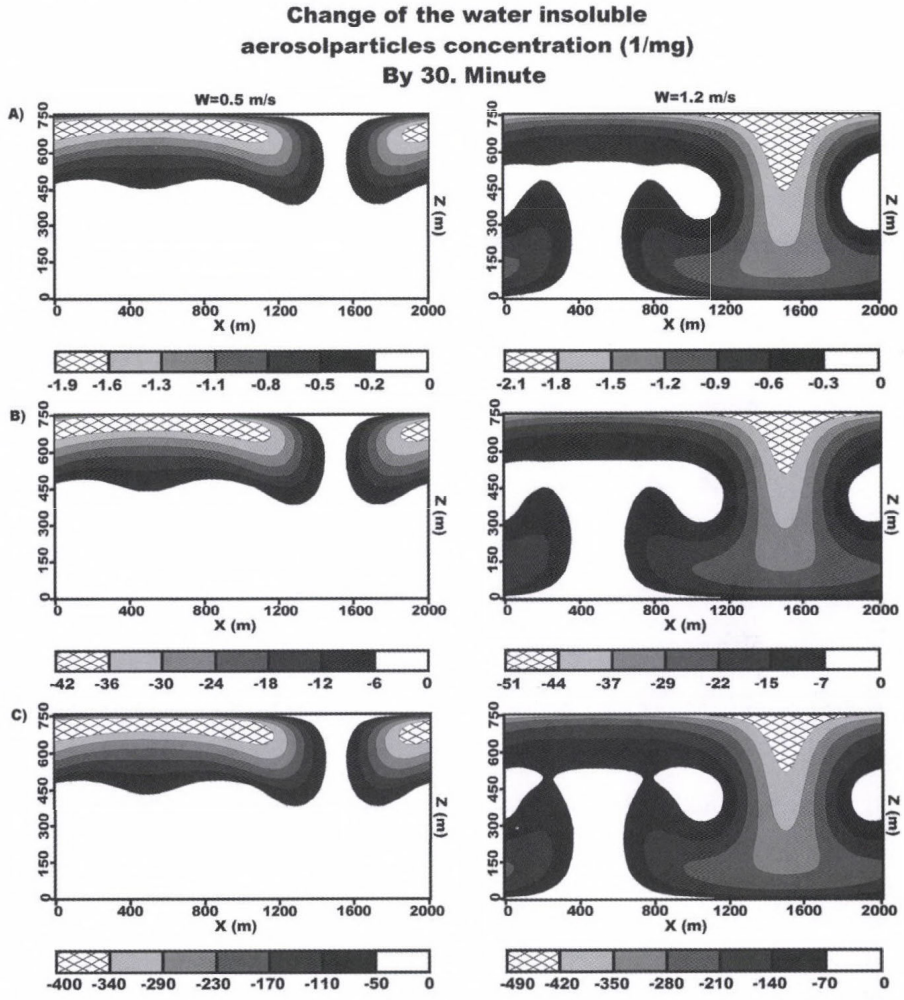

Fig. 7. Concentration of the water droplets in maritime (a), rural (b), and remote continental (c) air mass types at two different maximum updrafts velocities by the end of the simulation. Scale is given in 1/mg.

The reduction in mass of the water insoluble aerosol particles was just a few tenth percents in each case. It follows from the fact that relatively more small particles were collected than large ones. The relative efficiency of scavenging of

the aerosol particles less than 0.1 μm means that scavenging of the water insoluble particles was mostly governed by the Brownian effect inside the cloud.

To investigate the efficiency of the scavenging in different regions of the domain, the following equation was calculated:

$$Scav_{eff} = \frac{N_0 - N_t}{N_0}, \tag{8}$$

where N_0 and N_t are the number concentration of the aerosol particles at a given grid point at the beginning and the end of the simulation, respectively. *Figs. 8a* and *8b* show the efficiency of scavenging in the case of remote continental airmass, when the maximum of the updraft velocity was 0.5 m/s and 1.2 m/s, respectively.

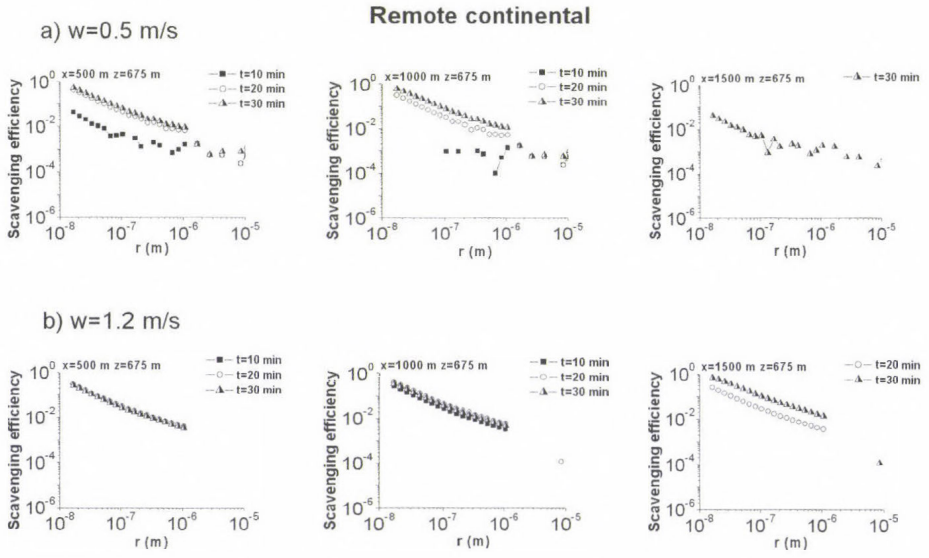

Fig. 8. Collection efficiency of the Brownian, phoretic, gravitational and dynamical processes at maximum updraft velocities of 0.5 m/s (a) and 1.2 m/s (b) in the remote continental airmass at three different grid points.

The three grid points represent three different regions of the domain. The left side figures in *Figs. 8a* and *8b* represent the updraft region near to the top of the cloud. Figures at x = 1000 m represent the cloud region where only horizontal flow occurs. The right side figures show the scavenging efficiency in the downdraft regions. It is clearly shown that the steepness of the curves is very similar at different grid points and at different maximum updraft velocities, as well. The difference between *Figs. 8a* and *8b* indicates that it takes longer time to reach the steady state in the case of weaker updraft. The aerosol particles less

than 0.1 μm were collected most efficiently by Brownian motion. The effect of Brownian motion strongly decreased above this particle size (*Young*, 1974). In the size range of 0.1 μm to 1 μm, only less than 1 percent of the particles were scavenged due to phoretic forces. The effect of the gravitational force was negligible. This force would have changed the concentration of the micron size particles considerably if the size of the hydrometeor had reached the value of 100–200 μm.

4. Summary

The aim of our research was to study the cycle of aerosol particles in stratocumulus clouds using a detailed microphysical scheme in the case of maritime, rural, and remote continental air mass types and at different dynamic conditions. In this study we focused on the following processes:

4.1. Drop formation and regeneration of aerosol particles

The model was able to simulate the regeneration of the water soluble aerosol particles. Neglecting the effect of numerical deficiency caused by the limits of information about the mass of the aerosol particle inside of the drops, the initial size distribution of the water soluble aerosol particles and the size distribution of the regenerated aerosol agree well.

The size distribution of the wet aerosol particles was mostly affected by the nucleation scavenging. Because the mean drop size was relatively small even in the case of maritime airmass, the collision-coalescence of the water drops hardly affected the size distribution of the regenerated aerosol particles.

4.2. Scavenging of water soluble and water insoluble aerosol particles

The water soluble aerosol particles diminished more than 90% in number and more than 99% in mass during the drop formation. Only about 0.1% of the water soluble particles were collected due to Brownian and phoretic forces.

The efficiency of scavenging of water insoluble aerosol particles depended on the initial concentration of the water soluble aerosol particles and on the intensity of the updraft.

Depending on the initial concentration of aerosol particles and the intensity of the updraft, about from 1 to 14% of the insoluble aerosol particles were collected by the different scavenging processes. In the case of more intense updraft, the aerosol particles were removed most efficiently in the downdraft core. The decrease of the number concentration was most significant in the size range of 0.01–0.1 μm due to the Brownian motion.

The results of numerical simulation show that phoretic effects hardly affect the washout of the aerosol particles in the case of the precipitable stratocumulus.

Thus the aerosol particles which do not contain water soluble fraction and their size is between 0.1 and 1.0 μm can have a relative long atmospheric retention time. Further research about how the other cloud types with more efficient precipitation formation can affect the washout these particles is necessary.

Acknowledgements—I would like to thank to *Dr. István Geresdi* for his contribution to the present work and for reviewing the manuscript, and also for using his numerical code. I also should like to thank to the anonymous reviewers for their comments and suggestions.

References

Ackerman, A.S., Toon, O.B., Hobbs, P.V., 1995: A model for particle microphysics, turbulent mixing, and radiative transfer in the stratocumulus-topped marine boundary layer and comparisons with measurements. *J. Atmos. Sci. 52*, 1204-1236.

Bott, A., 2000: A numerical model of cloud-topped planetary boundary-layer: influence of the physico-chemical properties of aerosol particles on effective radius of statiform clouds. *Atmos. Res. 53*, 15-27.

Caro, D., Wobrock, W., Flossmann, A.I., Chaumerliac, N., 2004: A two-moment parametrization of aerosol nucleation and impaction scavenging for a warm cloud microphysics: description and results from two-dimensional simulation. *Atmos. Res. 70*, 171-208.

Charlson, R.J., Vong, R., Hegg, D.A., 1983: The sources of sulphate in precipitation: 2. Sensitivities to chemical variables. *J. Geophys. Res. 88*, 1375-1377.

Chen, J.P., Lamb, D., 1994: Simulation of cloud microphysical and chemical processes using multicomponent framework. Part I: Description of the microphysical model. *J. Atmos. Sci. 51*, 2613-2630.

Cohard, J.M., Pinty, J., Bedos, C., 1998: Extending Twomey's analytical estimate of nucleated cloud droplet concentration from CCN spectra. *J. Atmos. Sci. 55*, 3348-3357.

Feingold, G., Heymsfield, A.J., 1992: Parametrizations of condensational growth of droplets for use in general circulation models. *J. Atmos. Sci. 49*, 2325-2342.

Feingold, G., Kreidenweis, S.M., Stevens, B., Cotton, W.R., 1996: Numerical simulations of stratocumulus processing of cloud condensation nuclei through collision-coalescence. *J. Geophys. Res. 101*, 21.391-21.402.

Feng, J., 2007: A 3-mode parametrization of below-cloud scavenging of aerosols for use in atmospheric dispersion models. *Atmos. Environ. 41*, 6808-6822.

Geresdi, I., 1998: Idealized simulation of the Colorado hailstorm case: comparison of bulk and detailed microphysics. *Atmos. Res. 45*, 237-252.

Geresdi, I., Rasmussen, R., 2005: Freezing drizzle formation in stably stratified layer clouds. Part II: The role of giant nuclei and aerosol particle size distribution and solubility. *J. Atmos. Sci. 62*, 2037-2057.

Geresdi, I., Mészáros, E., Molnár, A., 2006: The effect of chemical composition and size distribution of aerosol particles on droplet formation and albedo of stratocumulus clouds. *Atmos. Environ. 40*, 1845-1855.

Gilliani, N.V., Schwartz, S.E., Leaitch, W.R., Strapp, J.W., Isaac, G.A., 1995: Field observations in continental stratiform clouds: Partitioning of cloud particles between droplets and unactivated interstitial aerosols. *J. Geophys. Res. 100*, 18.687-18.706.

Gwen, A., Cederwall, R.T., 2004: Precipitation scavenging of atmospheric aerosols for emergency response applications: testing an updated model with new real-time data. *Atmos. Environ. 38*, 993-1003.

Hall, W.D., 1980: A detailed microphysical model within a two-dimensional dynamic framework: model description and preliminary results. *J. Atmos. Sci. 37*, 2486-2507.

Hoose, C., Lohmann, U., Bennartz, R., Croft, B., Lesins, G., 2008: Global simulation of aerosol processing in clouds. *Atmos. Chem. Phys. Discuss. 8*, 13.555-13.618.

Jaenicke, R., 1988: Aerosol physics and chemistry. In *Zahlenwerte und Funktionen aus Naturwissenschaften und Technik.* (ed.: *L. Boernstein) 4b*, 391-457, Springer-Verlag.

Kulmala, M., Korhonen, P., Laaksonen, A., Charlson, R.J., 1997: A generalized reformulation of Köhler theory: Effects of soluble trace gases and slightly soluble substances. *J. Aeros. Sci. 28*, S749-S750.

Leroy, D., Monier, M., Wobrock, W., Flossmann, I.A., 2006: A numerical study of the effect of the aerosol spectrum on the development of the ice phase and precipitation formation. *Atmos. Res. 80*, 15-45.

Masahiro, H., Sachio, O., Naoto, M., Sadamu, Y., 2003: Activation capability of water soluble organic substances as CCN. *J. Aeros. Sci. 34*, 419-448.

Metres, S., Galgon, D., Schwirn, K., Nowak, A., Lehmann, K., Massling, A., Wiedensohler, A., Wieprecht, W., 2005: Evolution of particle concentration and size distribution observed upwind, inside and downwind hill cap clouds at connected flow conditions during FEBUKO. *Atmos. Environ. 39*, 4233-4245.

Mircea, M., Stefan, S., Fuzzi, S., 2000: Precipitation scavenging coefficient: influence of measured and raindrop size distributions. *Atmos. Environ. 34*, 5169-5174.

Morrison, H., Grabowski, W.W., 2007: Comparison of bulk and bin warm-rain microphysics models using kinematic framework. *J. Atmos. Sci. 64*, 2839-2861.

Pruppacher, H.R., Klett, J.D., 1997: *Microphysics of Clouds and Precipitation.* Kluwer Academic Publishers, Dordrecht/Boston/London.

Rasmussen, R., Geresdi, I., Thompson, G., Manning, K., Karplus, E., 2002: Freezing drizzle formation in stably stratified layer clouds: The role of radiative cooling of cloud droplets, cloud condensation nuclei and ice initiation. *J. Atmos. Sci. 59*, 837-860.

Reisin, T., Levin, Z., Tzivion, S., 1996: Rain production in convective clouds as simulated in an axisymmetric model with detailed microphysics. Part II: Effect of varying drops and ice initiation. *J. Atmos. Sci. 53*, 1815-1837.

Sassen, K., Mace, G.G., Wang, Z., Poellot, M.R., Sekelsky, S.M., McIntosh, R.E., 1999: Continental stratus clouds: A case study using coordinated remote sensing and aircraft measurements. *J. Atmos. Sci. 56*, 2345-2358.

Smolarkiewicz, K.P. and *Margolin, L.G.*, 1998: MPDATA: A finite-difference solver for geophysical flows. *J. Comput. Phys. 140*, 459-480.

Svenningsson, B., Hansson, H., Martinsson, B., Wiedensohler, A., Swietlicki, E., Cederfelt, S., Wendish, M., 1997: Cloud droplet nucleation scavenging in relation to the size and hygroscopic behavior of aerosol particles. *Atmos. Environ. 31*, 2463-2475.

Szumowski, M.J., Grabowski, W.W., Ochs, H.T., 1998: Simple two-dimensional kinematic framework designed to test warm rain microphysical models. *Atmos. Res. 45*, 299-326.

Targino, A.C., Noone, K.J., Drewnick, F., Schneider, J., Krejci, R., Olivares, G., Hings, S., Borrmann, S., 2007: Microphysical and chemical characteristics of cloud droplet residuals and interstitial particles in continental stratocumulus clouds. *Atmos. Res. 86*, 225-240.

Tzivion, S. Reisin, T.G., Levin, Z., 1999: A numerical solution of kinetic collection equation using high spectral grid resolution: a proposed reference. *J. Comput. Phys. 148*, 527-544.

Wang, P.K., 2002: Sharpe microdynamics of ice particle and their effect, in cirrus clouds. In: *Advances in Geophysics* (eds.: *R. Dmowska, B. Saltzman*) *45.* Academic Press.

Young, K.C., 1974: The role of contact nucleation in ice phase initiation in clouds. *J. Atmos. Sci. 31*, 768-776.

Zhang, L., Michelangeli, D.V., Taylor, P.A., 2004: Numerical studies of aerosol scavenging by low-level, warm stratiform clouds and precipitation. *Atmos. Environ. 38*, 4653-4665.

Zhang, L., Vet, R., 2006: A review of current knowledge concerning size- dependent aerosol removal. *China Particuol 4*, 272-282.

IDŐJÁRÁS

Quarterly Journal of the Hungarian Meteorological Service
Vol. 115, No. 3, July–September 2011, pp. 167–178

Determination of winter barley yield by the aim of multiplicative successive approximation

Erzsébet Enzsölné Gerencsér, Zsuzsanna Lantos, Zoltán Varga-Haszonits, and **Zoltán Varga***

Department of Mathematics and Physics,
Faculty of Agricultural and Food Sciences, University of West Hungary,
Vár 2, H-9200 Mosonmagyaróvár, Hungary
E-mail: varzol@mtk.nyme.hu

**Corresponding author*

(Manuscript received in final form October 20, 2010)

Abstract—The aim of our study was to analyze the climate-winter barley yield relationship by means of a model which took impact of successive periods into account. This approximation is a step from statistical models to dynamic models.

Study was based on data of an agroclimatological database, which contained daily values of meteorological elements during 1951–2000 measured by the Hungarian Meteorological Service and yearly county average values of winter barley yield published by Hungarian Central Statistical Office. In order to investigate the impact of meteorological factors on yield, we separated the influence of weather and technology. Impact of meteorological factors on yield was examined by regression equations during selected periods, but only time periods with significant influence on yield were taken into consideration. Applying this model, trend function was determined firstly, then relationship between trend ratio and meteorological element of first significant time period was calculated. This process was continued until the last function of meteorological impact had been determined.

Verification and validation of results were accomplished by studying of correlation between measured and calculated values and determination of frequency distribution of estimation errors.

The multiplicative successive model is suitable for estimating yields of winter barley, which grows in the cool and wet part of the year. It demonstrates how successive periods of growing season influence yield. This method is a better tool for studying the effects of climatic variability or a possible climate change than a simple statistical model.

Key-words: winter barley, yield, multiplicative successive model, water supply, temperature

1. Introduction

Winter barley is an important fodder grain crop in Hungary. This is a mesotherm plant which prefers cold spring weather. Its temperature demand and absorption of radiation are similar to those of winter wheat, but its cold hardening is worse. Mainly, cold weather without snow seems to be unfavorable for winter barley. Length of sowing-emergence phenophase is usually longer than that of winter wheat, because of higher water demand of barley (*Szakály*, 1968). Peak of water demand can be observed between shooting and heading, after heading water demand decreases (*Varga-Haszonits et al.*, 2000). This plant can be harvested first (in the second half of June) among grain crops; therefore, it is less affected by summer droughts. Winter barley is mainly used as fodder and its nutrition value is higher than that of winter wheat. It usually has the third biggest harvested area, which follows the area of winter wheat and maize. This harvested area of winter barley did not increase over the last some years, but a drying tendency can change that (*Varga-Haszonits et al.*, 2000, 2006).

2. Material and methods

Study was based on data of an agroclimatological database which had been built by Meteorological Group of Institute of Mathematics, Physics and Informatics of University of West Hungary. That database contains daily values of meteorological elements during 1951–2000 measured by Hungarian Meteorological Service and yearly county average values of winter barley yield published by Hungarian Central Statistical Office.

Yield of winter barley is mainly influenced by agrotechnical factors (variety, nutrient supply, plant protection) and meteorological elements. Weather is a key component, because in most cases high percentage of the variability of the yield (20% – 80%) is due to the variability in weather conditions (*Fageria*, 1992; *Porter* and *Semenov*, 2005). Agrotechnical factors change slowly year by year in a given area, that is why these factors show trend of change (*Fig. 1*). Variability of meteorological elements from year to year can be significant, this is the reason of the fluctuation around the trend. In order to investigate the impact of meteorological factors on yield, we have to separate the influence of weather and technology. This can be evaluated by the method of making ratio or difference between the trend and the actual yield or by the help of simulation using different model-calculations (*Andresen et al.*, 2001; *Thompson*, 1962, 1969, 1975, 1986).

Fig. 1 shows that course of barley yields in the second half of the 20th century can be expressed by means of a polynomial of the third degree. Relative

position of single points to trend function indicates that variability of yield increases with rising yields. For this reason, meteorological effect is expressed by trend ratio instead of the trend anomalies. So it can be calculated as follows:

$$\frac{Y(t)}{f(t)} = f(m), \tag{1}$$

where $Y(t)$ is actual yield in the tth year, $f(t)$ is yield calculated by means of trend function in the tth year, and $f(m)$ is a function of meteorological impact.

In this manner, actual yield can be expressed as follows:

$$Y(t) = f(t)f(m). \tag{2}$$

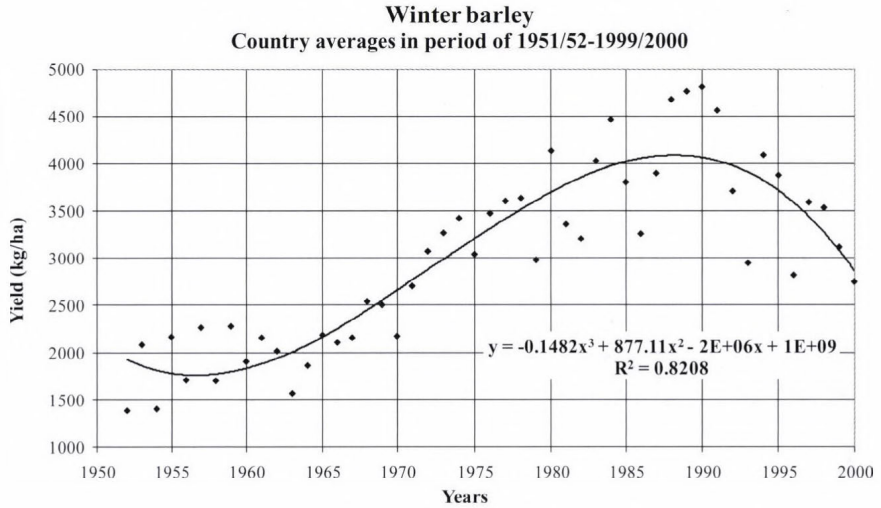

Fig. 1. Tendency of yearly variability in winter barley yield (kg/ha).

It seems to be practical to divide the growing season into different stages. These stages can be natural periods (phenological phases, intervals determined by threshold values) or calendar terms (seasons, months, ten or five days periods). Impact of meteorological factors on yield is examined by regression equations during selected periods, but only time periods with significant influence on yield are taken into consideration (*Szabó* and *Tóth*, 1989). These agrometeorologically important time periods are joined in a model based on multiplicative successive approximation. This dynamically estimating yield model makes possible to predict the crop yield before ripening (*Fuqin* and *Tian*, 1991; *Panofsky* and *Brier*, 1963; *Varga-Haszonits*, 1986, 1987, 1992).

Applying this model, trend function was determined firstly, then relationship between trend ratio and meteorological element (m_1) of first significant time period was calculated. First function of meteorological impact ($f_1(m_1)$) was determined this way:

$$\frac{Y(t)}{f(t)} = f_1(m_1). \tag{3}$$

Then the ratio of $Y(t)$ actual yield and $f(t)\cdot f_1(m_1)$ estimating function is created, and this ratio has to be correlated with m_2 meteorological element of next significant time period for determining $f_2(m_2)$ function:

$$\frac{Y(t)}{f(t)f_1(m_1)} = f_2(m_2). \tag{4}$$

This process is continued until the last function of meteorological impact has been determined. Herewith $Y^*(t)$ estimating function is worked out, and the model can be described as follows:

$$Y^*(t) = f(t)f_1(m_1)f_2(m_2)\ldots f_k(m_k), \tag{5}$$

where $f_1(m_1)$, $f_2(m_2)$, ..., $f_k(m_k)$ are functions of meteorological impact of significant time periods which are calculated by the aim of successive approximation.

Verification and validation of results (*Mavi* and *Tupper*, 2004) were accomplished by studying of correlation between measured and calculated values and determination of frequency distribution of errors.

Crop yield models are divided into three groups by *Ritchie* and *Alagarswamy* (2002). These are groups of statistical, mechanistic, and functional models. Statistical models are used to make large-area yield predictions. Nowadays, these models have been replaced by complex simulation models (*Abbaspour et al.*, 1992). Mechanistic models include mathematical descriptions of plant growth and development. Functional models contain simple equations or empirical relationship to describe the plant process and its environment (*Hoogenboom*, 2000).

This model belongs to the first (statistical) group, because it is based on dividing agrotechnical and meteorological impact and calculating meteorological impact as trend ratio. Calculation took into consideration ten-day periods with significant thermal effects, and it was accomplished by the aim of a multiplicative successive approximation.

3. Results and discussion

It is practical to start from the principle that – as we mentioned earlier – yields are influenced by agrotechnical factors and meteorological elements. Four production levels were distinguished (*Hoogenboom*, 2000; *Penning de Vries*, 1962) for these impacts. Yields would be determined by meteorological impact on first production level, if water and nutrient supply are basically favorable. Following this temporary water shortage, lack of nitrogen or phosphorus and potassium deficit can be observed on second, third, or fourth production level, respectively.

First and second levels can be interpreted as unchanged levels of meteorological elements in our study. In the case of third and fourth production levels, change of the yield was thought to be caused by change of nutrient supply and procedure of plant protection. Influences exerted on yield were examined agroclimatologically, and effects of nutrient supply and plant protection were took into account by means of trend in the case of third and fourth levels.

Yield of first two levels was essentially determined by meteorological elements. These meteorological factors can be divided into two groups: thermal (radiation and temperature) and humidity (relative humidity, precipitation, evapotranspiration, and soil moisture) factors. Water supply is influenced by humidity factors directly. That is the reason why humidity conditions of winter barley during growing season were analyzed (*Fig. 2*).

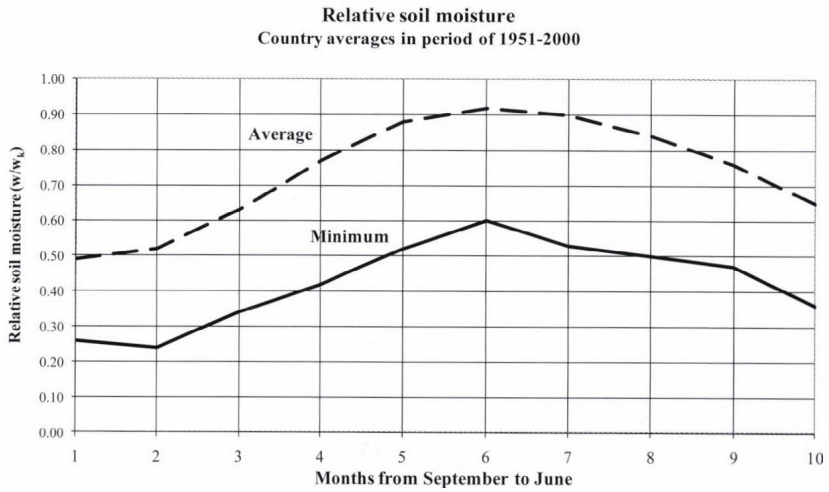

Fig. 2. Temporal changes in relative soil moisture (%) during the growing season of winter barley.

3.1. Water supply conditions of winter barley during growing season

Growing season of winter barley lasts from the second half of September to the second half of June. If survey is based on calendar terms, then months between September and June could be taken in account. Run of soil moisture during that period can be studied (*Fig. 2*). Soil moisture is expressed in the form of relative soil moisture in the first 1 meter depth of upper layer in soil:

$$w_r = \frac{w_a - WP}{FC - WP} = \frac{w}{w_k}, \tag{6}$$

where w_a is the actual soil water content (in mm), WP is the soil water content at wilting point (in mm), FC is the soil water content at field capacity (in mm), w is the available water content, and w_k is the available water capacity (in mm). All soil moisture values are related to 1 meter depth of upper layer in soil.

Lower limit of soil moisture demand of winter barley is 45% of available water according to *Szalóki* (1989, 1991). Soil moisture values above this threshold value are favorable for that crop. Higher limit of soil moisture demand is hard to be defined. Generally, high soil moisture values below field drained upper limit decrease air porosity causing oxygen shortage in pores and unfavorable water uptake.

Fig. 2 shows temporal changes in relative soil moisture during growing season of winter barley in Hungary (country average). It can be seen in *Fig. 2,* that mean values are above 45% of available water during the whole growing season. On the other hand, minimum values of relative soil moisture are below 45% between September and the middle of January and in the last month of the growing season. As we can see later, soil moisture conditions of autumn-early winter period have just a little effect on yields, and only May–June interval means a certain risk. The results were very similar in the case of other stations.

Hence, it can be presumed that water supply conditions are generally favorable for winter barley, but value of humidity factors can become critical in certain years. In this study, favorable water supply is assumed and impact of temperature on yield is analyzed.

3.2. Influence of temperature on yields of winter barley

Firstly, the growing season has to be divided into shorter periods. In this work a calendar term, namely ten-day period was chosen, because experience suggests that the same effect of meteorological conditions rarely extends for a longer interval, that meteorological impact of shorter periods varies, in turn, year by year.

Table 1a. Correlation coefficients of quadratic relationship between average temperature of ten-day periods and trend ratios of winter barley (from September to January)

Stations	Ten days periods in months														
	September			October			November			December			January		
	1	2	3	1	2	3	1	2	3	1	2	3	1	2	3
Győr	0.28	0.30	0.03	0.16	0.10	0.38	0.11	0.30	0.25	0.29	0.37	0.45	0.18	0.11	0.20
Szombathely	0.17	0.27	0.08	0.31	0.10	0.40	0.21	0.35	0.31	0.38	0.36	0.42	0.30	0.28	0.25
Zalaegerszeg	0.18	0.31	0.12	0.26	0.11	0.20	0.16	0.50	0.41	0.46	0.30	0.30	0.11	0.20	0.16
Kaposvár	0.15	0.29	0.23	0.15	0.36	0.18	0.00	0.57	0.33	0.18	0.20	0.18	0.13	0.22	0.25
Pápa	0.20	0.22	0.16	0.12	0.07	0.34	0.09	0.43	0.23	0.24	0.26	0.31	0.15	0.12	0.30
Tatabánya	0.17	0.26	0.19	0.13	0.09	0.24	0.31	0.39	0.24	0.39	0.29	0.34	0.14	0.14	0.22
Martonvásár	0.28	0.25	0.16	0.17	0.22	0.30	0.09	0.39	0.15	0.21	0.35	0.28	0.26	0.11	0.27
Iregszemcse	0.19	0.28	0.25	0.11	0.34	0.23	0.18	0.51	0.20	0.12	0.18	0.19	0.15	0.14	0.22
Pécs	0.20	0.20	0.11	0.06	0.35	0.05	0.25	0.55	0.33	0.13	0.26	0.25	0.23	0.30	0.15
Kecskemét	0.10	0.27	0.16	0.16	0.24	0.25	0.17	0.49	0.30	0.16	0.30	0.22	0.19	0.19	0.24
Budapest	0.20	0.28	0.21	0.10	0.19	0.23	0.07	0.32	0.28	0.39	0.34	0.34	0.18	0.22	0.26
Szolnok	0.25	0.28	0.23	0.22	0.39	0.44	0.15	0.43	0.22	0.25	0.51	0.35	0.14	0.32	0.31
Szeged	0.10	0.17	0.21	0.09	0.28	0.35	0.14	0.31	0.21	0.07	0.46	0.37	0.33	0.19	0.30
Békéscsaba	0.19	0.35	0.27	0.43	0.34	0.34	0.14	0.31	0.18	0.00	0.52	0.45	0.26	0.15	0.33
Debrecen	0.18	0.36	0.06	0.35	0.31	0.38	0.18	0.29	0.33	0.23	0.57	0.42	0.09	0.03	0.23
Nyíregyháza	0.11	0.44	0.21	0.23	0.27	0.28	0.21	0.22	0.29	0.17	0.57	0.42	0.17	0.19	0.04
Miskolc	0.06	0.31	0.10	0.13	0.14	0.48	0.26	0.03	0.19	0.36	0.47	0.37	0.15	0.16	0.04
Kompolt	0.32	0.24	0.10	0.05	0.25	0.40	0.34	0.29	0.34	0.25	0.29	0.31	0.20	0.20	0.12
Balassagyarm.	0.30	0.15	0.04	0.18	0.03	0.29	0.43	0.11	0.25	0.07	0.23	0.42	0.40	0.20	0.33

Table 1b. Correlation coefficients of quadratic relationship between average temperature of ten-day periods and trend ratios of winter barley (from February to June)

Stations	Ten days periods in months														
	February			March			April			May			June		
	1	2	3	1	2	3	1	2	3	1	2	3	1	2	3
Győr	0.39	0.36	0.15	0.15	0.21	0.08	0.12	0.30	0.32	0.25	0.32	0.34	0.48	0.25	0.25
Szombathely	0.34	0.37	0.05	0.18	0.08	0.12	0.13	0.13	0.33	0.36	0.35	0.37	0.32	0.27	0.13
Zalaegerszeg	0.42	0.43	0.15	0.22	0.13	0.23	0.13	0.06	0.37	0.18	0.29	0.21	0.26	0.19	0.13
Kaposvár	0.35	0.34	0.15	0.23	0.17	0.02	0.22	0.18	0.20	0.10	0.03	0.23	0.27	0.07	0.14
Pápa	0.35	0.36	0.01	0.02	0.06	0.14	0.23	0.18	0.28	0.18	0.31	0.45	0.39	0.28	0.21
Tatabánya	0.54	0.51	0.21	0.08	0.07	0.17	0.28	0.15	0.34	0.01	0.26	0.24	0.48	0.06	0.42
Martonvásár	0.35	0.27	0.10	0.14	0.09	0.13	0.22	0.26	0.26	0.19	0.33	0.37	0.35	0.16	0.26
Iregszemcse	0.35	0.31	0.17	0.18	0.17	0.19	0.15	0.37	0.32	0.32	0.07	0.15	0.30	0.15	0.17
Pécs	0.26	0.29	0.23	0.20	0.14	0.16	0.09	0.44	0.27	0.29	0.11	0.12	0.25	0.08	0.19
Kecskemét	0.38	0.41	0.24	0.21	0.15	0.09	0.27	0.42	0.25	0.23	0.23	0.29	0.26	0.15	0.24
Budapest	0.34	0.36	0.18	0.20	0.09	0.18	0.32	0.20	0.39	0.13	0.36	0.42	0.37	0.07	0.26
Szolnok	0.37	0.39	0.13	0.26	0.19	0.07	0.17	0.23	0.28	0.15	0.35	0.40	0.39	0.02	0.22
Szeged	0.36	0.20	0.29	0.30	0.28	0.13	0.26	0.37	0.39	0.30	0.31	0.33	0.39	0.05	0.11
Békéscsaba	0.31	0.24	0.24	0.45	0.12	0.29	0.16	0.30	0.46	0.22	0.26	0.27	0.40	0.06	0.08
Debrecen	0.41	0.37	0.11	0.37	0.07	0.23	0.10	0.31	0.48	0.20	0.29	0.28	0.37	0.05	0.18
Nyíregyháza	0.32	0.49	0.02	0.28	0.29	0.10	0.32	0.26	0.33	0.12	0.32	0.44	0.40	0.26	0.42
Miskolc	0.37	0.29	0.04	0.08	0.22	0.41	0.18	0.13	0.39	0.18	0.09	0.21	0.56	0.12	0.26
Kompolt	0.43	0.38	0.11	0.12	0.07	0.35	0.17	0.16	0.34	0.13	0.16	0.22	0.55	0.05	0.27
Balassagyarm.	0.49	0.47	0.18	0.09	0.16	0.06	0.49	0.24	0.38	0.26	0.15	0.31	0.40	0.15	0.52

Relationship between temperature and trend ratio was studied for all ten-day periods of growing season. *Table 1a* shows correlation coefficients of these relationships for September–January period and *Table 1b* demonstrates *r* values of January–June interval.

Temperature values of the third ten days period of October and the second ten-day period of November are in close correlation with yields as it can be seen in *Table 1a.* This is because of the relatively poor frost-tolerance of winter barley (*Varga-Haszonits et al.*, 2006). In winter, mostly the third ten-day period of December (see *Table 1a*) and the first and second ten-day periods of February (see *Table 1b*) influence barley yield. It suggests that the success of barley production is basically influenced by permanent cold weather without snow-cover. Thus, significant influence of winter temperature values on yield are demonstrated also by investigations based on data of ten-day periods. In spring (and in early summer) mainly the third ten-day period of April, the third ten days period of May and the first ten-day period of June have great influence on productivity.

Selection of the most significant periods was done separately in the case of all stations, that is why these ten-day periods of our model can differ in different places. Data of *Tables 1a* and *1b* make it possible to choose appropriate intervals which can be used in the multiplicative successive model. Selected ten-day periods can be seen in *Table 2*.

Table 2. Ten-day periods chosen by means of sensitivity analysis

Stations	Selected periods			
	Period 1	**Period 2**	**Period 3**	**Period 4**
Győr	Nov 11–Nov 30	Dec 11–Dec 20	Feb 1–Feb 20	Apr 21–Jun 10
Szombathely	Nov 11–Nov 20	Dec 11–Dec 20	Feb 1–Feb 20	Apr 21–Jun 10
Zalaegerszeg	Nov 11–Nov 20	Dec 21–Dec 31	Apr 21–Apr 30	Apr 21–Apr 30
Kaposvár	Nov 11–Nov 20	Dec 11–Dec 31	Jan 1–Feb 20	Jan 1–Feb 20
Pápa	Nov 11–Nov 20	Dec 11–Dec 31	Feb 1–Feb 20	May 11–Jun 10
Tatabánya	Nov 11–Nov 20	Dec 11–Dec 31	Apr 21–Apr 30	Jun 1–Jun 10
Martonvásár	Nov 11–Nov 20	Dec 11–Dec 31	Jan 21–Feb 20	May 11–Jun 10
Iregszemcse	Oct 11–Oct 31	Nov 11–Nov 30	Feb 1–Feb 20	Apr 11–May 31
Pécs	Nov 11–Nov 20	Dec 11–Dec 20	Feb 1–Feb 20	Apr 11–May 10
Kecskemét	Nov 11–Nov 20	Dec 11–Dec 20	Feb 1–Feb 20	Mar 1–Jun 10
Budapest	Nov 11–Nov 20	Dec 1 –Dec 20	Feb 1–Feb 20	Mar 1–Jun 10
Szolnok	Nov 11–Nov 20	Dec 11–Dec 20	Feb 1–Feb 20	Mar 1–Jun 10
Szeged	Nov 11–Nov 20	Dec 11–Dec 20	Feb 1–Feb 20	Apr 1–Jun 10
Békéscsaba	Nov 11–Nov 20	Dec 11–Dec 20	Feb 1–Feb 20	Mar 1–Jun 10
Debrecen	Nov 11–Nov 20	Dec 11–Dec 20	Feb 1–Feb 20	Mar 1–Jun 10
Nyíregyháza	Nov 11–Nov 20	Dec 11–Dec 20	Feb 1–Feb 20	Mar 1–Jun 10
Miskolc	Nov 11–Nov 20	Dec 11–Dec 20	Feb 1–Feb 20	Mar 1–Jun 10
Kompolt	Oct 21–Feb 20	Apr 21–Apr 30	Jun 1–Jun 10	Jun 1–Jun 10
Balassagyarmat	Dec 21–Dec 31	Feb 1 –Feb 20	Apr 21–Apr 30	Jun 1–Jun 10

Calculations displayed in Section 2 can be done on the base of temperature data of those intervals. *Table 3* contains our results.

Table 3. Correlation coefficients of estimating functions for selected periods

Station	Trend	Correlation coefficients of estimating function			
		Period 1	Period 2	Period 3	Period 4
	$f(t)$	$f(t)\cdot f_1(m_1)$	$f(t)f_1(m_1)f_2(m_2)$	$f(t)f_1(m_1)$ $f_2(m_2)f_3(m_3)$	$f(t)f_1(m_1)$ $f_2(m_2)f_3(m_3)f_4(m_4)$
Győr	0.9139	0.9319	0.9325	0.9405	0.9514
Szombathely	0.8627	0.8889	0.8903	0.9146	0.9275
Zalaegerszeg	0.9042	0.9241	0.9276	0.9252	0.9252
Kaposvár	0.9187	0.9460	0.9479	0.9588	0.9588
Pápa	0.9173	0.9451	0.9466	0.9504	0.9706
Tatabánya	0.8575	0.8955	0.8933	0.8922	0.9092
Martonvásár	0.8958	0.9288	0.9295	0.9429	0.9568
Iregszemcse	0.9207	0.9225	0.9499	0.9580	0.9630
Pécs	0.9054	0.9378	0.9381	0.9468	0.9524
Kecskemét	0.8139	0.8807	0.8921	0.8972	0.9233
Budapest	0.8545	0.8826	0.8859	0.8865	0.9014
Szolnok	0.8961	0.9290	0.9457	0.9523	0.9538
Szeged	0.8313	0.8511	0.8852	0.8932	0.9117
Békéscsaba	0.9162	0.9201	0.9409	0.9480	0.9519
Debrecen	0.8424	0.8647	0.9099	0.9314	0.9300
Nyíregyháza	0.8138	0.8315	0.8847	0.9282	0.9281
Miskolc	0.8430	0.8437	0.8809	0.9011	0.9197
Kompolt	0.8559	0.8939	0.8947	0.9075	0.9076
Balassagyarmat	0.8641	0.8873	0.9138	0.9125	0.9304

As it can be seen in *Table 3*, we have got better and better estimating functions by the aim of multiplicative successive approximation, and correlation coefficients came closer to the value of 1. According to our results it can be stated that if ten-day periods with no significant impact are used then the accuracy of estimation will essentially diminish.

The check-up of method was done by comparison of calculated and measured values. According to our results coefficient of determination (r^2 values) were higher than 0.9 at all stations. It means that correlation coefficients (r values) were close to 1. *Fig. 3* shows such a relationship.

The accuracy of estimation was checked by error of estimation – that is the difference between calculated and measured value – and then by studying the frequency of these errors. Results are indicated in *Table 4*.

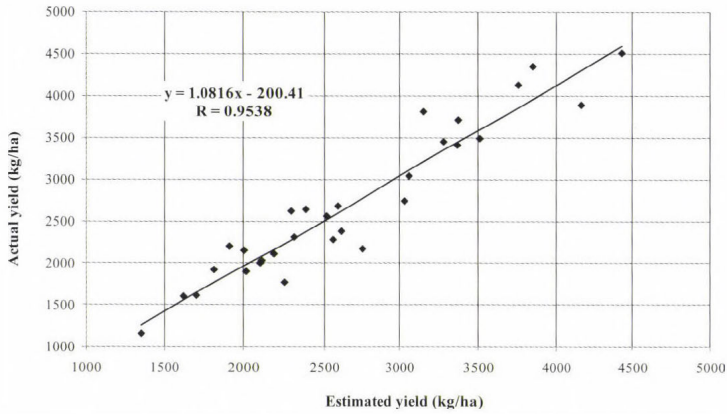

Fig. 3. Comparison of calculated and measured yield (kg/ha) values.

Table 4. Cumulative frequency of the difference between measured and calculated values

Stations	Error of estimation (%) under					
	5%	10%	15%	20%	25%	30%
Győr	47	77	87	93	93	97
Szombathely	33	77	80	90	97	97
Zalaegerszeg	27	73	83	90	97	100
Kaposvár	43	73	80	97	97	100
Pápa	37	77	97	97	97	100
Tatabánya	40	73	80	93	93	93
Martonvásár	37	77	90	93	97	100
Iregszemcse	37	73	83	93	100	100
Pécs	33	70	83	90	97	100
Kecskemét	60	70	83	90	93	93
Budapest	27	70	77	90	93	97
Szolnok	37	70	87	93	93	100
Szeged	37	70	87	87	97	97
Békéscsaba	27	73	87	90	90	100
Debrecen	20	70	90	93	97	97
Nyíregyháza	43	73	83	100	100	100
Miskolc	40	70	80	87	90	93
Kompolt	30	70	80	87	93	97
Balassagyarmat	33	77	83	87	93	97

The error of estimation was expressed in % of actual yield. As it can be seen in *Table 4*, our model gives acceptable results for yield estimation. When we used this method, the error of estimation was less than 5% in 30–40% of all cases and it was less than 10% in 70–80% of all cases. It means that inaccuracy of estimation remained under 10% in two third of all studied cases.

4. Conclusions

Our results suggest that multiplicative successive model is suitable for estimating yields of winter barley which grows in the cool and wet part of the year in Hungary. Considering the fact that yield of cultivated plants is mainly influenced by meteorological conditions, water supply, nutrient supply and plant protection, yields can be accurately estimated if impact of agrotechnical factors (variety, nutrient supply, plant protection) is defined numerically by means of a trend function, and impact of meteorological factors is calculated as the fluctuation around trend values. This model becomes more simply if we suppose that water supply is favorable during the growing season of winter barley. Unfavorably dry spells usually occur only from July in Hungary.

Our model demonstrates how successive periods of growing season influence the yield. In this way, this method takes impact of successive periods into account, and it is a step from statistical models to dynamic models. Our results demonstrated that autumn frosts and permanent cold winter weather without snow-cover have great influence on productivity of winter barley.

This model is a better tool for studying the effects of climatic variability or a possible climate change, than a simple statistical model. The multiplicative successive model is a useful tool to estimate the effect of the possible climate change on the yield of winter barley and to feternime the past of the growing season in which the changes would occur.

References

Abbaspour, K.C, Hall, J.W. and *Moon, D.E.*, 1992: A yield model for use in determining crop insurance premiums. *Agr. Forest Meteorol. 60*, 33-51.

Andresen, J.A., Alagarswamy, G., Rotz, C.A., Ritchie, J.T. and *LeBaron, A.W.*, 2001: Weather impacts on maize, soybean, and alfalfa production in the Great Lakes Region, 1895–1996. *Agron. J. 93*, 1059-1070.

Fageria, N.K., 1992: *Maximizing Crop Yields*. Marcel Dekker, New York.

Fuqin, L. and *Tian, G.* 1991: *Research on Remote Sensing – Meteorological Model for Wheat Yield Estimation*. 12th Asian Conference on Remote Sensing. Asian Association of Remote Sensing (AARS), Oct. 30 - Nov. 5, 1991, Singapore. (http://www.aars.org/acrs/proceeding/ACRS1991/Papers/AGV91-4.htm)

Hoogenboom, G., 2000: Contribution of agrometeorology to the simulation of crop production and its applications. *Agr. Forest Meteorol. 103*, 137-157.

Mavi, H.S. and *Tupper, G.J.*, 2004: *Agrometeorology. Principles and Applications of Climate Studies in Agriculture*. Food Product Press, New York.

Panofsky, H.A. and *Brier, G.W.*, 1963: *Some Applications of Statistics to Meteorology*. The Pennsylvania State University, Pennsylvania.

Penning de Vries, F.W.T., 1962: System analysis and models of crop growth. In *Simulation of plant growth and crop production* (eds.: *F.W.T. Penning de Vries* and *H.H. van Laar*). Simulation Monographs, Pudoc, Wageningen, 99-19.

Porter, J.R. and *Semenov, M.A.*, 2005: Crop responses to climatic variation. *Philos. Trans. R. Soc. Lond. B Biol. Sci. 360*(1463), 2021-2035.

Ritchie, J.T. and *Alagarswamy, G.*, 2002: Overview of crop models for assessment of crop production. In *Effect of Climate Change and Variability on Agricultural Production System* (eds.: *O.C. Doering, III, J.C. Randolph, J. Southworth, R.A. Pfeifer*). Kluwer Academic Publishers, Boston, 43-68.

Szabó, T. and *Tóth, R.*, 1989: Determination of significant periods influencing the productivity on the basis of meteorological factors (in Hungarian). *Növénytermelés 38*, 55-67.

Szakály, J., 1968: Meteorological conditions of early development of rye and winter barley and temperature sums of developmental periods (in Hungarian). *Beszámolók az 1966-ban végzett tudományos kutatásokról. 31*, Országos Meteorológiai Szolgálat, Budapest, 152-162.

Szalóki, S., 1989: Water Demand, Water Use and Irrigation Water Need of Crops (in Hungarian). In: *Manual of irrigation* (ed.: *Szalai, Gy.*). Mezőgazdasági Kiadó, Budapest, 100-154.

Szalóki, S., 1991: Water and irrigation demand of plants (in Hungarian) (eds.: *Lelkes, J.* and *Ligetvári, F.*). Fólium Könyvkiadó Kft., Budapest, 21-42.

Thompson, L.M., 1962: Evaluation of weather factors in the production of wheat. *J. Soil Water Conservation 17*, 218-230.

Thompson, L.M., 1969: Weather and technology in the production of wheat in the United States. *J. Soil Water Conservation 24*, 219-224.

Thompson, L.M., 1975: Weather variability, climatic change, and grain production. *Science 188*, 535-541.

Thompson, L.M., 1986: Climatic change, weather variability, and corn production. *Agron. J. 78*, 649-653.

Varga-Haszonits, Z., 1986: Principal-methodical basis of multiplicative crop-weather models (in Hungarian). *Beszámolók az 1983-ban végzett tudományos kutatásokról*. Országos Meteorológiai Szolgálat, Budapest, 155-164.

Varga-Haszonits, Z., 1987: Relationship between winter wheat yield and weather determined by multiplicative model using successive approximation (in Hungarian). *Beszámolók az 1985-ben végzett tudományos kutatásokról*. Országos Meteorológiai Szolgálat, Budapest, 184-196.

Varga-Haszonits, Z., 1992: *Complex Agroclimatological Model for Characterizing the Productivity of Winter Wheat* (in Hungarian). PhD Thesis,Hungarian Academy of Sciences, Budapest.

Varga-Haszonits, Z., Varga, Z., Lantos, Zs., Vámos, O. and *Schmidt, R.*, 2000: *Agroclimatological Analysis of Climatic Resources in Hungary* (in Hungarian). LÓRIPRINT, Mosonmagyaróvár.

Varga-Haszonits, Z., Varga, Z., Lantos, Zs. and *Enzsölné Gerencsér, E.* 2006: *Climatic Variability and Ecosystems* (in Hungarian). Monocopy, Mosonmagyaróvár.

IDŐJÁRÁS

Quarterly Journal of the Hungarian Meteorological Service
Vol. 115, No. 3, July–September 2011, pp. 179–204

Air quality around motorway tunnels in complex terrain – computational fluid dynamics modeling and comparison to wind tunnel data

Márton Balczó[1*], Miklós Balogh[1], István Goricsán[1], Torsten Nagel[2], Jenő M. Suda[1], and Tamás Lajos[1]

[1]*Theodore von Kármán Wind Tunnel Laboratory, Department of Fluid Mechanics, Budapest University of Technology and Economics (BME), Bertalan L. u. 4-6, H-1111 Budapest, Hungary*
E-mails: balczo@ara.bme.hu; baloghm@ara.bme.hu; goricsan@ara.bme.hu; suda@ara.bme.hu; lajos@ara.bme.hu

[2]*Lohmeyer Consulting Engineers*
An der Roßweid 3,76229, Karlsruhe, Germany
E-mail: t.nagel@lohmeyer.de

[*]*Corresponding author*

(Manuscript received in final form September 21, 2010)

Abstract—The current paper describes numerical simulations of flow and dispersion performed in a complex suburban area of Budapest using the microscale model MISKAM and accompanying wind tunnel tests which provided reference concentration data for validation of the model results. Main pollutant sources are traffic related and include a planned motorway section of 9 km length consisting of sections running in tunnel, on ground, and on viaduct. Four different route alternatives were investigated. In the paper, first a condensed review is given about problems related to air quality around motorway tunnels in complex terrain. The effect of larger scales on microscale air quality was determined using background concentrations from monitoring station time series with removal of short-term fluctuations, for which a simple method is introduced here. The validation wind tunnel tests were carried out at several wind directions on a 1:1000 scale model containing topography, buildings, and vegetation with measurement of tracer concentrations in 50 sampling locations. In the microscale CFD simulation, flow and dispersion considering topography, vegetation, and buildings were calculated three-dimensional in a large domain using k–ε model, and advective diffusion equation was set up on a Cartesian grid treating air pollutants as non-reactive scalars. Results give more detailed information about the flow, for example local speedup above hills, slowdown in vegetation zones, separation regions are resolved well. Deviation of pollutant plume paths from the mean wind direction caused by the topography could be also observed. NO_x concentration maps showed that air quality limit exceedances occur near motorway tunnel portals in form of large surface plumes, which can only be avoided by the application of

tunnel ventilation stacks. These will exhaust polluted tunnel air in larger heights. The comparison of numerical results to the wind tunnel reference data was performed using statistic metrics (fractional bias, normal mean square error, geometric mean bias, geometric variance, correlation coefficient) showing a generally good agreement.

Key-words: air quality, complex terrain, tunnel portal, CFD simulation, background concentration, model validation, wind tunnel measurement

1. Introduction

The prediction of air quality in urban or suburban areas often requires sophisticated tools when the surrounding terrain is complex. The major pollutant sources are mostly traffic related, emitting pollutants along main road or motorway routes. Buildings and vegetation have also strong influence on the dispersion process. Additional problems can emerge due to the concentrated exhaust of polluted air from roadway tunnel portals. A short literature overview of these topics will be given in the following subsections, followed by a short description of the investigated area in the north of Budapest, which includes, besides existing main roads, a 9 km long planned motorway section with longer tunnels. Section 2 discusses the proper input data collected for the microscale numerical simulations and wind tunnel tests, which are then described in detail in Section 3. In Section 4, we give an overview of the CFD results and compare them to the wind tunnel data. Additionally, we also summarize the proposed arrangements for reducing air pollution from the tunnel portals.

1.1. Flow over complex terrain

Complex terrain can produce a variety of flow patterns, mainly depending on the topography, vegetation cover, and the thermal stratification (Froude number), as described in standard texts, for example in *Plate* (1982) and *Kaimal* and *Finnigan* (1994). Basic mechanisms are discussed by *Belcher* and *Hunt* (1998), and an overview of research in the last 50 years is given by *Wood* (2000).

To validate the modeling tools for complex terrain flows, numerous studies were performed. Beyond isolated and simplified 2D or 3D slopes and hills measured in wind tunnels (e.g., *Ayotte* and *Hughes*, 2004), the Askervein hill project (*Taylor* and *Teunissen*, 1987; *Walmsley* and *Taylor*, 1996) has gained specific importance, with an on-site measurement campaign being performed in 1982–1983, which served as reference data for dozens of wind tunnel and numerical studies. The wind tunnel method gave good agreement with the measurement reference data (see e.g., particle image velocimetry (PIV) measurements of *Rodrigues*, 2005). *Bowen* (2003) discusses aspects of physical modeling like model scale and roughness in detail. In CFD modeling, besides the Reynolds-averaged Navier-Stokes (RANS) approach using mostly k–ε turbulence closure (*Kim* and *Patel,* 2000; *Castro et al.*, 2003), in the last decade

even more large-eddy simulation (LES) was used to model the Askervein hill flow (e.g., *Silva Lopes et al.*, 2007).

The application focus of the practical studies in this field is on wind turbine siting, heavy gas dispersion, and the determination of airport wind conditions. Several authors reported wind tunnel tests of real-world, very complex terrain. *Cermak* (1984) performed tests for different stratifications. Further studies to mention are those of *Snyder* (1990), *Liu et al.* (2001), and *McBride et al.* (2001). Numerical application examples using a RANS k–ε model and comparison with on-site measurements are shown for example in *Brodeur* and *Masson* (2006) and *Palma et al.* (2008).

1.2. Tunnel related air quality problems

In roadway tunnels, a large amount of traffic pollution can be accumulated, which is removed by the pressure difference, the piston effect of moving vehicles, and the tunnel ventilation system mostly through the tunnel portal. The tunnel ventilation system for one directional tunnel of medium length consists of axial fans mounted in the tunnel pipe, which drive air into the driving direction and exhaust polluted air at the forward tunnel exit. An overview of tunnel related air quality problems is given by *Longley* and *Kelly* (2008) and *Bettelini et al.* (2001), the latter is also showing modeling results near a tunnel portal with a Gaussian model and CFD. *Oettl et al.* (2003) compared results from two specific portal dispersion models with on-site measurements.

Wind tunnel measurements of a tunnel portal with moving vehicles were reported by *Nadel et al.* (1994) and *Plate* (1999). They observed high concentrations near the portal and recognized the influence of traffic induced turbulence. *Contini et al.* (2003) measured flow and dispersion near tunnel portals behind a 2D hill. Tunnel emissions were released from a point source in the middle of the tunnel.

Tunnel ventilation systems are designed according to national standards like those of Switzerland (*ASTRA*, 2004). To avoid large concentrations outside the portals of longer tunnels, it is often necessary to install separate ventilation stacks which direct polluted air from the tunnel into larger heights or filter facilities which remove a part of pollutants.

1.3. Site description

The area of investigation covers about 8 km × 5 km. The topography has moderate slopes similar to Askervein hill, with height differences of about 200–300 m (*Fig. 1*). In the south-eastern part of the domain, outskirts of Budapest are located with 10–15 storey block buildings and a population of about 70,000. On the northern and western side, four suburban towns can be found in the complex terrain of Buda Mountains with 20,000 inhabitants. Deciduous forests cover a smaller part of the not habited areas, mainly hilltops.

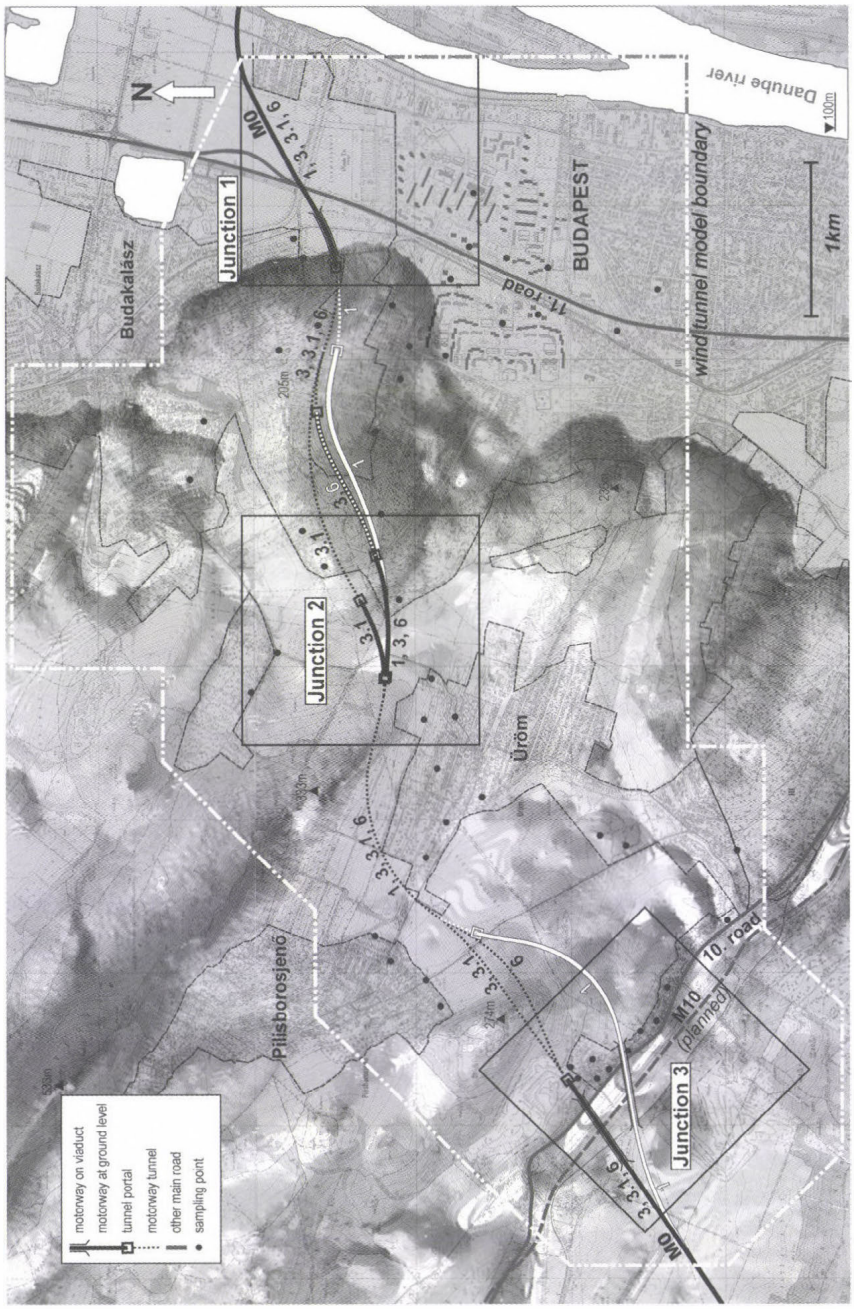

Fig. 1. The investigated domain with existing main roads and planned route alternatives 1, 3, 3.1, and 6 of the M0 motorway. Route colors are black or white. Please note that the routes are partly overlapping. Circular black dots: wind tunnel sampling points (50); thin continuous black rectangles: close investigation areas of numerical simulation in the 3 junctions; thin dashed line: inhabited areas.

Major pollutant sources are traffic sources, existing main roads (national roads No. 10 and No. 11) and most importantly, a planned section of the ring motorway M0 of Budapest, consisting of three traffic junctions. Four route alternatives have been investigated: 1, 3, 3.1, and 6, all of them include several bridges and tunnels.

The planned ring motorway section connects national road No. 10 and planned motorway M10 in the northwest of Budapest with national road No. 11 in the north of Budapest. Route 1 (marked white in *Fig. 1*) is the most southern from the alternatives, and has shorter tunnels. Route 3.1 and 6 differ from route 3 only in the middle and eastern part: route 6 runs in Junction 2 longer eastwards on surface and has a shorter eastern tunnel. Route 3.1's surface section and eastern tunnel's portal in Junction 2 are shifted to the north. On the far eastern side, in Junction 1 near the national road No. 11, all routes are identical. In Junction 1 and 3, the routes cross the valleys on viaducts. In Junction 2, the routes run in deep cutting.

Rush-hour traffic on the new section is expected to reach about 2,800 vehicle h^{-1} in the year 2018 with further growth to 4,400 vehicle h^{-1} until 2023. The planned one-directional tunnels are up to 3.2 km long, and their original design included longitudinal ventilation using axial fans without separate ventilation stacks (see later in *Fig. 10*). As a consequence, all pollutants produced in the tunnel are supposed to leave the tunnel through the forward portal.

Due to the closeness to inhabited areas, air quality and noise impacts of the new motorway were of most concern. The availability of high-resolution pollutant concentration maps of the area is thus crucial for the decision makers to help them find the best route alternative, and also for the public[1] to accept the selected route.

2. Input data

Unlike the investigations, focusing on the dispersion phenomenon itself, at the end of environmental impact assessment studies like this, exact concentrations should be calculated as a decision basis for the authorities. Any errors in input data like background concentrations, wind statistics, or car emissions will also be reflected in the results. Thus, one has to pay specific attention to the collection of high-quality input data.

2.1. Background concentrations

Pollutant dispersion is a multi-scale process in both space and time. Besides the possibility of a full coupling of different scale models (nesting), a demanding task for modelers, the usual approach is to consider the effect of larger scales in the microscale dispersion model as a background concentration. The background

[1] Short reports prepared for the public about this project can be found at www.karman-wtl.com (in Hungarian).

concentration might be significantly different in urban and rural areas, and can be determined in several ways: (a) by taking the output of a mesoscale / urban scale model or (b) using measurement data from urban background stations.

In *Mensink et al.* (2008), coupling of the Gaussian mesoscale dispersion model IFDM and the street canyon scale model OSPM was realized. Example of the second method can be seen in *Berkowicz* (2000), a simple urban background model developed for Copenhagen, using the urban emission inventory, rural background measurement data, and wind statistics.

When applying the second method, one has to consider the fact that urban background stations are also subject to short-term variations due to local pollution sources. Their effect should hence be removed to obtain clean background values. *Cremades* (2000) demonstrated two methods for this in a hypothetical case, while *Jones et al.* (2008) removed the effect of nearby traffic sources by comparing weekend and weekday concentrations at an urban monitoring station in London and determined the urban background values and urban non-traffic increments of PM_{10} . *Tchepel* and *Borrego* (2010) analyzed spectra of air quality monitoring data using spectral methods and found that short-term fluctuations correlate with daily variations in traffic and wind speed. Long-term variance over a 21-day period caused by long-range pollutant transport was also observed. In *Tchepel et al.* (2010), after spectral analysis of the concentration time series, short-term components above a frequency threshold were flattened using the Kolmogorov-Zurbenko filter.

In the present case, data from two background stations in Budapest were analyzed for the years 2007–2008. Pesthidegkút station is located in a suburban area, and thus, it is characteristic for Junction 2 and 3, while Gilice tér station is in an outer district of the city, which can provide background data for the semi-urban environment of Junction 1 (*Fig. 1*). Both stations are influenced by local sources with daily peaks in the morning and afternoon rush-hours (*Fig. 2*), especially for NO_x, which indicates a relatively close traffic release.

This local influence was removed by separating the baseline and short-term parts of the time series using Fourier transformation.

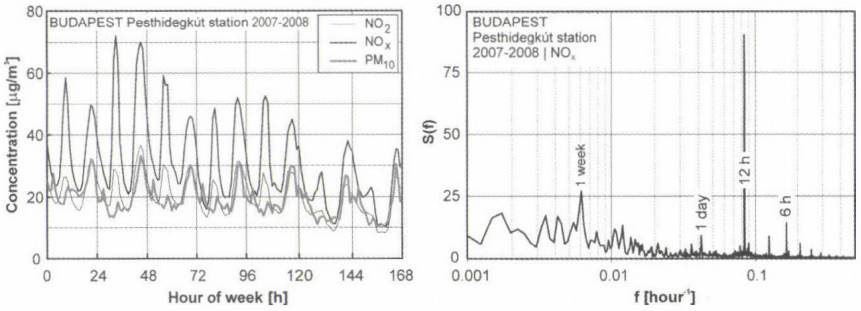

Fig. 2. Left: Average weekly concentrations at Pesthidegkút station in Budapest; right: spectrum of NO_x concentrations with a strong 12 h peak.

Because local traffic influence is reflected in the strong 12 h and 6 h components of the FFT spectrum (*Fig. 2*), the separation frequency was chosen as 0.056 h^{-1}, corresponding to the period of 18 h. After the separation, the average absolute value of the short-term signal was subtracted from the mean value of the original time series to obtain the annual mean background concentration without the contribution of local sources (*Table 1*).

Table 1. Background concentrations [μg m^{-3}]

	Annual mean		Fluctuations removed	
	NO_x	PM_{10}	NO_x	PM_{10}
Budapest, Pesthidegkút[a]	31.5	19.2	15.8	13.2
Budapest, Gilice tér[b]	39.6	31.2	20.0	20.4

[a] Suburban background station, 47.5617°N, 18.9608°E, Junction 2 and 3

[b] Urban background station, 47.4298°N, 19.1812°E, Junction 1

2.2. Emissions

Car emissions can be determined from traffic density and the emission factors of different vehicle categories. These are again dependent from fleet composition, traffic situation, slope, and so on. In this project, fleet-average emission factors for the reference year 2006 and realization year 2018 had to be determined. The Handbook of Emission Factors – HBEFA 2.1 (*Infras*, 2004) is the emission factor database of several mid-European countries (D, A, CH, NL) based on emission factors determined for individual vehicle groups, the so-called vehicle subsegments. Vehicles of the same class, engine power, and emission category have obviously similar emission factors, which were determined by dynamometer measurements. These may vary depending on traffic situation, speed, slope, road quality, and temperature. The accumulated emission factor valid on a specific road section (urban, rural, motorway etc.) is then an average of subsegment factors weighted by the actual traffic composition, which is also included in the database. The method was validated in several studies, e.g., through emission measurements in the Gubrist tunnel by *Colberg et al.* (2005).

To apply the method in Hungary, the national vehicle database of the years 2001–2006 was analyzed, and the fleet was divided into vehicle subsegments defined in the HBEFA database. As a rough estimate, a four-year delay compared to the vehicle fleet in Germany was demonstrated for passenger cars and light duty vehicles[2].

[2] In the meantime, the new HBEFA version 3.1 was released, supporting also vehicle fleets of Norway and Sweden. Further validation of emission factors and the new emission models applied lead in the upgrade to higher NO_x and PM emission factors for passenger cars and lower ones for light and heavy-duty vehicles. These changes might increase the accuracy of the concentration predictions, however, it could not anymore considered in this paper.

The fleet-averaged emission factors for the M0 motorway with 80 km/h speed limit and ±2% slope are shown in *Table 2*. The general improvement of factors over the years is due to the replacement of older vehicles with vehicles that comply with the EURO4 and newer standards. Also, non-exhaust PM_{10} emissions from abrasion and resuspension were considered, based on an on-site measurement campaign along a motorway (*Ketzel et al.*, 2007).

Table 2. Accumulated exhaust and non-exhaust emission factors [g km^{-1} veh^{-1}] for different vehicle categories calculated from the subsegment emission factors of the HBEFA 2.1 database and Hungarian fleet composition data. Traffic situation: motorway with 80 km/h speed limit and ±2 % slope

Emission factor	**NO_x**		**PM_{10}**[a]		**$PM_{10,\ n\text{-}e}$**[b]
Year	**2006**	**2018**	**2006**	**2018**	**All years**
Passenger car	0.60	0.17	0.008	0.007	0.022
Light duty vehicle	1.17	0.54	0.193	0.034	0.022
Coach	7.86	3.66	0.494	0.052	0.200
Heavy duty vehicle	5.04	2.81	0.120	0.037	0.200

[a] exhaust factors

[b] non-exhaust factors (*Ketzel et al.*, 2007)

2.3. Wind statistics

Long-term wind statistics were only available at a station of the Hungarian Meteorological Service (HMS) about 5 km from the site in a flat area. To determine local wind statistics, which may be different from the flat terrain measurements and could show systematic mesoscale changes due to the Buda Mountains, the mesoscale diagnostic wind field model DIWIMO[3] was run on a 30 km × 16.3 km domain shown in *Fig. 3*. Elevation in this domain varies between 87 and 562 m above sea level.

The model generates a mass-consistent wind field based on the measured wind statistics in one point of the domain considering the topography, stratification, varying surface roughness, and surface coverage of the area. The model's parameterizations are described in detail by *Moussiopoulos et al.* (1988).

The model uses a terrain-following mesh, in the current simulation with a horizontal grid resolution of 100 m, while in vertical direction the domain of 800 m height was divided into 26 layers of varying thickness. The lowermost layer's thickness changed between 7 and 19 m due to the stretching of the vertical grid to the terrain.

[3] Further description can be found at www.stadtklima.de/EN/E_1tools.htm#DIWIMO and on the webpage of Lohmeyer Consulting Engineers: www.lohmeyer.de/modelle/diwimo.htm (in German).

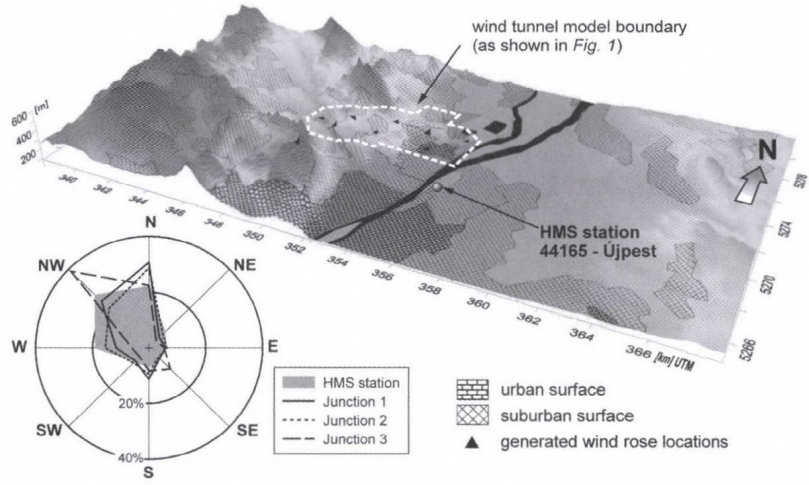

Fig. 3. Top: Domain of DIWIMO simulation with land usage patterns and generated wind rose locations. Elevation is scaled by 5. Bottom left: original wind statistics of the HMS station simplified for eight main wind directions (grey plot); mean wind roses, averaged from all calculated wind roses in the specific junction.

The model was run with 36 wind directions, and wind statistics were generated at 9 locations in the closer investigation area (3 in each traffic junction) using the known wind statistics at the location of the HMS station. These were averaged in each of the three junctions and simplified for the 8 main wind directions. The averaged wind roses can be seen as representative for the individual junctions, and can also be used as inlet boundary condition for the microscale investigation of the junctions.

In Junction 1 and 2, the wind roses show higher mean wind speed and distortions due to topographic effects towards the north (*Fig. 3*, bottom left). At Junction 3, influence of a NW–SE oriented valley can be clearly recognized. Based on the wind statistics, 5–7 important incident wind directions were selected at each junction for further microscale investigation, covering about 80% of the wind conditions in a year.

3. Microscale investigation methods

3.1. MISKAM flow and dispersion simulations

In the last decade, dozens of different CFD models were developed and applied for the investigation of microscale air pollution problems, where the effect of a singular or a group of obstacles is not negligible, and thus, the solution of the full equations of motion is necessary. On behalf of the numerous publications in this topic, most of them are concentrating on built urban areas, more specifically

street canyons, only the reviews of *Vardoulakis et al.* (2003) and *Holmes* and *Morawska* (2006) may be cited here. Besides the models utilizing the RANS (Reynolds-averaged Navier-Stokes) approach with k–ε type turbulence closures, large-eddy simulation is applied with promising results (e.g., *Xie* and *Castro*, 2009), however, on the price of a very high computational demand (needing multi-processor computer clusters), which is in most cases not accessible for environmental agencies and consulting engineers.

The code used in the current investigation, MISKAM gained currency in environmental assessment practice due to the relatively simple model setup and the fast code able to run on a single processor PC. The model solves the RANS equation using a k–ε turbulence closure on a Cartesian grid. Buildings are represented as blockouts from the grid. Dispersion of an inert pollutant is calculated afterwards by the advection-diffusion equation using the wind field simulation results. Vegetation effects can be accounted for by additional terms in the flow and turbulence equations. Details of the MISKAM model are given in *Table 3* or in more depth in *Eichhorn* (2008).

Extensive model evaluation activities were undertaken according to *VDI* (2005) by *Eichhorn* and *Kniffka* (2010) and in the framework of COST Action 732[4] (*Goricsán et al.*, 2011) using the MUST data set. The implemented vegetation model (*Ries* and *Eichhorn*, 2001), which introduced additional terms in the motion and turbulence equations, was validated in *Balczó et al.* (2009) using the CODASC[5] wind tunnel data set.

Besides these, the model has been used in several validation and comparison studies. *Ketzel et al.* (2000) compared MISKAM data to on-site measurements, as it was also done in the Podbi-exercise (*Lohmeyer et al.*, 2002). Comparison of MISKAM simulation data to urban wind tunnel measurements can be found in *Ketzel et al.* (2002), *Sahm et al.* (2002), *Goricsán et al.* (2004), and for a simple stack-building configuration in *Olesen et al.* (2009). Several authors used MISKAM results as input for other transport and chemistry models (*Stern* and *Yamartino*, 2001; *Dixon* and *Tomlin*, 2007), or for emergency response tools (*Donnelly et al.*, 2009).

Although MISKAM is able to model the effect of stable stratification on dispersion by decreasing turbulence production in the equations of k and ε, and in general, CFD modeling of stratification and thermal induced flows is possible (see, e.g., the adaptation of CFD solvers for stratified flows in *Kristóf et al.*, 2009), in this case we limited the influence of thermal stratification to neutral conditions to preserve the compatibility of CFD results with the wind tunnel measurements.

---

[4] COST Action 732: Quality Assurance and Improvement of Micro-Scale Meteorological Models, www.mi.uni-hamburg.de/Home.484.0.html

[5] CODASC data base, (COncentration DAta for Street Canyons), Laboratory of Building and Environmental Aerodynamics, IfH Karlsruhe Institute of Technology, www.codasc.de

Table 3. Description of the MISKAM model

Model equations	
Model version	MISKAM 5.01
Flow model	Reynolds-averaged Navier-Stokes equation with turbulence closure
Turbulence model	Modified version of Kato-Launder k–ε (*Kato* and *Launder*, 1993; *López*, 2002)
Model constants	$C_\mu = 0.09$, $C_{\varepsilon 1} = 1.44$, $\sigma_\kappa = 1$, $\sigma_\varepsilon = 1.3$, $\kappa_\mu = 0.4$
Wall treatment	Logarithmic wall function
Vegetation treatment	Porosity-based model
Dispersion model	Reynolds-averaged advective diffusion equation
Turbulent Schmidt number	0.74
Numerical schemes	
Order in time	1st order explicit
Advection terms	
– momentum equation	Upstream
– dispersion equation	MPDATA scheme (*Smolarkiewicz* and *Grabowski*, 1989)
Diffusive terms	ADI (Alternating Direction Implicit) method
Computational grid	
Grid type	Arakawa-C non-equidistant Cartesian grid (staggered grid), with buildings and topography blocked out from the grid
Variable definition	u, v, w defined at the centre of the corresponding face of the cell, scalar quantities defined at the centre of the cell
Boundary conditions	
Flow variables	
Inlet velocity profile	Logarithmic profile with roughness length z_0 fitted to reference height H_{ref} and velocity u_{ref}
Inlet turbulence profile	Generated from the assumption of equilibrium boundary layer
Ground \& building surfaces	No-slip (with wall function)
Top boundary	Constant values of u, v, w, k, ε taken from the top of the inlet profile
Lateral boundaries	No-flux
Outflow boundary	No-flux with pressure correction to ensure overall mass conservation
Dispersion variables	
Inflow boundary	$c = 0$
Lateral and outflow boundaries	No-flux
Source cells	Volume source strength Q with optional vertical momentum w prescribed
Vegetation cells	Leaf drag coefficient $c_D = 0.2$ and LAD (leaf area density) prescribed

The computational domains and grids were created following the Best Practice Guideline of *Franke et al.* (2007) using an in-house preprocessor. In each junction, close investigation areas of 1.5 km × 1.5 km were defined (see black rectangles in *Fig. 1*), for which grids of uniform horizontal resolution were generated. Inflow and outflow zones of sufficient length were attached to these to prepare correct inflow conditions in the investigated area (*Fig. 4*).

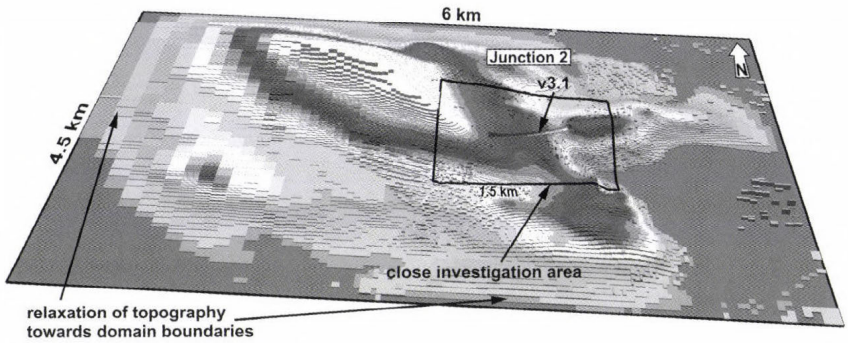

Fig. 4. View of the MISKAM model domain of Junction 2 showing the non-uniform grid with the highest grid resolution around the two tunnel portals and the relaxation of topography at the boundaries.

The domain height was 2 km to ensure a low blockage ratio of 3%. Terrain height sunk to zero at the boundaries. The cell number of each grid was above 5 million. The simulation time on a 3 GHz Intel Core2 computer was about one week for a case. Further details of the simulations are given in *Table 4.*

Table 4. Grid and simulation details. In each junction, simulations were run for every wind direction and every source, resulting in a high number of simulations

	Unit	Junction 1	Junction 2	Junction 3
No. of grid cells	–	246 × 255	206 × 321	252 × 273
– vertical direction	–	97	77	97
Highest resolution	m	5 × 7.5		
– vertical direction	m	1.5		
Max. cell growth ratio	–	1.2		
Cell number	million	5.526	5.244	5.225
Wind directions investigated	–	N, SE, S, WSW, W, WNW, NW	N, NE, S, W, NW	N, SE, S, W, NW
Leaf area density	$m^2\ m^{-3}$	0.5 (in forest areas)		
Vent. stack vertical velocity	$m\ s^{-1}$	6		
No. of dispersion simulations	–	107	92	52

3.2. Source treatment and simulations on a simplified tunnel model

Traffic pollutants released in a one-directional motorway tunnel are exhausted usually through the forward tunnel portal in a low-speed jet. In the MISKAM simulations, as it is not allowed for the user to prescribe horizontal momentum, this jet was replaced by a point source without momentum located in a certain

distance in front of the tunnel portal. To justify the above simplification, several numerical simulations were performed using the more flexible FLUENT code. The FLUENT 6.3 simulations used a simple tunnel portal geometry shown in *Fig. 5* on the left.

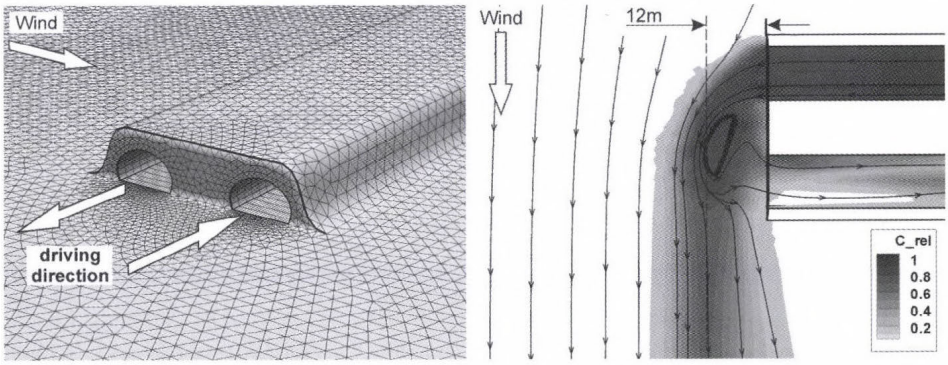

Fig. 5. Left: simplified tunnel geometry and grid for the preliminary investigation of flow around the portals using FLUENT with tunnel cross-section of 12 m × 6.5 m, portal height 10 m, tunnel axis distance 24 m. Right: simulation results in a horizontal cross-section at 3 m height with streamtraces and relative concentration contours. Tunnel outflow velocity is 3 m s^{-1}. Note the plume displacement of 12 m as well as the unfavorable suction of polluted air into the other tunnel.

First, the flow conditions inside a one-directional tunnel were investigated. Vehicle traffic moving with 80 km h^{-1} was substituted in the simulation by momentum sources determined from drag coefficient c_D, vehicle cross-section A_{veh}, and the traffic density. The piston effect of a single vehicle can be expressed according the Swiss standard (*ASTRA*, 2004) by the pressure difference caused by it:

$$0.5\rho(u_{veh}-u_{air})^2 c_D A_{veh} A_{tunnel}^{-1}. \quad (1)$$

In the FLUENT simulation utilizing this assumption, at maximal traffic density and without the use of a longitudinal tunnel ventilation system, an average tunnel air velocity u_{air} of 1.8 m s^{-1} was developed.

Following this simulation, the tunnel portal model was placed in an atmospheric boundary layer flow to observe the pollutant plume's displacement at several wind directions. The simulations utilized the RANS approach with standard k–ε turbulence closure on a mesh consisting of 800,000 tetrahedral and polyhedral cells. External flow velocity was 3 m s^{-1} at 100 m height, tunnel air velocity was also 3 m s^{-1}. Simulation at cross-flow wind showed a plume displacement of about 12 m from the tunnel portal (*Fig. 5*, right). Remarkably, the other one-directional tunnel is sucking in a part of polluted air released by

the other tunnel. (This short-circuit is unfavorable and can be prevented by increasing the distance between the two portals, e.g., shifting the two portals away in longitudinal direction, or by building a separation wall between them.)

Based on the results mentioned, the pollutants sources in the MISKAM simulations were placed 10 m in front of the portals. To account for the high concentration gradients, the grid density in the portal region was increased to 5 m × 7.5 m × 1.5 m.

3.3. Wind tunnel testing

Wind tunnel testing proved to be a sufficient physical modeling method of the real scale dispersion processes in the past (*Cermak,* 1984; *Plate,* 1999), and thus, it can serve as reference data source for the current CFD simulations.

As in most environmental wind tunnels, only the modeling of neutral conditions was possible in the current wind tunnel test campaign. The atmospheric boundary layer profile was modeled by a horizontal grid, spikes, and roughness elements (*Fig. 6*) and was checked by two-component hot-wire measurements (cross-wire sensor with DISA 55M CTA bridges). The profile measurement results are shown in *Fig. 7.*

The wind tunnel measurements were carried out on a modular 1:1000 scale model with a total area of 28.5 m^2 (largest extents about 8 m × 5 m), resolving the topography, buildings, vegetation, and pollutant sources of the surroundings. From the modules, models of the three junctions at various wind directions and route alternatives could be constructed and investigated separately in the wind tunnel. The elevation at the model boundaries was relaxed to zero level using artificial slopes.

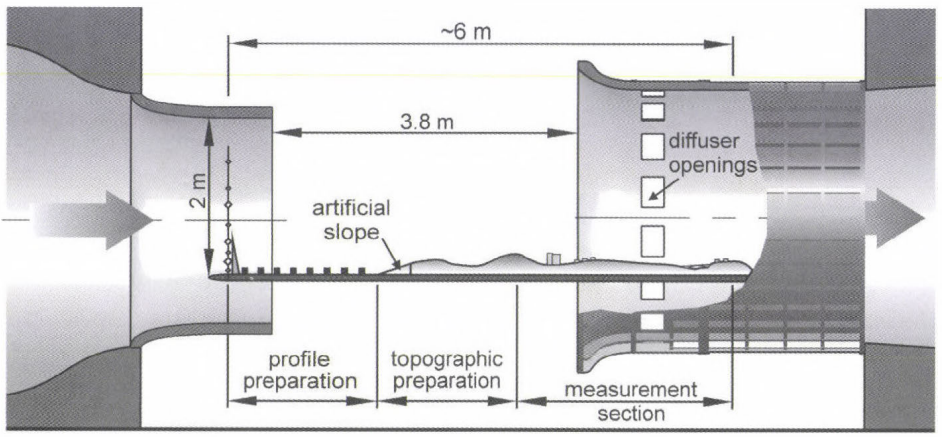

Fig. 6. Vertical cross section view of the model arranged in the test section of the Göttingen-type wind tunnel.

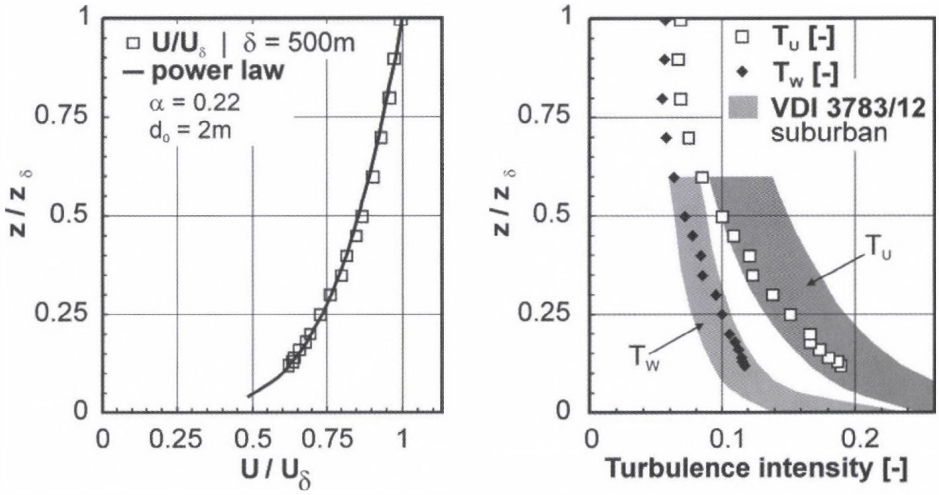

Fig. 7. Inlet profiles of mean velocity and turbulence measured by two-component CTA. The reference height δ is 500 m at full scale.

Fifty sampling points were distributed on the model (see black dots in *Fig. 1*) near tunnel portals and road sections, and inside inhabited areas and locations of specific care, for example at school buildings. Unfortunately, detailed concentration field mapping along lines or arcs could not be fitted into the four-month timeframe of the wind tunnel tests.

Methane was used as tracer gas, and source strengths Q_i were controlled using digital mass flow controllers. Road segments were treated as line sources, and therefore, tracer was released from underfloor source units lying in line with the model's surface. The construction ensured homogeneous exhaust along the road following the line source construction principle of *Meroney et al.* (1996). The pollutants produced in the road tunnels were supposed to leave the tunnel at the portal in the direction of traffic and were modeled accordingly as point sources with a small horizontal momentum. Air samples were collected simultaneously by an automatic 24-channel sampling system built from stepmotor-driven sampling cylinders and magnetic valves, and they were analyzed by a flame ionization detector (FID) afterwards. The system was calibrated with gas samples of known concentration. Repeatability tests of the whole measurement system gave an average relative uncertainty of 9% over a range of 10^2–10^4 ppm CH_4 concentration.

To a further check of the concentration measurement system, a simple test case known from the literature was measured, consisting of a line source placed into a crosswind boundary layer flow. The measured concentration downwind the source was inside the limits given by the VDI guideline 3783/12 (*VDI*, 2004). This test also proved that the use of methane as tracer

gas, regardless of its different density is proper, if testing wind speed is high enough, and thus, buoyancy effects are suppressed.

Afterwards, the Reynolds number dependency of concentration results was checked on the terrain model by repeating concentration measurements at different wind speeds. It was found that above the mean flow velocity u_{ref} of 3 m s^{-1} (at H_{ref}= 50 mm height), normalized concentrations

$$c^{+} = c u_{ref} H_{ref}{}^{2} Q^{-1} \tag{2}$$

remain constant, thus independent of the Reynolds number. In the final tests, u_{ref} was set to 4.5 m s^{-1}.

The horizontal momentum of polluted air inlet at the tunnel portals was determined by keeping the ratio of tunnel air momentum and incident wind momentum ($\rho_Q u_Q{}^2 \rho_{air}{}^{-1} u_{ref}{}^{-2}$) constant in both full and model scale. This gave 3 m s^{-1} model scale tunnel air velocity for 2.3 m s^{-1} full scale tunnel air velocity.

In total, 126 sets of concentration measurements, each consisting of 10 to 22 sampling points, were performed. The wind tunnel's background concentration and calibration gas were sampled in each set. The influence of each individual source i (road segment, tunnel portal) on the concentration distribution was measured separately at each wind direction to determine the contribution of the different sources to the total concentration.

Full scale concentrations c_{FS} [g m^{-3}] of NO_X, PM_{10}, and CO at a specific wind direction were determined based on the similarity of normalized concentrations c_i^{+} in both model and full scale by taking into consideration the real traffic emissions $Q_{i,FS}$ [g s^{-1}] of the individual sources, and finally by adding the background concentrations c_{bg} from *Table 1*, as

$$c_{FS} = c_{hg} + u_{ref\,FS}{}^{-1} H_{ref\,FS}{}^{-2} \sum c_i^{+} Q_{iFS} . \tag{3}$$

4. Results and discussion

As the ratio of the emitted pollutant mass flow and the corresponding concentration limit value is far the highest for NO_x (among the pollutants mentioned above), the distribution maps of NO_x will be analyzed further in Section 4. Although the photochemical reactions, which lead to the formation of more dangerous NO_2 and O_3, were not included in this study, annual mean values of NO_x can be correlated to those of NO_2 based on long-term station observations, and thus, a prediction can be given also for annual NO_2 concentrations.

4.1. General observations

The flow field at the three junctions could be analyzed using velocity profiles, streamlines, and contour plots of the CFD results. An example is shown in *Fig. 8*.

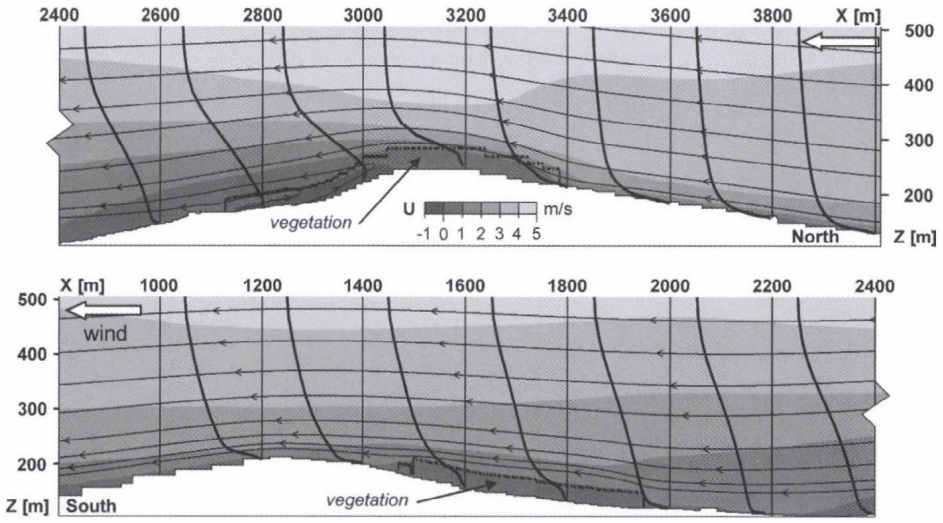

Fig. 8. North-south cross section of the flow over hills of Junction 3 for a north wind with streamlines and vertical profiles of the U velocity component. Boundaries of deciduous forests are shown with dotted lines. Note the speedup above the hills and the small separation region and backward flow on the lee side of the northern hill.

The most important factors affecting the flow field are listed in the following:

(1) The influence of topography ranges from slight changes of wind direction and wind speed to the full three-dimensionality of flow. Speed-up could be observed above the hill ridges. Separation zones can develop behind steeper hills (see at Junction 3 in *Fig. 8* and later in *Fig. 12*).

(2) Building effects are only worth mentioning near the 10–15 storey block buildings of Junction 1, while at the other junctions detached houses of suburban towns act rather like roughness elements because the grid resolution is not sufficient to resolve the small flow structures around them (buildings accommodate only a few grid cells).

(3) Vegetation zones are slowing down the flow and at the same time shifting the main flow upwards (*Fig. 8*).

Based on both wind tunnel measurements and CFD simulations we can draw the following conclusions about the concentration field:

(1) In the case of road segments running on the surface, concentration limits are exceeded only in a narrow strip of about 50 m along the road.

(2) On the other hand, the emission from tunnel portals can cause plumes of more than 100 m length above the hourly concentration limit (200 μg m^{-3}), reaching even populated areas (*Fig. 9*).

(3) The direction of the tunnel plumes is slightly modified by the topography; see, for example, at Junction 2 with a northeast wind direction (*Fig. 9*).

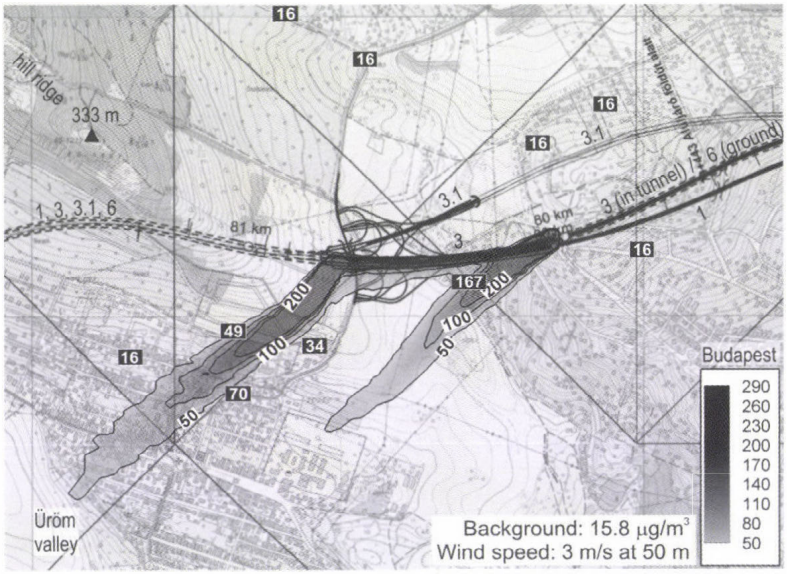

Fig. 9. Concentrations of NO_x [μg m^{-3}] at Junction 2, 3 m above the surface with a NE wind direction and a wind velocity of 3 m s^{-1}, in the case of route alternative 3 without ventilation stacks operating. White numbers: concentrations from wind tunnel measurement, contour plot; bold black numbers: simulation results. (The other route alternatives are drawn in the figure but are not in operation.)

(4) In separation zones, upwind dispersion is possible due to the recirculating flow.

(5) Pollution coming from viaducts has an almost negligible footprint at the surface due to the higher wind speed and the higher altitude of release (*Fig. 12*).

4.2. Modeling of ventilation stacks

To account for the most prominent observation made in Section 4.1, the large pollutant plumes released from tunnel portals, which threaten the air quality of nearby settlements at low wind speeds and rush-hour traffic density, the design of the tunnel ventilation system was extended by ventilation stacks. These will be put into operation if the above mentioned conditions are met and will then exhaust the polluted tunnel air at more than 20 m height above ground. In this way, large concentrations at ground level in the vicinity of the portals can be avoided. In *Fig. 10*, the revised ventilation concept can be seen. The stacks are located near the tunnel portals.

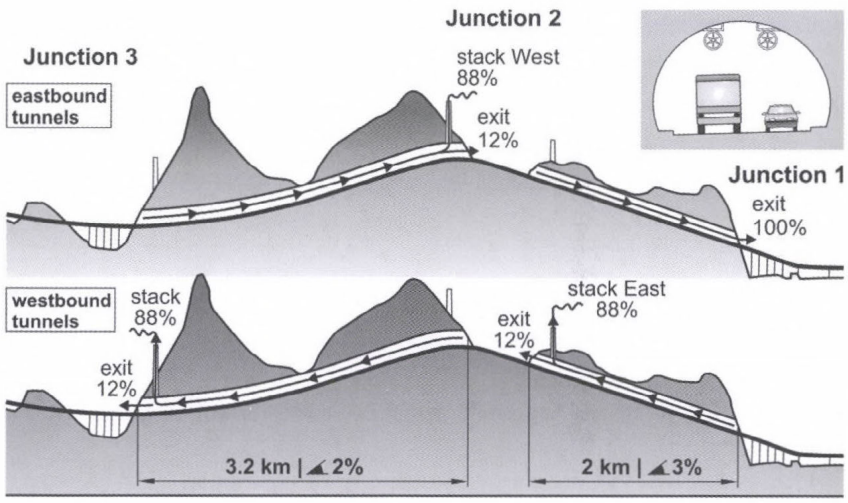

Fig. 10. Tunnel ventilation concept with stack locations. The ventilation of the eastbound and westbound one-directional tunnels is independent, and thus, shown separately. Elevation is scaled approximately by 10. Upper right corner: cross-section of a one-directional tunnel with axial ventilation fans.

The concept was checked in further MISKAM simulations. Stack heights range between 20–25 m, and vertical outflow velocity of the exhaust was set to 6 m s^{-1}. Based on the simulation results, if external wind speed is 3 m s^{-1} at 50 m height, at least 88% of the polluted tunnel air has to be exhausted through the stacks to avoid concentration limit exceedance near the portals. When comparing *Figs. 9* and *11*, the decrease of the area with concentrations above the hourly concentration limit (200 μg m^{-3}) is obvious, while footprints of stack plumes on the surface are well below the limit. The plume of the west stack is also modified by the topography, more specifically by the NW oriented nearby hill ridge.

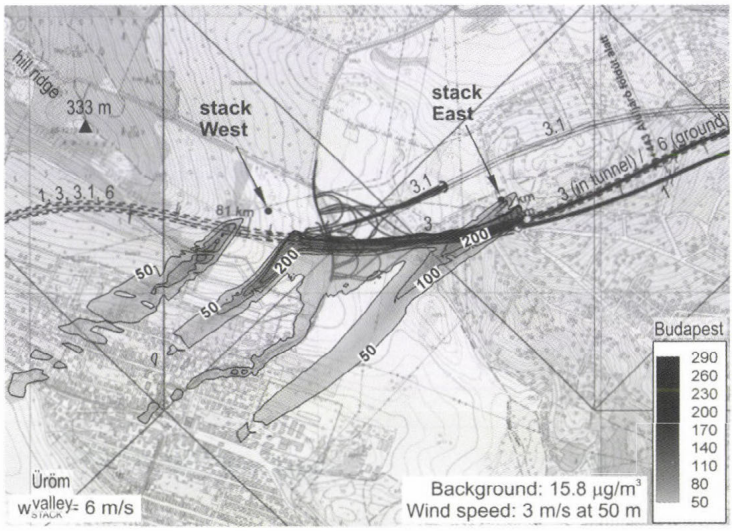

Fig. 11. Concentrations of NO_x [μg m^{-3}] at Junction 2, 3 m above the surface with a NE wind direction and a wind velocity of 3 m s^{-1}, in case of route variant 3. Ventilation stacks are in operation, vertical stack velocity is 6 m s^{-1}. Compare this figure to *Fig. 9.*

Detailed analysis of the flow and concentration fields showed that plume axes run at about 40 m height above ground (see *Fig. 12*). Surface concentrations below the stack plumes are significantly smaller than those at the tunnel portals, although they exhaust seven times more pollutant. *Fig. 12* also demonstrates the ability of CFD models in resolving three-dimensional flows above complex terrain.

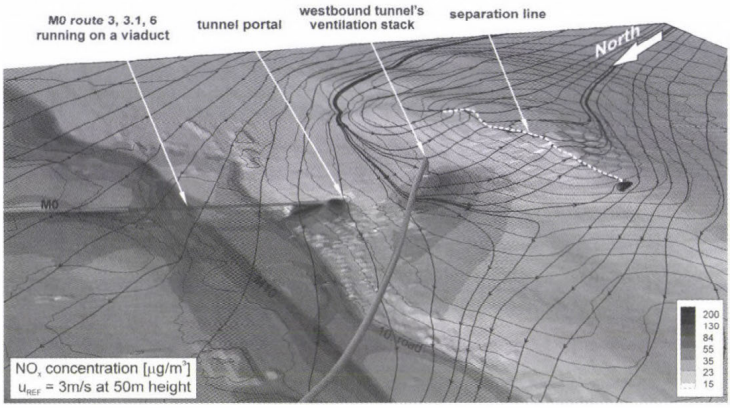

Fig. 12. MISKAM simulation of Junction 3 with a north wind direction and 3 m s^{-1} wind velocity at 50 m height. Tunnel ventilation stacks are in operation. Streamlines (thicker black lines) at 6 m height above ground show a separation behind the northern hill and the modification of the ventilation stack's plume centerline (dark grey rod). Thin black lines: topographic level curves; surface color: concentration (logarithmic scale).

To decrease the power consumption of the ventilation system, it is proposed to operate it only at lower wind speeds with full power. In case of higher wind speeds pollutant dilution is faster, thus, a larger portion of polluted tunnel air can be released through the portal without causing limit exceedances. Similarly, in periods with low traffic, further ventilation energy can be saved.

4.3. Comparison of experimental and numerical results

The comparison of experimental and numerical concentrations (in total 499 non-zero value pairs) in the left part of *Fig. 13*, shows acceptable agreement in general. However, some larger deviations were observed, which are partly due to limitations of the modeling methods. The deviations were analyzed point by point and the most typical causes found are listed in the following.

(1) Known limitations of $k-\varepsilon$ models: *Castro et al.* (2003) concluded from their Askervein Hill simulations that speed-up above the hilltop is underpredicted. Furthermore, being originally a steady-state simulation, the time-dependency, especially in recirculating zones, is not captured by the models. In our case this is not problematic, as we are interested in mean values only. Concerning the dispersion results, according to the validation tests in *Eichhorn* and *Balczó* (2008), MISKAM 5 predicts thinner and longer pollutant plumes from point sources than those measured in wind tunnel.

(2) Minor geometrical differences between the wind tunnel and numerical model: Near the line sources very large concentration gradients can occur, meaning that even a small displacement of a sampling point in the physical and numerical model could cause errors of above 50%.

(3) Different initial dilutions of the pollutant sources can again affect near-source measurements (passive scalar released in source grid cells in CFD vs. tracer gas released along a line from the surface of the wind tunnel model).

(4) Different vegetation modeling: In the numerical model, the parameter expressing the vegetation density, known as leaf area density (*LAD*), was 0.5, an average value for deciduous forests taken from the literature. This corresponds according to *Balczó et al.* (2009) and *Gromke* and *Ruck* (2009) at the model scale of 1:1000 to a crown porosity of about 96–97% in the wind tunnel measurement. In the physical model, however, artificial grass of lower porosity was used for forest modeling (approximately 94%), leading to smaller wind velocities and higher displacement thicknesses in vegetation covered areas.

(5) Coarse numerical grid resolution: Because of the staggered grid (without terrain-following coordinate system), slopes, especially in the

inflow and outflow zones, have higher roughness, influencing the near-surface balance of k and, in consequence, the dispersion.

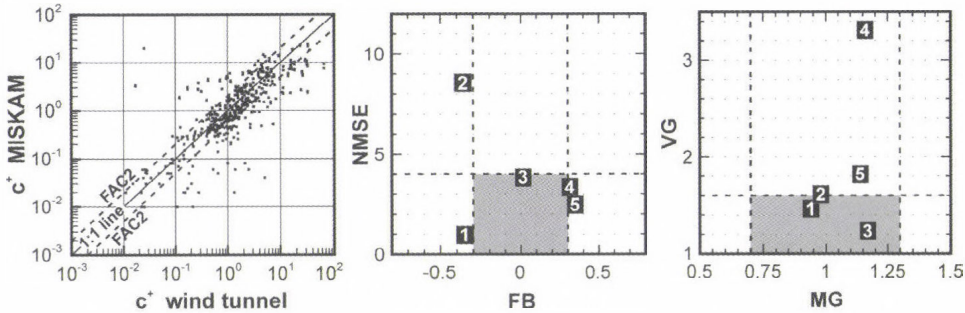

Fig. 13. Left: logarithmic scatter plot of measured and simulated concentrations c^+. The plot contains all non-zero value pairs which were measured respectively simulated in the 50 sampling point locations (see *Fig. 1*), in total about 499 points. Dashed lines show 50% and 200% of the measurements. Points between the two lines represent predictions within a factor of two of observations (FAC2).

Middle and right: Plots of linear and logarithmic validation metrics of normalized concentration c^+ from different MISKAM simulations. Cases compared: (1) perpendicular flow in a street canyon with vegetation of *Balczó et al.* (2009); (2) simulation of the Mock Urban Setting Test (*Eichhorn* and *Balczó*, 2008) using MISKAM 5.02; (3) simulation of the Mock Urban Setting Test using MISKAM 6; (4) present simulation, all non-zero values; and (5) present simulation, all values > 0.5. The model acceptance range is marked grey.

4.4. Validation metrics

To quantify the extent of deviations between results from numerical and physical modeling, statistic metrics after *Chang* and *Hanna* (2004) were calculated. The values can be seen in *Table 5*; many of them are within or at least close to the limits of acceptance proposed for state-of-the-art models. The larger positive value of the fractional bias (FB) shows that wind tunnel results are moderately underestimated by the simulation at large concentrations. However, this is not the case at medium and small concentrations, because geometric mean bias (MG), which is not dominated by the large concentration values, is very good. The worse value of geometric variance (VG) while at the same time the normal mean square error (NMSE) is clearly inside the limit, can be explained by the scattering of small concentration values due to the measurement error. After filtering c^+ values smaller than 0.5, metrics of the remaining 336 data points improve significantly.

In *Fig.13*, middle and right, one can see the metrics of concentrations from already published validation studies using the MISKAM code. Point 1 of the figure refers to a simulation in a street canyon with a building height to street width ratio of 1:1 and a street length to width ratio of 10:1, at perpendicular flow direction and with tree planting inside the canyon, described in detail in *Balczó et al.* (2009).

Table 5. Calculated statistic metrics for concentration (after *Chang* and *Hanna*, 2004)

Validation metric	Abbreviation	Limit	All non-zero values	Values < 0.5 filtered	Classification
Correlation coefficient	R	0.8	0.608	0.722	Fair
Fractional bias	FB	±0.3	0.313	0.347	Nearly good
Normalized mean square error	NMSE	0–4	3.35	2.47	Good
Geometric mean bias	MG	0.7–1.3	1.16	1.14	Good
Geometric variance	VG	0–1.6	3.31	1.82	Nearly good
Fraction of predictions within a factor of two of observations	FAC2	0.5	0.655	0.723	Good

Points 2 and 3 show test results from the Mock Urban Setting Test (*Eichhorn* and *Balczó*, 2008). The Mock Urban Setting Test (MUST) was a full-scale measurement campaign on a rectangular grid-like arrangement of 120 standard shipping containers in Utah as described by *Yee* and *Biltoft* (2004), wind tunnel tests of the same arrangement were carried out by *Leitl et al.*, (2007). MISKAM was used to simulate dispersion from a source between the containers at slanted −45° flow. Tracer dispersion data was compared in 256 data points. This test case was run with the current and future MISKAM versions 5.02 (point 2 in *Fig. 13*) and 6 (point 3).

Point 4 refers to all non-zero c^+ values of the current study, point 5 to all c^+ values larger than 0.5. A comparison of these data with those mentioned above indicates clearly, that in case of practical applications and complex geometries like this investigation, the code performs less accurately, but an acceptable level of accuracy can be still achieved.

5. *Conclusions*

The current paper gives an overview about a larger microscale CFD and wind tunnel test campaign performed in a suburban area of complex terrain in the north of Budapest. Emission determination, mesoscale influences on local wind statistics, and background concentrations were also discussed.

The CFD simulations and accompanying wind tunnel measurements showed that open road sections cause limit exceedance along a narrow strip of some 50 m along the investigated motorway routes, while pollutant plumes from the tunnel portals can spread more hundred meters away. They also provided information on the necessary changes of the tunnel ventilation system. The effect of the proposed ventilation stacks on air quality was estimated by CFD. The NO_x concentration maps delivered by this investigation helped the authorities to select the final route, which is a slightly modified version of route alternative 3.1.

Numerical simulation using the RANS approach with k–ε closure proved to be a reliable tool to understand and predict flow and dispersion phenomena, resolving all main features of the three-dimensional flow, but deviations from the

experimental results signal that the use of wind tunnel or on-site reference data is still useful. These can provide valuable information for the evaluation and assessment of simulation results, as shown here with the application of statistic metrics.

Acknowledgements—Thanks are due to the Hungarian Meteorological Service, to department staff members *Tamás Régert*, *Viktor Szente*, *Zoltán Szucsán*, *Gábor Kalmár*, and finally to all participating students for their valuable contributions. The investigations presented in this paper were financed by the National Infrastructure Development Corporation of Hungary. This work is connected to the scientific program of the "Development of quality-oriented and harmonized R+D+I strategy and functional model at BME" project, which is supported by the New Széchenyi Plan (grant agreement no.: TÁMOP-4.2.1/B-09/1/KMR-2010-0002). *Miklós Balogh's* participation was also financed by his current project, which is supported by the European Union and co-financed by the European Social Fund (grant agreement no. TÁMOP 4.2.1./B-09/1/KMR-2010-0003).

References

ASTRA, 2004: *Guideline for the ventilation of road tunnels.* ASTRA Bundesamt für Strassen/Swiss Federal Roads Office FEDRO, Bern.

Ayotte, K., Hughes, D., 2004: Observations of boundary-layer wind-tunnel flow over isolated ridges of varying steepness and roughness. *Bound.-Lay. Meteorol. 112*, 525-556.

Balczó, M., Gromke, C., Ruck, B., 2009: Numerical modeling of flow and pollutant dispersion in street canyons with tree planting. *Meteorol Z. 18*, 197-206.

Belcher, S.E., Hunt, J.C.R., 1998: Turbulent flow over hills and waves. *Annu. Rev. Fluid. Mech. 30,* 507-538.

Berkowicz, R., 2000: A simple model for urban background pollution. *Environ. Monit. Assess. 65,* 259-267.

Bettelini, M., Brandt, R., Riess, I., 2001: Environmental aspects of tunnel ventilation. *AITES-ITA 2001 World Tunnel Congress,* Milano, June 10-13, 2001.

Bowen, A. J., 2003: Modelling of strong wind flows over complex terrain at small geometric scales. *J Wind. Eng. Ind. Aerod. 91,* 1859-1871.

Brodeur, P., Masson, C., 2006: Numerical simulations of wind distributions over very complex terrain. *44th AIAA Aerospace Sciences Meeting and Exhibit*, 9–12 January 2006, Reno, Nevada AIAA 2006-1362.

Castro, F.A., Palma, J. M. L. M., Silva Lopes, A., 2003: Simulation of the Askervein flow. Part 1: Reynolds averaged Navier-Stokes equations (k–ε turbulence model). *Bound.-Lay. Meteorol 107,* 501-530.

Cermak, J. E. 1984: Physical modelling of flow and dispersion over complex terrain. *Bound.-Lay. Meteorol. 30,* 261-292.

Chang, J.C., Hanna, S. R., 2004: Air quality model performance evaluation. *Meteorol. Atmos. Phys. 87,* 167-196.

Colberg, C. A., Tona, B., Stahel, W. A., Meier, M., Staehelin, J., 2005: Comparison of a road traffic emission model (HBEFA) with emissions derived from measurements in the Gubrist road tunnel, Switzerland. *Atmos. Environ. 39,* 4703-4714.

Contini, D., Procino, L., Massini, M., Manfrida, G., 2003: Ground-level diffusion of pollutant emitted at the portal of a road tunnel model. *Proceedings of PHYSMOD 2003 International Workshop on Physical Modelling of Flow and Dispersion Phenomena*, Prato, Italy, 244-251.

Cremades, L., 2000: Estimating the background air concentration excluding the contribution of an individual source. *Environ. Model. Assess. 5,* 119-124.

Dixon, N., Tomlin, A., 2007: A Lagrangian stochastic model for predicting concentration fluctuations in urban areas. *Atmos. Environ. 41,* 8114-8127.

Donnelly, R., Lyons, T., Flassak, T., 2009: Evaluation of results of a numerical simulation of dispersion in an idealised urban area for emergency response modelling. *Atmos. Environ. 43,* 4416-4423.

Eichhorn, J., 2008: MISKAM Manual for version 5. giese-eichhorn environmental meteorological software, Wackernheim, Germany

Eichhorn, J., Balczó, M., 2008: Flow and dispersal simulations of the Mock Urban Setting Test. The 12th Int. Conf. on Harmonization within Atmospheric Dispersion Modelling for Regulatory Purposes (HARMO12), Cavtat, Croatia, October 6-9, 2008. *Croatian Meteorol. J. 43,* 67-72.

Eichhorn, J., Kniffka, A., 2010: The numerical flow model MISKAM: State of development and evaluation of the basic version. *Meteorol. Z. 19,* 81-90.

Franke, J., Hellsten, A., Schlünzen, H., Carissimo, B., 2007: *Best practice guideline for the CFD simulation of flows in the urban environment.* COST Office Brussels ISBN: 3-00-018312-4.

Goricsán, I., Balczó, M., Régert, T., Suda, J. M., 2004: Comparison of wind tunnel measurement and numerical simulation of dispersion of pollutants in urban environment. *International Conference on UrbanWind Engineering and Building Aerodynamics, von Karman Institute,* Rhode-Saint-Genése, Belgium, May 5-7, 2004 D.6.1-D.6.10.

Goricsán, I., Balczó, M., Czáder, K., Rákai, A., Tonkó, C., 2011: Simulation of flow in an idealised city using various CFD codes. *Int. J. Environ. Pollut. 44,* 359-367.

Gromke, C., Ruck, B., 2009: On the impact of trees on dispersion processes of traffic emissions in street canyons. *Bound.-Lay. Meteorol. 131,* 19-34.

Holmes, N., Morawska, L., 2006: A review of dispersion modelling and its application to the dispersion of particles: An overview of different dispersion models available. *Atmos. Environ. 40,* 5902-5928.

Infras, 2004: *The Handbook of Emission Factors for Road Transport (HBEFA 2.1).*www.hbefa.net, CD-ROM database.

Jones, A. M., Yin, J., Harrison, R. M. 2008: The weekday-weekend difference and the estimation of the non-vehicle contributions to the urban increment of airborne particulate matter. *Atmos. Environ. 42,* 4467-4479.

Kaimal, J., Finnigan, J., 1994: *Atmospheric Boundary Layer Flows.* Oxford University Press.

Kato, M., Launder, B., 1993: The modelling of turbulent flow around stationary and vibrating square cylinders. *Ninth Symp. on Turbulent Shear Flows,* Kyoto, Japan, August 1993, 10.4.1-10.4.6.

Ketzel, M., Berkowicz, R., Lohmeyer, A., 2000: Comparison of numerical street dispersion models with results from wind tunnel and field measurements. *Environ. Monit. Assess. 65,* 363-370.

Ketzel, M., Louka, P., Sahm, P., Guilloteau, E., Sini, J. F., Moussiopoulos, N., 2002: Intercomparison of numerical urban dispersion models - Part II: Street canyon in Hannover, Germany. *Water Air Soil Pollution: Focus 2,* 603-613.

Ketzel, M., Omstedt, G., Johansson, C., Düring, I., Pohjola, M., Oettl, D., Gidhagen, L., Wahlin, P., Lohmeyer, A., Haakana, M., Berkowicz, R., 2007: Estimation and validation of PM2.5/PM10 exhaust and non-exhaust emission factors for practical street pollution modelling. *Atmos. Environ. 41,* 9370-9385.

Kim, H. G., Patel, V. C., 2000: Test of turbulence models for wind flow over terrain with separation and recirculation. *Bound.-Lay. Meteorol. 94,* 5-21.

Kristóf, G., Rácz, N., Balogh, M., 2009: Adaptation of pressure based CFD solvers for mesoscale atmospheric problems. *Bound.-Lay. Meteorol. 131,* 85-103.

Leitl, B., Bezpalcova, K., Harms, F., 2007: Wind tunnel modelling of the MUST experiment. *The 11th International Conference on Harmonisation within Atmospheric Dispersion Modelling for Regulatory Purposes (HARMO11).* Cambridge, UK, July 2–5. 435-439.

Liu, H., Zhang, B., Sang, J., Cheng, A. Y. S., 2001: A laboratory simulation of plume dispersion in stratified atmospheres over complex terrain. *J. Wind Eng. Ind. Aerod. 89,* 1-15.

Lohmeyer, A., Mueller, W. J., Baechlin, W., 2002: A comparison of street canyon concentration predictions by different modellers: final results now available from the Podbi-exercise. *Atmos. Environ. 36,* 157-158.

Longley, I., Kelly, F., 2008: Systematic literature review to address air quality in and around traffic tunnels. *National Health and Medical Research Council,* Commonwealth of Australia.

López, S. D., 2002*:* Numerische Modellierung turbulenter Umströmungen von Gebäuden. *PhD thesis, University of Bremen,* Germany.

McBride, M., Reeves, A., Vanderheyden, M., Lea, C., Zhou, X., 2001: Use of advanced techniques to model the dispersion of chlorine in complex terrain. *Process. Sa. Environ. 79,* 89-102.

Mensink, C., De Ridder, K., Deutsch, F., Lefebre, F., Van de Vel, K., 2008: Examples of scale interactions in local, urban, and regional air quality modelling. *Atmos. Res. 89,* 351-357.

Meroney, R.N., Pavageau, M., Rafailidis, S., Schatzmann, M., 1996: Study of line source characteristics for 2-D physical modelling of pollutant dispersion in street canyons. *J. Wind Eng. Ind. Aerod. 62,* 37-56.

Moussiopoulos, N., Flassak, T., Knittel, G., 1988: A refined diagnostic wind model. *Environ. Softw. 3,* 85-94.

Nadel, C., Vanderheyden, M. D., Lepage, M., Davies, A., Wan, P., Ginzburg, H., Schattanek, G., 1994: Physical modelling of dispersion of a tunnel portal exhaust plume. *8th International Symposium on Aerodynamics & Ventilation of Vehicle Tunnels*, Liverpool, UK.

Oettl, D., Sturm, P., Almbauer, R., Okamoto, S., Horiuchi, K., 2003: Dispersion from road tunnel portals: comparison of two different modelling approaches. *Atmos. Environ. 37,* 5165-5175.

Olesen, H., Berkowicz, R., Ketzel, M., Løfstrøm, P., 2009: Validation of OML, AERMOD/PRIME and MISKAM using the Thompson wind-tunnel dataset for simple stack-building configurations. *Bound.-Lay. Meteorol. 131,* 73-83.

Palma, J., Castro, F., Ribeiro, L., Rodrigues, A., Pinto, A., 2008: Linear and nonlinear models in wind resource assessment and wind turbine micro-siting in complex terrain. *J. Wind. Eng. Ind. Aerod. 96,* 2308-2326.

Plate, E.J. (ed.), 1982: *Engineering Meteorology.* Elsevier.

Plate, E. J., 1999: Methods of investigating urban wind fields – physical models. *Atmos. Environ. 33,* 3981-3989.

Ries, K., Eichhorn, J., 2001: Simulation of effects of vegetation on the dispersion of pollutants in street canyons. *Meteorol. Z. 10,* 229-233.

Rodrigues, C. A. V., 2005: Analysis of the atmospheric boundary layer flow over mountainous terrain. *Master's thesis, Von Karman Institute.*

Sahm, P., Louka, P., Ketzel, M., Guilloteau, E., Sini, J. F., 2002: Intercomparison of numerical urban dispersion models – Part I: Street canyon and single building configurations. *Water Air Soil Poll: Focus 2,* 587-601.

Silva Lopes, A., Palma, J., Castro, F., 2007: Simulation of the Askervein flow. Part 2: Large-eddy simulations. *Bound.-Lay. Meteorol. 125,* 85-108.

Smolarkiewicz, P., Grabowski, W., 1989: The multidimensional positive definite advection transport algorithm: Nonoscillatory option. *J. Computat. Phys. 86,* 355–375.

Snyder, W. H., 1990: Fluid modeling applied to atmospheric diffusion in complex terrain. *Atmos. Environ. Part A General Topics. 24,* 2071-2088.

Stern, R., Yamartino, R. J., 2001: Development and first evaluation of Micro-Calgrid: a 3-D, urban-canopy-scale photochemical model. *Atmos. Environ. 35,* 149-165.

Taylor, P. A., Teunissen, H. W., 1987: The Askervein Hill project: Overview and background data. *Bound.-Lay. Meteorol. 39,* 15-39.

Tchepel, O., Borrego, C., 2010: Frequency analysis of air quality time series for traffic related pollutants. *J. Environ. Monitor. 12,* 544-550.

Tchepel, O., Costa, A., Martins, H., Ferreira, J., Monteiro, A., Miranda, A., Borrego, C., 2010: Determination of background concentrations for air quality models using spectral analysis and filtering of monitoring data. *Atmos. Environ. 44,* 106-114.

Vardoulakis, S., Fisher, B. E. A., Pericleous, K., Gonzalez-Flesca, N., 2003: Modelling air quality in street canyons: a review. *Atmos. Environ. 37,* 155-182.

VDI, 2004: VDI 3783, Part 12: Environmental meteorology, Physical modelling of flow and dispersion processes in the atmospheric boundary layer. *Application of Wind Tunnels.* Beuth-Verlag, Germany.

VDI, 2005: *VDI 3783, Part 9:* Environmental meteorology. Prognostic microscale windfield models: *Evaluation for Flow Around Buildings and Obstacles.* Beuth-Verlag, Berlin, Germany.

Walmsley, J. L., Taylor, P. A., 1996: Boundary-layer flow over topography: Impacts of the Askervein study. *Bound.-Lay. Meteorol. 78,* 291-320.

Wood, N., 2000: Wind flow over complex terrain: A historical perspective and the prospect for large-eddy modelling. *Bound.-Lay. Meteorol. 96,* 11-32.

Xie, Z. T., Castro, I. P., 2009: Large-eddy simulation for flow and dispersion in urban streets. *Atmos. Environ. 43,* 2174-2185.

Yee, E., Biltoft, C.A., 2004: Concentration fluctuation measurements in a plume dispersing through a regular array of obstacles. *Bound.-Lay. Meteorol. 111,* 363-415.

IDŐJÁRÁS

Quarterly Journal of the Hungarian Meteorological Service
Vol. 115, No. 3, July–September 2011, pp. 205–216

Application of a new aridity index in Hungarian forestry practice

Ernő Führer[1]*, László Horváth[2], Anikó Jagodics[1], Attila Machon[2,3,4], and Ildikó Szabados[5]

[1]*Hungarian Forest Research Institute, Paprét 17, 9400 Sopron, Hungary*

[2]*Hungarian Meteorological Service, P.O. Box 39, 1675 Budapest, Hungary; E-mail: horvath.l@met.hu*

[3]*Center for Environmental Science, Eötvös Loránd University, Pázmány P. sétány 1/A, 1117 Budapest, Hungary*

[4]*Institute of Botany and Ecophysiology, Szent István University, Páter K. utca 1, 2103 Gödöllő, Hungary*

[5]*Hungarian Forest Research Institute, Várkerület 30/a, 9600 Sárvár, Hungary*

**Corresponding author; E-mail: fuhrere@erti.hu*

(Manuscript received in final form September 7, 2010)

Abstract—The ecophysiological observations and the investigations of the weather dependent vital processes of the forests have clearly proved that the water supply in the main growing–main water consumption period (from May to July) as well as in the critical months (July and August) have crucial influence on the growth, vitality, and organic matter production of the forest. Evapotranspiration rate is higher in these periods; and forest ecosystems are most sensitive to the extreme weather conditions this time. Relationship between meteorological parameters and girth-growth of trees (proportional with organic matter production) can be characterized by a simplified forestry aridity index (FAI) for Hungarian conditions: $FAI = 100\ T_{VII-VIII}/(P_{V-VII} + P_{VII-VIII})$, where $T_{VII-VIII}$ is the average temperature in July and August (°C), P_{V-VII} is the precipitation sum (mm) of the period from May to July, and $P_{VII-VIII}$ is the precipitation sum (mm) of July and August. By this index, the average weather conditions of different climate categories applied in forestry practice can be described. *FAI* values representative for different species are beech: < 4.75; hornbeam–oak: $4.75 - 6.00$; sessile oak and Turkey oak: $6.00 - 7.25$; forest-steppe: > 7.25.

Key-words: forest ecosystem, climate change, productivity, forestry aridity index, forestry climate categories

1. Introduction

The predicted climate change is one of the greatest challenges of the 21st century. In terms of Hungary's climate, warmer and drier weather circumstances will be expected (*Láng et al.*, 2007). Main reasons for the increasing aridity in air and soil would be the decrease and change of seasonal distribution of precipitation as well as the significant increase of air temperature (*Führer*, 2010; *Führer* and *Járó*, 1992; *Várallyai*, 2002, 2010; *Várallyai* and *Farkas*, 2008). All these changes have impact on the productivity of forests influencing not only the structure and species composition of forests but also, indirectly, the organic matter production (*Führer*, 1995). For these reasons, the investigation of the effect of the possible climate change on forestry practice is important not only from the point of view of change of spreading and vitality of species (*Berki et al.*, 2007, 2009; *Mátyás*, 2010; *Mátyás et al.*, 2009), and the increase of biotic and abiotic damages (*Csóka et al.*, 2007; *Molnár* and *Lakatos*, 2007). The detailed evaluation – from practical production biology approximation –, the climate effect on the growth properties of trees and stands will also be more and more necessary.

Aridity indices frequently used in agrometeorology are summarized in *Dunkel* (2009). Some of them take into account measured precipitation and temperature characteristics; others apply derived or complicated parameters as potential evapotranspiration, radiation balance, Bowen ratio, etc. The primary aim of this paper is to describe and specify the climatic-ecophysiological relationships and to propose a simple index based on meteorological parameters measured routinely and available all over the country.

2. Scientific background

2.1. Seasonal variation of tree growth

Regarding the annual tree growth, it is important to distinguish between the growing period and the vegetation period. On one hand, vegetation period is the season of the potential growth. In the temperate climate zone, this period ranges between the early and late frost (*Linderholm*, 2006). On the other hand, the growing period is a term when actual growing (shoot or thickness) or other physiological processes take place such as the formation of bud structure.

In Hungary, trunk thickness and growth-pattern observations have shown that more than 80% of organic material production takes place during the months from May to July in case of various tree species (*Szőnyi*, 1962; *Halupa*, 1967; *Járó* and *Tátraaljai*, 1984-85; *Führer*, 1994, 1995; *Manninger*, 2004). This means that in Hungary the low precipitation and high summer temperatures basically influence the intensity and magnitude of organic material production and they also have an impact on the ratio of spring and autumn tree rings.

Vegetation period out of main growing period and critical months only plays an important role when weather circumstances restrict the physiological processes leading to organic matter production. Such circumstances can be observed during the late May frost period or during April droughts.

2.2. Water supply and girth-growth of tree

Apart from the changing temperatures, the organic material production of trees is mostly influenced by the water supply. The growth of trees is restricted by the common water shortage in Hungary during warm months with high potential evapotranspiration rate. The annual water cycle of forests and the related organic matter production is based on three phases of water supply and water consumption, and three life cycles of growth (*Führer*, 1994, 1995, 2008, 2010; *Führer* and *Járó*, 2000; *Járó*, 1989). When evaluating the precipitation relations in different life-cycles, we have to take into consideration many dominating interdependent factors, both in time and space. These all may either strengthen or balance the effect of extreme weather circumstances.

From the point of view of water cycle, the winter season between November and April is the *storage period*, while regarding the growth it is the *dormant* and *initial growth* phase (*Fig. 1*). In this phase, most amount of precipitation, somewhat decreased by crown and litter interception infiltrates into the soil, and gradually fills it up. The physiological water consumption is negligible. During winter drought in storage period when precipitation deficit exceeds the 40% compared to regular years, the effect of water deficiency on the growth is difficult to define since transpiration process starts only later.

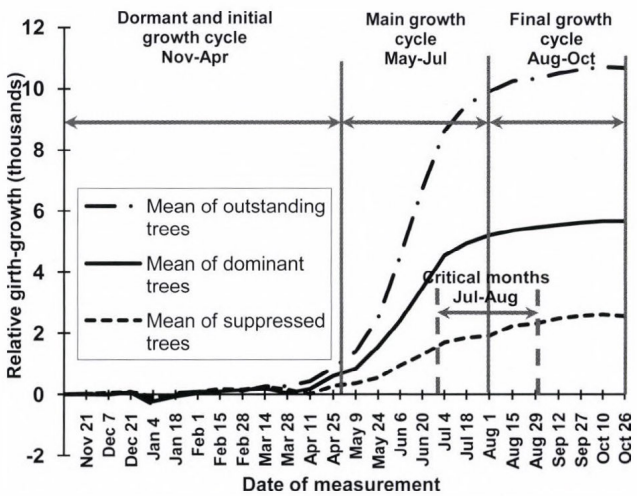

Fig. 1. Average annual girth-growth of a Brennbergbánya beech forest over five years in relative units (1988–1992) (*Führer*, 1994, 2010).

The period between May and July is called *main utilization phase* or *main growth cycle*. At this time, the precipitation decreased by crown and litter interception gets into only the upper layers of the soil. It is used later – together with the water left from the storage period – mostly for organic matter production and less for other physiological processes. In this cycle, 80% of the increment of the forest occurs, and this is why the extreme weather conditions, namely the effect of deficient precipitation can be more effective. This happens in case of increment decrease, i.e., in case of *partial aridity damage*.

The period between August and October is called *final growth phase*. At this time, the precipitation decreased by interception fills up only the upper layers of the soil recovering the amount of water used up during the main growth cycle; supplying the water demand of physiological processes apart from thickness growing (e.g., cropping). Low precipitation can only result in small increment decrease.

If significant deficit of precipitation in the main and final growth phase (May to October) is accompanied by extremely high temperatures in July and August (critical months), not only increment loss can be observed, but even organic matter production of trees can stop. This may happen because water is used for transpiration to keep the heat balance of trees during extreme circumstances. In extreme cases, the physiological debilitation of trees might result in decrease in trunk number of trees. This so-called total drought damage is mostly characteristic for hybrid poplars and spruces planted at marginal sites in Hungary.

3. Results

3.1. Forestry aridity index (FAI)

The principle of the further development of forest management shall be the ecosystem based evaluation of ecological (site) factors of forest management regions. In this system, climate has become a dynamically changing site factor. The ecophysiological observations and the investigation of the physiological processes of forests depending on weather have clearly proved that water supply in the *main growth cycle – main utilization cycle* (May to July) and in the *critical months* (July and August) essentially influences the growth and organic matter production of the forests. In this period, evapotranspiration is most intensive, therefore, forest reacts sensitively to the extreme weather conditions.

To describe the relationship between weather conditions and thickness growth of tree stands, we propose a simplified forestry aridity index applicable for Hungarian conditions. The index is based on meteorological parameters, namely on precipitation and temperature that have been measured extensively all over Hungary with adequate precision, so adaptation and up-scaling for the whole country can be surely done. In the formula, based on monthly temperature

and precipitation averages, theoretical approximations of the aridity index for arable land proposed by *Pálfai* (2002, 2007, 2010) and the critical water supply index applied for dry forestry regions (*Führer* and *Járó*, 2000), appear together. Consequently, the *FAI* index takes into account the ratio of the average temperature of the critical months (July and August) and the precipitation sums in main growth cycle (May to July) plus the precipitation sums in the critical months (from July to August) (*Führer*, 2008, 2010):

$$FAI = 100\, T_{VII-VIII}/(P_{V-VII} + P_{VII-VIII}), \tag{1}$$

where $T_{VII-VIII}$ is the average temperature in July and August (°C), P_{V-VII} is the precipitation sum (mm) in the period from May to July, and $P_{VII-VIII}$ is the precipitation sum (mm) in July and August.

In the future, we aim to refine the *FAI* values with developing more exact relationships, i.e., we have to apply some correction factors taking into account: (i) the weather circumstances in dormant season (from November to March), (ii) especially in April, when weather conditions may influence the start of vegetation, (iii) the correct weighting in the formula for the magnitude of the role of different months in organic matter production, (iv) the exposure and slope circumstances.

With the help of the *FAI* we are able to classify the average climate of a spot or even a region from forestry viewpoint. On the other hand, we can characterize the expansion area of certain tree species, and we are also able to measure the impact of extreme weather conditions.

It clearly follows from Eq. (1) that increasing *FAI* means warmer and dryer weather in the main growth cycle and in the critical months and vice versa; decreasing *FAI* indicates cooler and wetter climate.

3.2. Relation between FAI and tree growth

The adaptability of the forestry aridity index is tested by an experiment (*Führer* and *Jagodics*, 2009), where mass of organic material (dendromass) were measured above and below the ground of a beech, hornbeam-English oak, and Turkey oak ecosystem. The age of the investigated ecosystems is 50−70 years; the canopy density is between 95−100%. Stands are located on deep, brown forest soil, and the source of water is solely the precipitation infiltrating into the soil. The climate of stands differs. The total mass of organic matter of a stand at a given forest site is basically determined by the production capacity (ecological potential) of the site. Taking into account that production capacity strongly depends on the climate parameters, the mass of organic matter is less (191 tC ha^{-1}) where the forestry aridity index is higher (*FAI* = 5.50 as for Turkey oak) (*Fig. 2*). In contrast, in beech stand with cooler and wetter climate (*FAI* = 4.45) the mass of organic matter is high (292 tC ha^{-1}).

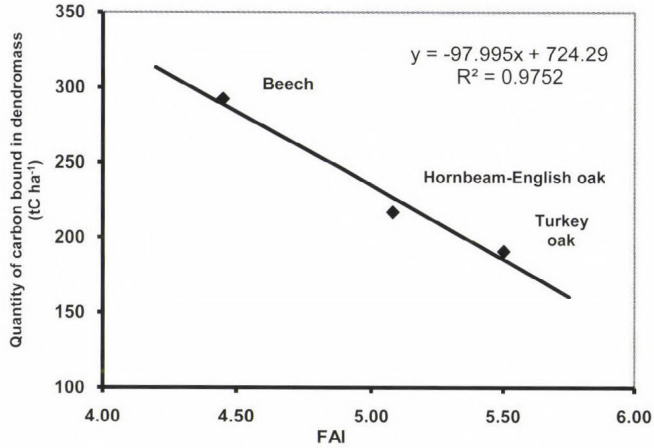

Fig. 2. Correlation between carbon bound in dendromass and *FAI* (*Führer* and *Jagodics*, 2009).

The applicability of *FAI* is also justified by another experiment evaluating the annual thickness (girth) growing of a hundred-year-old beech stand at Brennbergbánya research site. Increase of girth of trees was observed weekly by dendrometer bands located at stems of emergent, dominant, and suppressed trees. Basal area growth was calculated from girth-growth data. In *Fig. 3* we can see that variation of annual *FAI* values from average was always inverse in the examined 9 years (1999–2007) compared to the difference from the average basal area growth of beech. This means that warmer and drier years (represented by higher *FAI*) resulted in less of growth increment (*Fig. 4*).

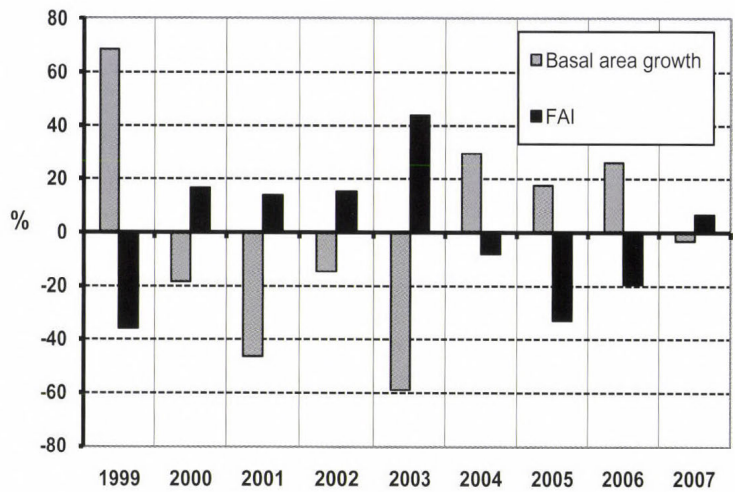

Fig. 3. Annual difference from average annual *FAI* values and basal area growth.

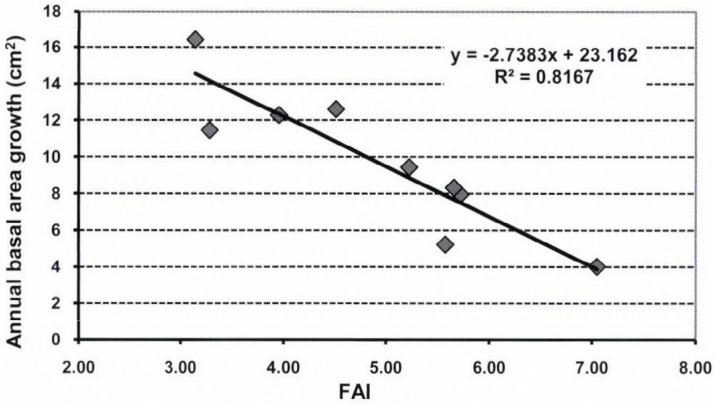

Fig. 4. Annual basal area growth as the function of *FAI*.

3.3. Calculation of FAI by means of meteorological data used at earlier forestry evaluations; characterization of forestry climate categories

Current forestry climate classification in Hungary is based on air humidity circumstances, since water-loss of trees (transpiration) is strongly determined among others by the relative humidity.

On the basis of agrometeorological investigations, daily relative humidity at 2 p.m. in July seemed to be the most suitable index, because humidity is the function of the temperature of the warmest summer month and more or less of the precipitation needed for evaporation. From data of 62 meteorological stations, between 1901 and 1950 we can draw the following conclusion (*Führer* and *Járó*, 2000); when the mean relative air humidity in July, 2 p.m. is higher than 58%, the natural plant community is beech. Between 53–58% and 48–53%, the plant community hornbeam-oak and sessile oak / Turkey oak, respectively. When air humidity is lower than 48%, the area is originally treeless (forest-steppe climate). Beside July, low relative humidity can also be observed in August; sometimes it is even lower than in July, therefore, mean humidity of critical months (July–August) would represent better the weather of climate categories according to our newest knowledge. Unfortunately, the exact characterization by air temperature and precipitation data – according to the climate categories – of annual periods essential in the physiological processes of trees has not been realized yet. So far, in forestry practice, the climate categories have been determined according to occurrence of test species (beech, hornbeam, sessile oak, and Turkey oak) in Hungary.

However, *FAI* index takes into account the temperature and precipitation characteristics of the period when organic matter production is directly influenced by these parameters. According to this criterion, we evaluated the data of meteorological stations in the important growth periods, which were earlier taken into consideration in the characterization of forestry regions.

Using data of 94 meteorological stations between 1901 and 1950 covering the whole area of the country, on the basis of the *Járó-type* evaluation (*Führer* and *Járó*, 2000), there are 11 stations in the beech climate, 16 in the hornbeam–oak climate, 43 in the sessile oak / Turkey oak, while 24 stations of them belong to the forest-steppe climate. On the basis of the mean of 50-year long measurement record (*Table 1*), we can conclude that:

Table 1. Meteorological features of forestry climate categories (*Führer*, 2010)

Meteorological parameters			Forestry climate categories			
			Beech	**Hornbeam–oak**	**Sessile oak–Turkey oak**	**Forest-steppe**
			(*FAI* <4.75)	**(*FAI*: 4.75–6.00)**	**(*FAI*: 6.00–7.25)**	**(*FAI* >7.25)**
Precipitation (mm)	annual	mean	752	663	598	546
		S.D.	31.0	55.4	43.4	29.0
	Nov–Apr	mean	297	267	248	233
		S.D.	25.9	36.5	26.1	18.7
	May–Jul	mean	259	218	192	174
		S.D.	12.5	15.0	11.3	6.6
	May–Oct	mean	455	395	350	313
		S.D.	22.0	25.5	22.7	13.0
	Jul–Aug	mean	167	139	118	101
		S.D.	8.6	12.8	8.9	5.4
Temperature (°C)	annual	mean	8.80	9.40	9.90	10.4
		S.D.	0.87	0.73	0.61	0.29
	Nov–Apr	mean	2.30	2.70	3.00	3.40
		S.D.	0.95	0.85	0.66	0.35
	May–Jul	mean	16.6	17.50	18.20	19.0
		S.D.	0.84	0.80	0.66	0.33
	May–Oct	mean	15.2	16.20	16.80	17.5
		S.D.	0.82	0.71	0.62	0.34
	Jul–Aug	mean	18.5	19.60	20.30	21.1
		S.D.	0.79	0.74	0.67	0.39
FAI		**mean**	**4.36**	**5.51**	**6.56**	**7.65**
		S.D.	0.30	0.41	0.38	0.31

(a) In the *beech climate*, where the climate marker species is beech, the sum of annual average precipitation reaches the 750 mm. During winter (in the storage period, from November to April), the average precipitation is nearly 300 mm; in the main growth phase (from May to July) it is 260 mm, whilst in the critical months it is 170 mm. The annual average temperature ranges between 8.5 and 9.0 °C, and during the warmest, critical months it is 18.5 °C.

(b) In the *hornbeam–oak climate*, where the climate marker species is hornbeam, the annual average precipitation sum is higher than 660 mm,

and in the water storage period it is nearly 270 mm. In the main growth phase and in the critical months, it reaches 225 and 140 mm, respectively. These values are about 10–15% lower than in the beech climate. The annual average temperature is 9.4 °C, but in the critical months it is higher than 19.5 °C.

(c) In the *sessile oak–Turkey oak* climate, where the climate marker species depending on the acidity of the soil is either the sessile oak (acidic site) or the Turkey oak (alkaline site), the annual average precipitation is around 600 mm, and in the water storage period it hardly reaches 250 mm. In the main growth cycle and in the critical months it is 190 and 120 mm, respectively. These values are about 10% lower than in the hornbeam–oak climate. The annual average temperature can reach 10 °C, and in the critical months it is higher than 20 °C.

(d) The *forest-steppe* climate cannot be characterized by tree species since it is originally treeless area. The lowest annual average precipitation sum under 550 mm is found here. In the storage period it is 230 mm and in the main growth cycle it is 175 mm. In the critical months the value goes down to 100 mm. This climate is the warmest in Hungary, the annual average temperature is nearly 10.5 °C and the average temperature in the critical months is higher than 21.0 °C.

(e) The average data of the climate categories significantly differ from each other at the confidence level of 90%.

Average value of forestry aridity index in the beech climate is nearly 4.4. Lowest value in Hungary can be derived at the meteorological station of Kékestető ($FAI = 3.3$), Hungary's highest peak (1005 m above sea level). The average *FAI* value at the stations in the hornbeam–oak climate is 5.5. The average *FAI* value in the sessile oak–Turkey oak climate nearly reaches 6.6. At stations of the forest-steppe climate, the average *FAI* value is higher than 7.6. The highest value ($FAI = 8.3$) was calculated for Csongrád town, in the warmest and lowest area of the Great Hungarian Plain.

Although the spatial distribution of considered meteorological stations only partially agrees with the distribution of marker stands representing various climate categories, we can still draw – on the basis of calculated mean *FAI* values and its deviation – the borders of different forestry climate categories with sufficient reliability, and we can also specify the classification of meteorological stations taking into consideration in our evaluation.

This means that in the *beech climate* zone the *FAI* index is 4.75 or below. *Hornbeam–oak climate* can be characterized by *FAI* value between 4.75 and 6.00, while we have *sessile oak–Turkey oak climate* between the values of 6.00 and 7.25. The *forest-steppe climate* can be found over higher *FAI* values.

4. Application of forestry aridity index for future estimations

On the basis of different climate scenarios during the summer months, the average temperature in Hungary increases, while precipitation will be less in this period (*Bartholy*, 2006). The *FAI* number allows us to model the expected impact of climate change on the basis of different scenarios, in other words, how the area of the certain climate categories will change.

In a simple way when we increase the mean temperature of critical months in calculation of *FAI* index with parallel decrease of precipitation according to the scenarios, we get the *FAI* representing the expected climate category in the future. Based on 30-year average meteorological data for 1961–1990, we have determined the distribution of the forestry climate categories. The distribution of categories in Transdanubian region will substantially be modified by a moderate temperature increase (1.0 °C) in summer (*Figs. 5* and *6*). Taking into account higher temperature increase (1.7 °C) and lower precipitation (8.2%) in summer (*Fig. 7*), 90% of the beech climate will disappear and the territory of the hornbeam-oak climate will decrease by 50%. The area ratio of the Turkey oak climate will remain the same, but it will be moved to the area of the today's hornbeam-oak climate. Expectedly, the area of the forest-steppe climate will be 4 times larger, and it will occupy the area of the current Turkey oak climate and partly in some extent that of hornbeam-oak climate.

The practical impact of this new situation (the change of areas of climate categories) is significant. It basically modifies the future forestry strategy of the country and the principle of forestry management from the point of view both of ecology aspects (species selection) and cultivation technology (regeneration, nursing sylvicultural treatment), as well as profitability.

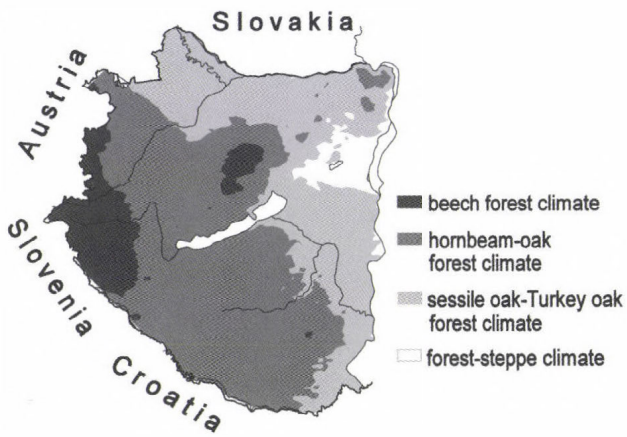

Fig. 5. Current distribution of climate categories in Transdanubian region according to today's weather conditions.

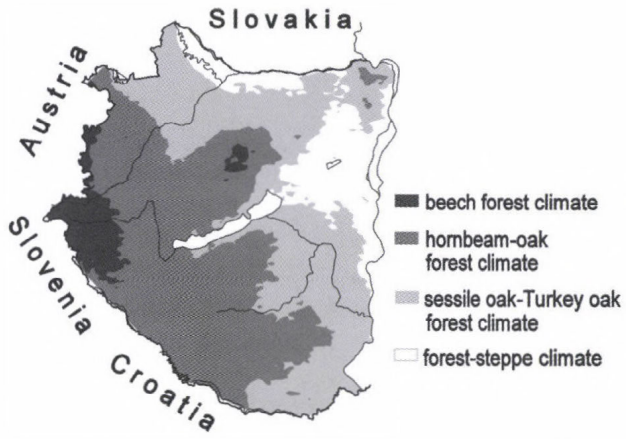

Fig. 6. Distribution of climate categories in Transdanubian region with a weak summer temperature (1.0 °C) increase scenario.

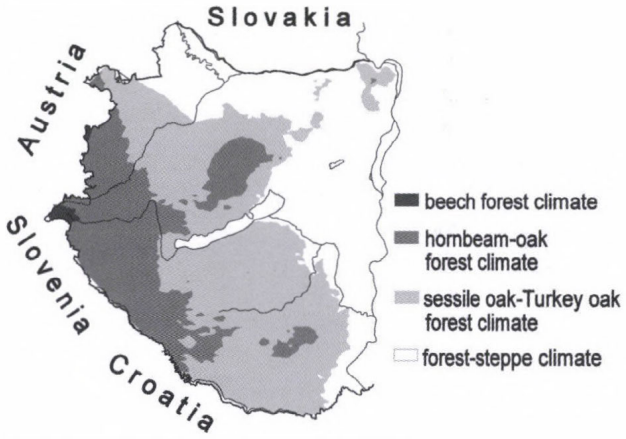

Fig. 7. Distribution of climate categories in Transdanubian region with a summer temperature increase of 1.7 °C and summer precipitation decrease of 8.2% scenario.

Acknowledgements—The authors acknowledge funding by a Hungarian research project NKTH–OTKA 80305 and 80335 CK.

References

Bartholy, J., 2006: The possible climate consequences of the global climate change in Hungary (in Hungarian). "*AGRO-21*" *Füzetek 48*, 12-18.

Berki, I., Móricz, N., Rasztovits, E. and *Vig, P.*, 2007: Determination of the drought tolerance limit of beech (in Hungarian). *Proceedings of the V. Erdő és klíma konferencia* (eds.: *Cs. Mátyás, P. Vig*). Nyugat-Magyarországi Egyetem, Sopron, 213-228.

Berki, I., Rasztovits, E., Móricz, N. and *Mátyás, Cs.*, 2009: Determination of the drought tolerance limit of beech forests and forecasting their future distribution in Hungary. *Cereal Research Communications 37*, 613-616.

Csóka, Gy., Koltay, A., Hirka, A. and *Janik, G.*, 2007: Influence of drought on health of sessile oak and beech stands in Hungary (in Hungarian). *Proceedings of the V. Erdő és klíma konferencia* (eds.: *Cs. Mátyás, P. Vig*). Nyugat-Magyarországi Egyetem, Sopron, 229-239.

Dunkel, Z., 2009: Brief surveying and discussing of drought indices used in agricultural meteorology. *Időjárás 113*, 23-38.

Führer, E., 1994: Precipitation measurements in beech, sessile oak and spruce ecosystems (in Hungarian). *Erdészeti Kutatások 84*, 11-35.

Führer, E., 1995: The effect of weather on the productivity and health state of the forests (in Hungarian). *Erdészeti Lapok 130*, 176-178.

Führer, E., 2008: Forest management (in Hungarian). In *Klímaváltozásról mindenkinek* (eds.: *Zs. Harnos, M. Gaál, L. Hufnagel*). Budapesti Corvinus Egyetem, Kertészettudományi Kar, Matematikai és Informatikai Tanszék, Budapest, 90-102.

Führer, E., 2010: Tree growth and the climate (in Hungarian). *"Klíma-21" Füzetek 61*, 98-107.

Führer, E. and *Jagodics, A.*, 2009: Carbon stocks in the stands of climate indicator tree species (in Hungarian). *„Klíma-21" Füzetek 57*, 43-55.

Führer, E. and *Járó, Z.*, 1992: Auswirkungen der Klimaänderung auf die Waldbestände Ungarns. *Österreichische Forstzeitung 9*, 25-27.

Führer, E. and *Járó, Z.*, 2000: The effectiveness of drought and drainage water in the sylviculture of the Great Plain I. (in Hungarian). *Erdészeti Tudományos Intézet Kiadványai 12*, 1-144.

Halupa, L., 1967: Data to the investigation of the growing process of saline oak forests (in Hungarian). *Erdészeti Kutatások 63*, 95-108.

Járó, Z., 1989: Water cycle in the forest (in Hungarian). *Az Erdő 38*, 352-355.

Járó, Z. and *Tátraaljai, E.*, 1984-85: Yearly growth of trees (in Hungarian). *Erdészeti Kutatások 76-77*, 221-234.

Láng, I., Csete, L. and *Jolánkai, M.* (eds.), 2007: Global climate change: home impacts and answers (in Hungarian). *A VAHAVA jelentés*, Szaktudás Kiadó Ház, Budapest, p. 227.

Linderholm, H.W., 2006: Growing season changes in the last century. *Agr. Forest Meteorol. 137*, 1-14.

Manninger, M., 2004: Annual and periodic growth pattern of forest trees and its relation to ecological factors (in Hungarian). In *Proceedings of the IV. Erdő és klíma konferencia* (eds.: *Cs. Mátyás, P. Vig*). Nyugat-Magyarországi Egyetem, Sopron, 151-162.

Mátyás, Cs., 2010: Forecasts needed for retreating forests. *Nature 464 (7293)*, 1271.

Mátyás, Cs., Nagy, L. and *Ujvári-Jármay, É.*, 2009: Climatic stress and the genetically determined response of tree species at the aridity limit of distribution: analysis and predictions (in Hungarian). *"Klíma-21" Füzetek* 56, 57-65.

Molnár, M. and *Lakatos, F.*, 2007: Beech decline in Zala county: triggered by climate change? (in Hungarian). *Proceedings of the V. Erdő és klíma konferencia* (eds.: *Cs. Mátyás, P. Vig*). Nyugat-Magyarországi Egyetem, Sopron, 257-267.

Pálfai, I., 2002: Drought zones of Hungary (in Hungarian). *Vízügyi Közlemények 84*, 323-357.

Pálfai, I., 2007: Climate change and drought (in Hungarian). *"Klíma-21" Füzetek 49*, 59-65.

Pálfai, I., 2010: The frequency of droughts in the Carpathian Basin in the last three hundred years (in Hungarian). *"Klíma-21" Füzetek 59*, 42-45.

Szőnyi, L., 1962: Data to the girth growth of some tree species (in Hungarian). *Az Erdő 11*, 289-300.

Várallyai, Gy., 2002: Climate change and soil processes. *Időjárás 106*, 113-124.

Várallyai, Gy., 2010: Soil as water reservoir; soil aridification (in Hungarian). *"Klíma-21" Füzetek 59*, 3-25.

Várallyai, Gy. and *Farkas, Cs.*, 2008: Expected impacts of climate change on the soils in Hungary (in Hungarian). In *Klímaváltozás: környezet – kockázat – társadalom* (eds.: *Zs. Harnos, L. Csete*). Szaktudás Kiadó Ház, Budapest, 91-129.

BOOK REVIEW

Haszpra, László (editor), 2011: **Atmospheric Greenhouse Gases: The Hungarian Perspective**. Springer, Dordrecht – Heidelberg – London – New York. 393 pages, with nearly 120 figures and 50 tables (ISBN 978-90-481-9949-5).

Human induced global climate change is one of the biggest challenges humankind faces today. Increasing amount of atmospheric greenhouse gases play a crucial role in the evolution of the climate. Without the understanding of the contributing processes, feedbacks, and interactions we cannot predict the future changes and develop effective mitigation/adaptation strategies. To decrease the uncertainty of the global studies, detailed regional studies are needed surveying the regional characteristics of the atmospheric greenhouse gas budget and the influencing factors. The book covers a coherent subset of the Hungarian climate change oriented research that is directly related to greenhouse gases.

The 16 chapters written by 44 Hungarian and foreign authors are grouped into four parts. The first part of the book covers the atmospheric trends and fluctuations of the major greenhouse gases as observed in Hungary. Here, first, the interested readers can get acquainted with the history and technical background of the Hungarian atmospheric greenhouse gas measurements. The following two chapters present the concentration trends, seasonal and diurnal variations, as well as the characteristic changes observed during the measurement period. For these studies impressive 17–30 years long data series were available.

The second and third parts of the book deal with the exchange of greenhouse gases between the biosphere (including the soil) and the atmosphere. The response of the biosphere is an important feedback in the climate system. In the case of carbon dioxide and methane it can act as both a net source and a net sink depending on climate. Biospheric nitrous oxide emission also depends on climate. In turn, the greenhouse gas budget of the biosphere influences the climate through the control on the atmospheric greenhouse effect.

The first of these two parts covers the measurements, while the other focuses on the mathematical modeling of the processes. Both parts follow the same structure. They start with an introductory chapter presenting the measurement/modeling methods, then they discuss the grasslands, the forests, and the arable lands in separate chapters. The part on modeling finishes with a summary chapter giving the overall biospheric greenhouse gas budget of Hungary.

Atmospheric greenhouse gases cannot be discussed without mentioning the anthropogenic contribution. The three chapters of the last part of the book present the effect of the anthropogenic perturbation of the biosphere, the contribution of the different industrial processes (energy production, waste

management, etc.) giving also a methodological introduction to the emission estimations. The authors also review the trends in the Hungarian greenhouse gas emissions.

This book of 393 pages calls the attention to the regional properties, which may modulate the European scale or global picture on the variation of atmospheric greenhouse gases. Although, the book is intended primarily for scientists studying the atmospheric and biospheric greenhouse gas budgets, most of the topics are general enough also for students studying geosciences, ecology, or environmental sciences to get an overview on a part of atmospheric greenhouse gas budget research.

L. Bozó

INSTRUCTIONS TO AUTHORS OF *IDŐJÁRÁS*

The purpose of the journal is to publish papers in any field of meteorology and atmosphere related scientific areas. These may be

- research papers on new results of scientific investigations,
- critical review articles summarizing the current state of art of a certain topic,
- short contributions dealing with a particular question.

Some issues contain "News" and "Book review", therefore, such contributions are also welcome. The papers must be in American English and should be checked by a native speaker if necessary.

Authors are requested to send their manuscripts to

Editor-in Chief of IDŐJÁRÁS
P.O. Box 38, H-1525 Budapest, Hungary
E-mail: journal.idojaras@met.hu

including all illustrations. MS Word format is preferred in electronic submission. Papers will then be reviewed normally by two independent referees, who remain unidentified for the author(s). The Editor-in-Chief will inform the author(s) whether or not the paper is acceptable for publication, and what modifications, if any, are necessary.

Please, follow the order given below when typing manuscripts.

Title page: should consist of the title, the name(s) of the author(s), their affiliation(s) including full postal and e-mail address(es). In case of more than one author, the corresponding author must be identified.

Abstract: should contain the purpose, the applied data and methods as well as the basic conclusion(s) of the paper.

Key-words: must be included (from 5 to 10) to help to classify the topic.

Text: has to be typed in single spacing on an A4 size paper using 14 pt Times New Roman font if possible. Use of S.I. units are expected, and the use of negative exponent is preferred to fractional sign. Mathematical formulae are expected to be as simple as possible and numbered in parentheses at the right margin.

All publications cited in the text should be presented in the *list of references*, arranged in alphabetical order. For an article: name(s) of author(s) in Italics, year, title of article, name of journal, volume, number (the latter two in Italics) and pages. E.g., *Nathan, K.K.,* 1986: A note on the relationship between photo-synthetically active radiation and cloud amount. *Időjárás 90,* 10-13. For a book: name(s) of author(s), year, title of the book (all in Italics except the year), publisher and place of publication. E.g., *Junge, C.E.,* 1963: *Air Chemistry and Radioactivity.* Academic Press, New York and London. Reference in the text should contain the name(s) of the author(s) in Italics and year of publication. E.g., in the case of one author: *Miller* (1989); in the case of two authors: *Gamov* and *Cleveland* (1973); and if there are more than two authors: *Smith et al.* (1990). If the name of the author cannot be fitted into the text: *(Miller,* 1989); etc. When referring papers published in the same year by the same author, letters a, b, c, etc. should follow the year of publication.

Tables should be marked by Arabic numbers and printed in separate sheets with their numbers and legends given below them. Avoid too lengthy or complicated tables, or tables duplicating results given in other form in the manuscript (e.g., graphs).

Figures should also be marked with Arabic numbers and printed in black and white or color (under special arrangement) in separate sheets with their numbers and captions given below them. JPG, TIF, GIF, BMP or PNG formats should be used for electronic artwork submission.

Reprints: authors receive 30 reprints free of charge. Additional reprints may be ordered at the authors' expense when sending back the proofs to the Editorial Office.

More information for authors is available: journal.idojaras@met.hu

Published by the Hungarian Meteorological Service

Budapest, Hungary

INDEX 26 361

HU ISSN 0324-6329